1-1-2011

Functional in vitro analyses of lipid raft-associated cathepsin b: implication for the invasive phenotype of inflammatory breast cancer

Bernadette Caroline Victor
Wayne State University,

FUNCTIONAL IN VITRO ANALYSES OF LIPID RAFT-ASSOCIATED CATHEPSIN B: IMPLICATION FOR THE INVASIVE PHENOTYPE OF INFLAMMATORY BREAST CANCER

by

BERNADETTE C. VICTOR

DISSERTATION

Submitted to the Graduate School

of Wayne State University,

Detroit, Michigan

in partial fulfillment of the requirements

for the degree of

DOCTOR OF PHILOSOPHY

2011

MAJOR: CANCER BIOLOGY

Approved by:

_____

Adviser Date

_____

_____

_____

DEDICATION

I dedicate this dissertation to my entire family. To my parents, Dominic and Dody Palazzolo: you show unwavering love, support and encouragement always. You are the best parents, whom I deeply respect. I must recognize the encouragement and love of my sister, Frances and my brother, Dominic. I am indebted to you.

I especially dedicate this work to my husband Jonny and our amazing daughter, Lia Francesca. I love you dearly and cannot wait to spend more time with you.

ACKNOWLEDGMENTS

To Dr. Bonnie Sloane, my mentor, much heartfelt appreciation for accepting me into your laboratory. You provided an exceptional environment for my development into a young scientist, incredible opportunities to travel, network with leading researchers, attain independent funding, and publish. In addition, I have gained a great deal of knowledge and skill through your example as a woman with a very accomplished scientific career.

I also greatly appreciate all the time, effort and valuable advise from my doctoral committee: Drs. Raymond Mattingly, Rafael Fridman and James Granneman.

A huge thank you to all of my past and present colleagues in the Sloane laboratory for making it such a great place to work everyday. I owe a huge debt of gratitude to Izabela Podgorski, Dora Cavallo-Medved, Sue Sameni, Christopher Jedeszko and Mary Olive. My sincere thanks to Selvi Anbalagan, Mackenzie Herroon and Aimalie Hardaway for all of the great laughs and memories on the 6th floor of Scott Hall, especially in tissue culture. I will most certainly miss you. I would also like to acknowledge the Thursday night running club, especially Amy Roth.

Lastly, I would like to thank my beautiful family for their overwhelming love, encouragement and support.

TABLE OF CONTENTS

CHAPTER 3: RESULTS

LIST OF ABBREVIATIONS

2D	two-dimensional
3D	three-dimensional
AIIt	annexin II heterotetramer
CA074	N-(l-3-trans-propyl-carbamoyloxir-ane-2-carbonyl)-L-isoleucyl-L-proline
DAPI	(3-(4,5-Dimethylthiazol-2-yl)-2,5-diphenyltetrazolium bromide
ECM	extracellular matrix
EGFR	epidermal growth factor receptor
ER	estrogen receptor
IBC	inflammatory breast cancer
IHC	Immunohistochemical
MMP	matrix metalloprotease
MTT	4’,6-diamidino-2-phenylindole-dihydrochloride
MVA	mevalonic acid
PBS	phosphate buffered saline
PR	progesterone receptor
rBM	reconstituted basement membrane
TNBC	triple-negative breast cancer
uPA	urokinase plasminogen activator
uPAR	urokinase plasminogen activator receptor

LIST OF TABLES

LIST OF FIGURES

CHAPTER 1

INTRODUCTION

Inflammatory Breast Cancer. Inflammatory breast cancer (IBC) is the most lethal type of breast cancer with a three-year survival rate of 42% as compared to 85% for non-IBC (Chang et al., 1998b). The incidence of IBC is relatively low but varies depending on geographic region. For example, an analysis by Hance *et. al* reported that IBC accounts for approximately 2.5% of all breast cancer cases in the USA (Hance et al., 2005) whereas in parts of northern Africa rates may be as high as 10% (Boussen et al., 2010). The unique clinical presentation and symptoms of primary IBC, described below, are quite distinct from non-IBC (Walshe and Swain, 2005) and because it is rare, clinicians are less familiar with the disease. Upon physical examination, a palpable discrete mass is absent in many patients and IBC is often misdiagnosed as mastitis, a benign bacterial infection. Therefore, accurate and early diagnosis is critical due to the aggressiveness and rapid onset of IBC. In 2010, an international panel of leading experts recommended that the clinical consensus for a minimal standard diagnosis of IBC include erythema occupying at least one-third of the breast, hardening and retraction of the nipple, dimpling (peau d'orange) of the skin caused by enlarged hair-follicle pits that does not respond to antibiotic treatment (Dawood et al., 2010) (Figure 1.1). More than half to 85% of patients present with axillary or supraclavicular lymph node metastases

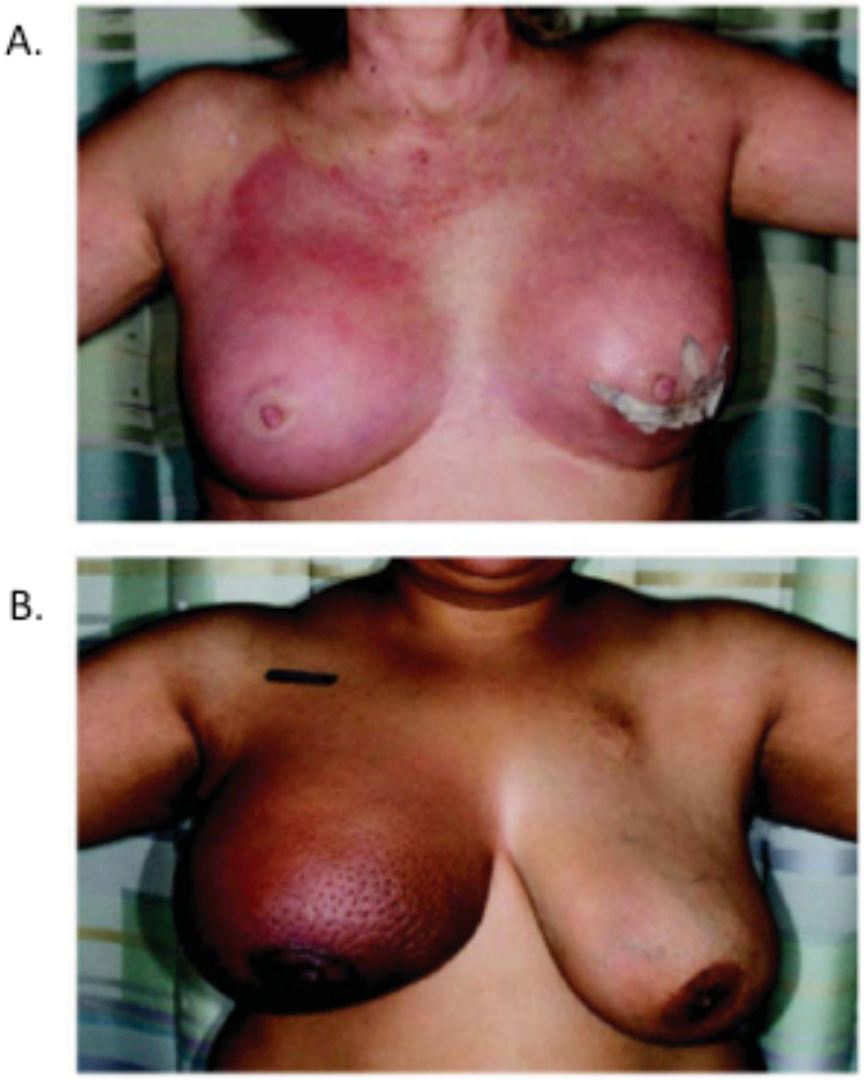

Figure 1.1. Clinical signs of IBC and variations in presentation. (A) Primary IBC with synchronous bilateral erythema with minimal breast edema. (B) An African American IBC patient with increased breast size and peau d'orange with minimal erythema. (Robertson et al., 2010)

(Walshe and Swain, 2005). Indeed, classification of IBC is considered at least Stage IIIB or higher depending on nodal status and the presence of distant metastases (Edge et al., 2010).

Mammographic and ultrasonographic imaging are both important for IBC diagnosis and disease assessment and often reveal the absence of an underlying discrete mass or lump. Ultrasonographic evaluation has proved significant for detection of skin, pectoral muscle and axillary lymph node involvement and also for revealing masses. Masses may be otherwise masked by accompanying inflammatory changes such as skin thickening and stromal coarsening and/or increased density when evaluated by mammography (Gunhan-Bilgen et al., 2002). The clinical manifestation and characteristic imaging profile of the involved breast are thought to reflect dermal lymphatic invasion, in which invasive cellular aggregates or tumor emboli in dermal lymphatics block drainage of these vessels.

IBC is an aggressive and fatal invasive breast cancer and therefore studies have focused on establishing epidemiological risk factors, identifying molecular features and defining the specific biology of IBC. Risk factors highly associated with IBC include younger age at diagnosis, high body mass index and African American ethnicity (Chang et al., 1998a; Levine and Veneroso, 2008). Over-expression of the Ras superfamily member RhoC and loss of WISP3 may be two key and related events in the development of IBC (Miao et al., 2003). IBC tumors, in comparison to non-IBC tumors, have a higher occurrence of *p53* gene

mutations (Riou et al., 1993; Gonzalez-Angulo et al., 2004), increased expression of angiogenic and lymphangiogenic factors including VEGF, IL-6, IL-8 and VEGF receptor 3 (Van der Auwera et al., 2004), and a greater incidence of HER2 positivity and EGF receptor (Guerin et al., 1989; Parton et al., 2004). In IBC, high levels of the cysteine protease cathepsin B correlate with increases in numbers of metastatic lymph nodes (Nouh et al., 2011). Caveolin-1, which was initially hypothesized to be a tumor suppressor in breast cancer (Bouras et al., 2004), is highly expressed in both IBC cells and tissues (Van Laere et al., 2005; Van den Eynden et al., 2006; Nouh et al., 2011). Recent data suggest that high expression of caveolin-1 is a characteristic of triple-negative and other basal-like breast cancers (Elsheikh et al., 2008), including IBC of a basal phenotype.

Caveolin-1 and Caveolae. Caveolin-1, a 22-kDa protein, was first identified in Rous sarcoma virus transfected fibroblasts as a phosphorylation substrate of v-Src (Glenney, 1989). Caveolin-1 belongs to a family of three highly conserved proteins. Caveolin-1 and caveolin-2 are expressed in most tissues and caveolin-3 is muscle specific. The caveolins have a hairpin loop structure that is inserted into the inner leaflet of the plasma membrane with the N- and C-termini exposed to the cytoplasm (Glenney and Soppet, 1992). Cholesterol binds caveolin-1 via a putative cholesterol-binding domain and this interaction is thought to facilitate its oligomerization (Murata et al., 1995). Assembly of caveolin-1 oligomers at the plasma membrane forms the structure

and scaffold of caveolae (Monier et al., 1995; Fernandez et al., 2002) with the integrity and function of caveolae dependent on membrane cholesterol (Rothberg et al., 1992). First identified in the 1950s by electron microscopy, caveolae are omega-shaped plasmalemmal invaginations approximately 50-100 nm in diameter. Caveolae are specialized cholesterol- and sphingolipid-rich microdomains that are distinct from other lipid rafts as well as from the general plasma membrane and clathrin-coated vesicles (Schnitzer et al., 1995b; Anderson and Jacobson, 2002). The lipid raft model originated from observations that glycosphingolipids first cluster in the Golgi apparatus before being sorted to the apical surface of epithelial cells (Simons and van Meer, 1988). Subsequent studies demonstrated that sphingolipid-cholesterol rafts (including caveolae) are insoluble in the detergent Triton X-100 at 4°C, resulting in detergent–insoluble or –resistant membranes. As a result of the elevated lipid content, these detergent-insoluble membranes float to a light buoyant density on sucrose gradients (Brown, 1994) along with associated proteins. This has led to purification techniques and use of cholesterol-modulating agents for the study of lipid rafts and caveolae (Sargiacomo et al., 1993; Smart et al., 1995; Song et al., 1996). In prostate cancer models, strategies to disrupt cholesterol-rich structures have elucidated their associated proteins and functions in tumor progression [for review see (Di Vizio et al., 2008)]. For example, targeted disruption of lipid rafts with cholesterol binding agents inhibits EGF receptor and Akt1 phosphorylation and reduced survival of prostate cancer cells (Zhuang et al., 2002; Oh et al.,

2007). Alternatively inhibiting cholesterol biosynthesis alters lipid raft composition, i.e. decreased cholesterol content and phosphorylated Akt, inhibits Akt pathway signaling and induces apoptosis in prostate cancer cells and xenografts (Zhuang et al., 2005). Recently, quantitative proteomics is being used to map the lipid raft proteome, studies which may identify tumor biomarkers and therapeutic targets (Staubach and Hanisch, 2011).

Specific Functions of Caveolae and Caveolin-1. Caveolae play functional roles in both endocytosis and transcytosis (Montesano et al., 1982; Schnitzer et al., 1994; Schnitzer et al., 1995a; Schnitzer, 2001). Caveolae associated signaling molecules have also been identified: a number of heterotrimeric G proteins (Oh and Schnitzer, 2001), non-receptor tyrosine kinases (Liu et al., 1997) and Ras (Rizzo et al., 1998). Thus, caveolae compartmentalize signaling pathways and may act as cell surface structures for regulated signal transduction. Caveolin-1 protein directly interacts with many of the aforementioned as well as several other proteins and lipids, e.g. insulin receptor and GM1 [for review see (Liu et al., 2002a)] indicating its role in lipid transport, lipid trafficking and signal transduction. We propose that caveolae also serve as sites on the cell surface linking signaling pathways and proteolytic networks that are involved in tumor invasion.

Proteases and Their Receptors in Caveolae. We previously hypothesized that the high levels of caveolin-1 expression in bladder, colon, esophageal and prostate cancers promote cell surface proteolytic events that lead to extracellular matrix (ECM) degradation and tumor invasion [for review see (Cavallo-Medved and Sloane, 2003)]. Annexin II, a member of a family of membrane-binding proteins that bind to negatively charged phospholipids in a calcium-dependent manner [for review see (Gerke and Moss, 2002), localizes to caveolae in many cell types (Sargiacomo et al., 1993; Lisanti et al., 1994; Cavallo-Medved et al., 2005). Annexin II (or p36), like caveolin-1, is a v-Src substrate (Soric and Gordon, 1986) and exists both as a monomer and in a heterotetrameric complex, referred to as the annexin II heterotetramer (AIIt). AIIt consists of two subunits of annexin II, the heavy chain, bound to a homodimer of S100A10 (also called p11), the light chain. The amino terminus of annexin II contains the binding site for its hydrophobic interactions with S100A10 (Rety et al., 1999). The heavy chain, annexin II, is a collagen I binding protein (Santoro et al., 1994). Chung *et al.* found that the annexin II tetramer interacts with an alternatively spliced segment of tenascin C on the cell surface of U-251MG human glioma cells (Chung and Erickson, 1994). Usually absent from most adult tissues, tenascin C reappears in places of active tissue regeneration and cell migration, i.e., in tumors and areas of wound healing (Mackie et al., 1988; Koukoulis et al., 1991). The AIIt is a receptor for and regulatory complex of plasminogen (MacLeod et al., 2003). Our laboratory demonstrated that the AIIt

serves as a binding platform for cathepsin B on the surface of tumor cells (Mai et al., 2000). More specifically, we have shown that in colon cancer cells cathepsin B and AIIt localize in caveolae (Cavallo-Medved et al., 2003). Proteases of the plasminogen cascade, specifically pro-urokinase plasminogen activator (pro-uPA) and its receptor uPAR have also been localized to caveolae (Stahl and Mueller, 1995; Cavallo-Medved et al., 2005). These findings may be of functional significance as cathepsin B is capable of processing the zymogen pro-uPA to its active derivative uPA (Kobayashi et al., 1991), which in turn can activate plasminogen bound to AIIt. A proteolytic pathway involving cathepsin B and uPA has been identified upstream of plasminogen on the surface of a number of cell lines (Kobayashi et al., 1992; Kobayashi et al., 1993; Guo et al., 2002). Moreover, uPAR complexes with caveolin-1 via β1-integrin, an association that has been shown to mediate uPAR-dependent adhesion and β1-integrin-induced signal transduction (Wei et al., 1999; Schwab et al., 2001). Localization of these enzymes and their receptors to caveolae supports the hypothesis that proteolytic cascades may be initiated in caveolae and participate in tumor invasion via the degradation of extracellular matrix components (Figure 1.2).

Cathepsin B: Intracellular Trafficking and Activity. Cathepsin B is a ubiquitously expressed lysosomal cysteine protease of the papain family. In the acidic lysosomal environment, cathepsin B functions in protein degradation in

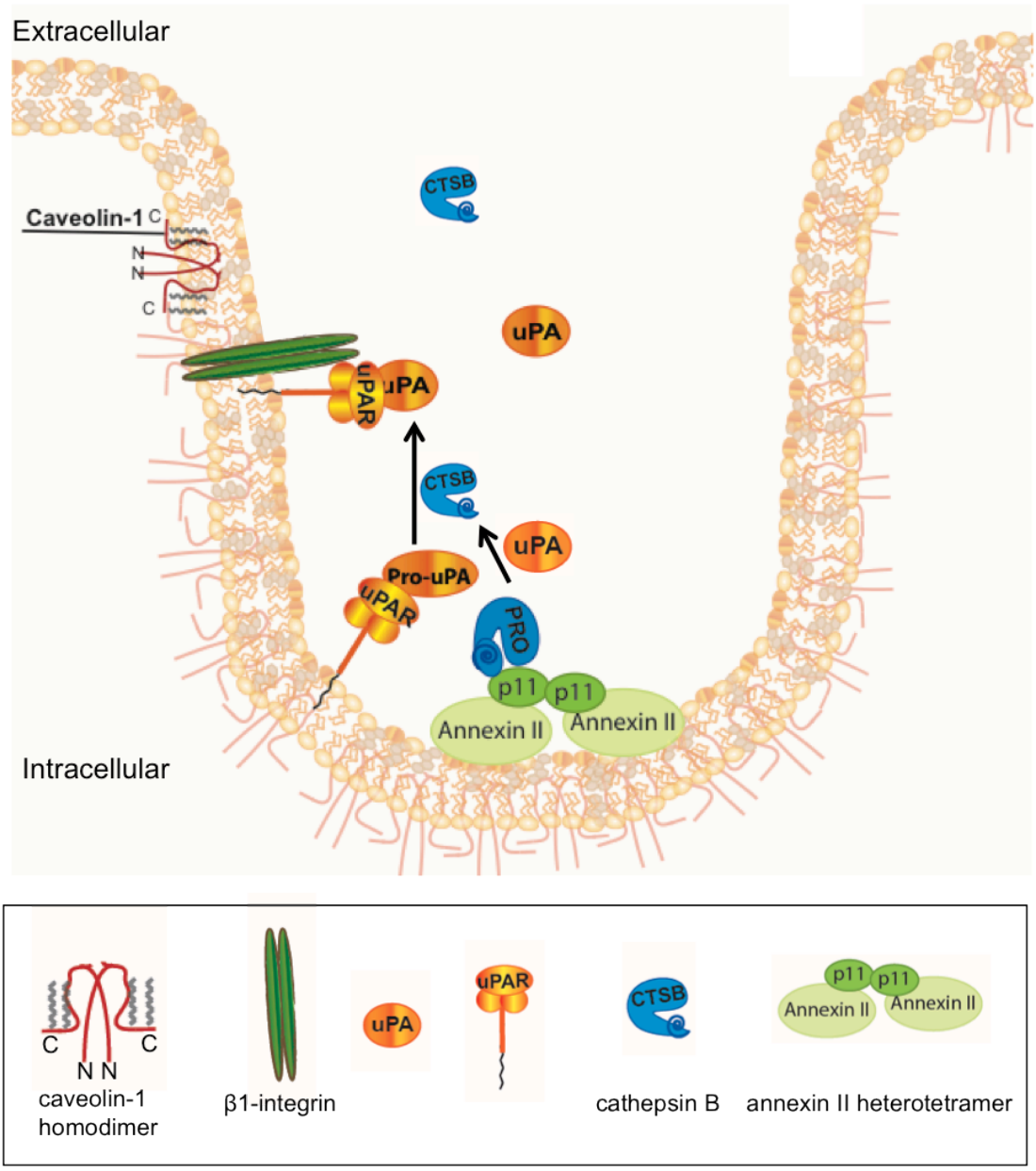

Figure 1.2. Proteases localize to caveolae at the surface of tumor cells. Caveolae are distinct lipid microdomains that are small invaginations of the plasma membrane formed by the oligomerization of the structural protein caveolin-1. Cathepsin B, uPA and their respective receptors, the annexin II heterotetramer and uPAR, localize at the tumor cell surface in caveolae. The bidirectional interaction between cathepsin B and uPA is one example of a proteolytic network clustering in caveolae that may affect tumor progression. Arrows indicate cleavage events that activate pro-enzymes. Adapted from (Rothberg et al., 2011).

mammalian cells, exhibiting broad substrate specificity (Mort and Buttle, 1997). Some redundancy in function of cysteine cathepsins might explain why the absence of cathepsin B is not lethal. Analyses of knockout mice have demonstrated significant roles for cathepsin B in trypsinogen activation in pancreatitis and also TNF-alpha specific. Non-redundant functions of cathepsin B suggest its involvement in processes of physiology and pathology (Guicciardi et al., 2000; Halangk et al., 2000).

The single human cathepsin B gene is located on chromosome 8p22 (Fong et al., 1986; Fong et al., 1992). Cathepsin B mRNA is translated as a preprocathepsin B on the rough endoplasmic reticulum. The signal recognition prepeptide directs translated mRNA into the rough endoplasmic reticulum. Two N-glycosylation sites, one within the 62 residue proregion and another present in the heavy chain, are co-translationally glycosylated. Following cleavage of the 17 residue prepeptide, the inactive proenzyme moves through the ER and is shuttled into the Golgi apparatus. Normal trafficking of cathepsin B to the lysosome follows the traditional mannose-6-phosphate pathway characteristic of lysosomal enzymes. Therefore, after entry into the Golgi complex, further modification of cathepsin B carbohydrate moieties to phosphorylated mannose residues enables recognition by membrane bound mannose-6-phosphate receptors (MPR). In the trans-Golgi, the 300-kDa cation-independent CI-MPR and the 46-kDa cation-dependent CD-MPR bind the phosphorylated carbohydrate moieties of procathepsin B (Ludwig et al., 1993). Normally

procathepsin B is trafficked from the Golgi to the pre-lysosomal compartment of late endosomes. The slightly acidic pH of the late endosomes results in dissociation of procathepsin B from MPRs. Removal of phosphate by acid phosphatase from the mannose-6-phosphate residues on cathepsin B prevents its retrograde trafficking. In the late endosome maturation of the enzyme by cleavage of the pro-region results in the 31-kDa active cathepsin B species (Mach et al., 1992). Cathepsin B is next transported to perinuclear lysosomes, where it normally functions in protein degradation and turnover of cellular components.

Therefore, there are several forms of intracellular cathepsin B. The molecular weight of the inactive species is 43 or 46-kDa, depending upon glycosylation. The active single chain form exists as a 31-kDa protein of 252 amino acids. In some tissues, additional proteolytic cleavage of the 31-kDa species occurs within the lysosome, the result of which is a double chain form composed of a 25/26-kDa heavy chain and 5-kDa light chain, bound by a disulfide linkage (Nishimura et al., 1988; Rowan et al., 1992). The difference in heavy chain molecular weight, 25 or 26 kDa, is due to removal of a carbohydrate moiety from the latter (Mach et al., 1992). The active site is within the 5-kDa light chain of the double chain form. The double chain cathepsin B is also short two amino acids in the heavy chain, a result of their cleavage during processing (Figure 1.3).

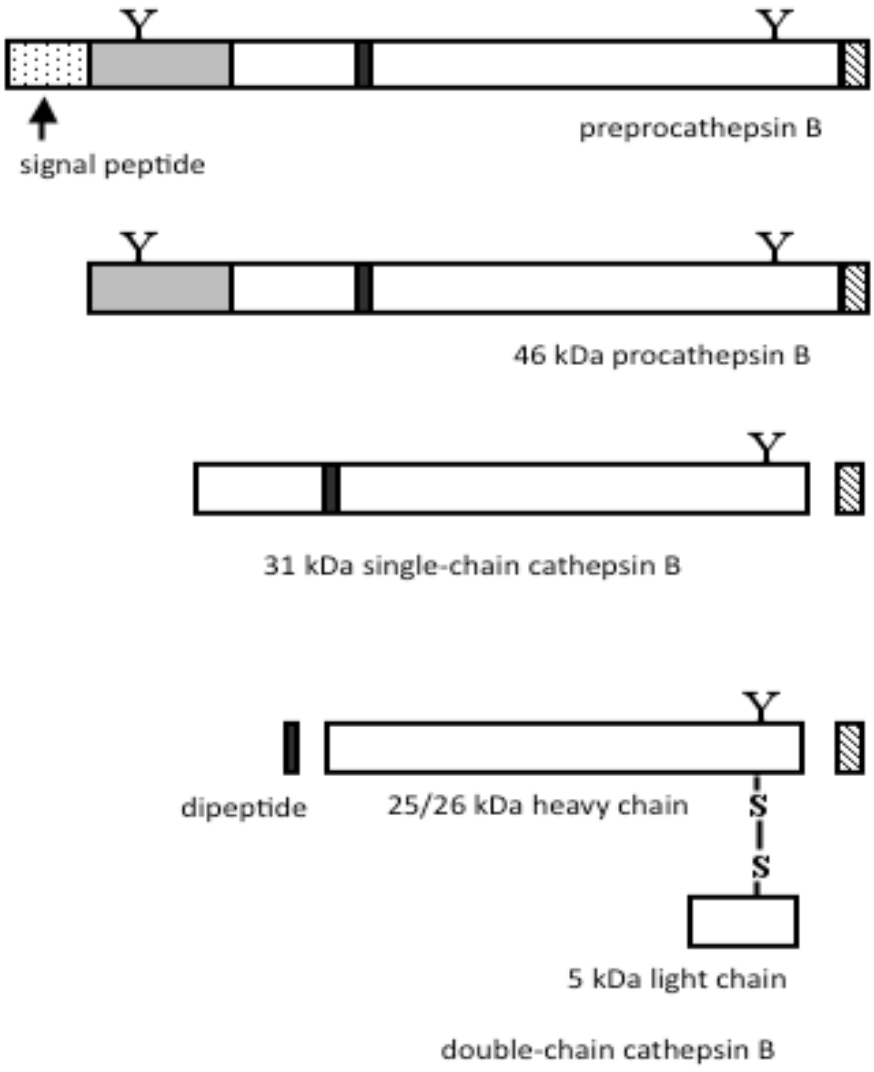

Figure 1.3. Cartoon illustrating the various cathepsin B species. Cathepsin B mRNA is translated as preprocathepsin B. The signal recognition prepeptide directs translated mRNA into the rough endoplasmic reticulum. The molecular weight of the inactive procathepsin B species is 43 or 46-kDa, depending upon glycosylation. Potential glycosylation sites are depicted as "Y". The active single chain form exists as a 31-kDa protein of 252 amino acids. In some tissues, additional processing of the 31-kDa species by cleavage of a dipeptide occurs within the lysosome, the result of which is a double chain form composed of a 25/26-kDa heavy chain and 5-kDa light chain that are linked by a disulfide bridge. Adapted from (Cavallo-Medved and Sloane, 2003).

Structurally, cathepsin B is a bilobal protein, containing two globular domains, between which the active site and substrate-binding site are located. In its active form, cathepsin B can act either as an endopeptidase, cleaving internal peptide bonds, or an exopeptidase, by removing C-terminal dipeptides from a substrate (Keppler and Sloane, 1996). Cathepsin B exhibits this dual peptidase activity due to a flexible structural element within the molecule, the occluding loop. At acidic pH, this occluding loop partially blocks the active site of the molecule, preventing large protein substrates from entering the active site and as a result the enzyme exhibits exopeptidase activity, specifically carboxydipeptidase activity. In a neutral pH environment, the loop is displaced and no longer blocks access of proteins to the active site, and therefore cathepsin B can act as an endopeptidase cleaving peptide bonds within a substrate.

Aberrant Trafficking of Cathepsin B. In normal cells less than five percent of the proenzyme is secreted (Hanewinkel et al., 1987). Unlike normal cells, cancer cells secrete significantly greater amounts of latent pro- and mature cathepsin B. This is observed in human malignancies of the breast (Poole et al., 1978) and colon (Maciewicz et al., 1989) as well as gliomas (McCormick, 1993). The normal location of lysosomes, and therefore cathepsin B, is perinuclear in the region of the microtubule organizing center and in the apical pole of polarized epithelial cells. There is altered intracellular distribution of the cathepsin B in

tumors, leading to cathepsin B in vesicles throughout the cytoplasm and at the cell periphery. As seen by cathepsin B staining of human colon cancer tissues, there is a shift in localization from the apical pole of the cell to the inner basal surface of the plasma membrane (Emmert-Buck et al., 1994). Not only is there a change in localization as noted here, but also increased message, protein, and/or activity are localized to regions of tumor invasion (Sinha et al., 1993; Emmert-Buck et al., 1994; Visscher et al., 1994).

The mechanism for the aberrant intracellular localization of cathepsin B, its trafficking to the cell surface and subsequent secretion are yet unknown (Figure 1.4). Experimental data support several hypotheses. For example, studies on macrophages and fibroblasts demonstrated that experimentally lowering cytoplasmic pH causes lysosomes to move toward the cell periphery (Heuser, 1989). This movement follows an alteration in microtubules, and does not occur if cells are treated with the microtubule depolymerizing agent nocodazole. When evaluating how malignant progression affects the intracellular distribution and secretion of cathepsin B, Rozhin *et al.* incubated malignant cells at slightly acidic pH. Not only did secretion of active cathepsin B increase and intracellular levels decrease, but vesicles positive for cathepsin B localized to the cell periphery. These effects were inhibited by treatment with both taxol, a microtubule stabilizer, and colchicine, a microtubule poison (Rozhin et al., 1994). The studies suggest that modulating pH disrupts the microtubule cytoskeleton resulting in the movement and even secretion of lysosomal constituents, i.e.,

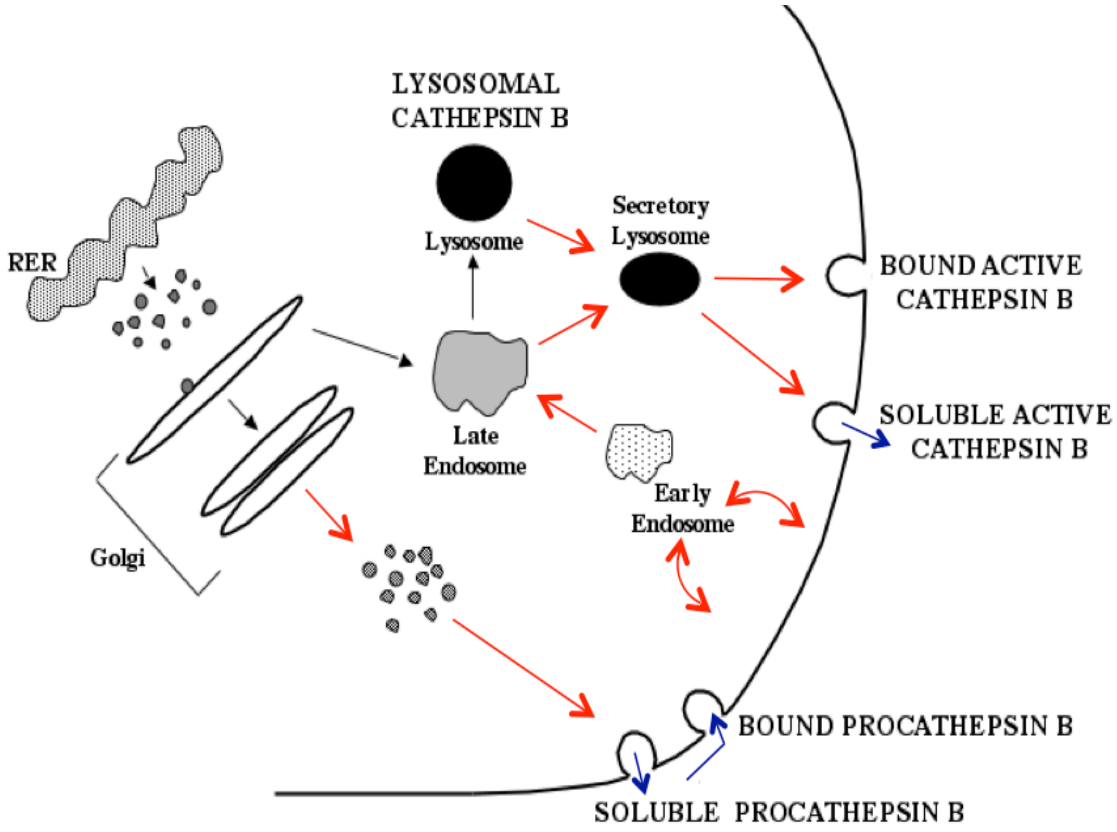

Figure 1.4. Classical and alternative trafficking pathways for cathepsin B. This diagram illustrates the potential pathways of cathepsin B trafficking in either normal or cancer cells. Normal trafficking of cathepsin B to the lysosome follows the traditional mannose-6-phosphate pathway characteristic of lysosomal enzymes, indicated by the black arrows. Cathepsin B mRNA is translated as a preprocathepsin B on the RER, transported through the Golgi complex, to late endosomes and finally to the lysosome. In tumor cells cathepsin B is still trafficked to the lysosome, but is also trafficked by alternative pathways, indicated by the red arrows: (1) Procathepsin B is secreted from tumor cells and exists as either a soluble or membrane bound form. (2) Active cathepsin B may also be translocated to the plasma membrane via secretory lysosomes that either fuse with the plasma membrane or undergo exocytosis and secrete soluble cathepsin B. The blue arrows indicate extracellular cathepsin B. Adapted from (Cavallo-Medved and Sloane, 2003).

release of active cathepsin B into the extracellular milieu. *In vitro* pH modulation may be relevant as it closely imitates the acidic tumor microenvironment found *in vivo* [for reviews, see (Wike-Hooley et al., 1984; Gillies et al., 2002)].

To understand cathepsin B functionality through qualitative analysis of secretion and membrane association, our lab developed an assay for measurement of cathepsin B activity in real time. Pericellular cathepsin B activity was shown to be forty to fifty percent membrane associated (Linebaugh et al., 1999). Other studies suggest that exocytosis of lysosomes is calcium mediated or that a yet unknown endosome functions in secretion of active cathepsin B (Rodriguez et al., 1997; Linebaugh et al., 1999; Andrews, 2000). Procathepsin B secretion is thought to be independent of the secretory lysosome theory, i.e., secretion of active cathepsin B. Procathepsin B is secreted through the default pathway as a result of the high levels of expression in tumors and swapping of available MPRs (Roshy et al., 2003).

Molecular Regulation of Cathepsin B. Molecular regulatory mechanisms controlling the biosynthesis of cathepsin B may play a role in the divergent protein trafficking seen in malignancy. Gene amplification, increased transcription, mRNA stability, use of alternative promoters, and alternative splicing have all been shown to affect the levels and/or localization of cathepsin B protein in pathologies [for review, see (Yan and Sloane, 2003)]. These molecular changes at the genetic level resulting in elevated protein, aberrant

localization, secretion, and in turn greater activity of cathepsin B, have been noted in several tumor types such as brain, colorectal, lung and prostate (Yan et al., 1998; Koblinski et al., 2000).

The cathepsin B transcript consists of at least 13 exons (Berquin et al., 1995). The 5'-untranslated region includes exons 1, 2, and 25 bp of exon 3. Translation of the preproprotein sequence begins at the initiation site within exon 3 and ends in exon 11, where the stop codon resides. The remainder of exon 11 and 12 constitute the non-coding 3'-untranslated region. Cao *et al.* were the first to isolate full-length preprocathepsin B cDNA clones from a human tumor source (Cao et al., 1994). In a later study, the same cDNA clones were assessed for any structural modifications that might result in membrane association and secretion of cathepsin B. Two new exons (exon 2a and exon 2b) and multiple transcription initiation sites in the 5'-UTR were identified (Berquin et al., 1995). The region upstream of exon 1 is high in GC content and lacks TATA and CAAT boxes, characteristics of a housekeeping-type promoter. This suggests that the cathepsin B gene may be constitutively expressed. This does not exclude the possibility of transcriptional regulation at the cathepsin B promoter. Cathepsin B expression and activity levels differ among tissue types or between normal and malignant tissues suggesting tissue specific regulation (San Segundo et al., 1986; Qian et al., 1989; Shuja et al., 1991). Within a region 200 base pairs upstream of the initiation site there are six Sp1, four Ets, and one USF (E box) binding sites (Jane et al., 2002). The presence of these additional elements may

induce transcription at the cathepsin B promoter. Sp1 and Ets factors regulate expression of cathepsin B in glioma (Yan et al., 2000). The same transcription factors, e.g., Ets1, that regulate expression of cathepsin B in glioma are also associated with components of a proteolytic cascade in this case uPA and caspase 3 (Delannoy-Courdent et al., 1998; Liu et al., 2002b).

Cathepsin B in Malignancy. Pathologies associated with cathepsin B include inflammatory airway diseases, acute pancreatitis, arthritis, and cancer [for reviews, see (Reinheckel et al., 2001; Vasiljeva et al., 2007; Reiser et al., 2010). Protease activity is important for tumor cell invasion and the many steps of tumor progression. Cathepsin B and other proteases function in the cleavage of enzymes secreted as inactive precursors, degradation of the basement membrane, invasion of surrounding tissues, and also angiogenesis. There is a substantial literature that supports a functional role for cathepsin B in malignancy [for reviews, see (Gocheva et al., 2006; Mohamed and Sloane, 2006).

Cathepsin B expression and/or its activity is increased in several tumor types. These include carcinomas of the breast (Krepela et al., 1989), colon (Campo et al., 1994), prostate (Sinha et al., 1995), lung (Sukoh et al., 1994) and stomach (Watanabe et al., 1989), gliomas (Rempel et al., 1994), and melanomas (Sloane et al., 1981). As is true for matrix metalloproteinases (MMPs) and serine proteases (van Kempen et al., 2002; Netzel-Arnett et al., 2003), tumor stromal interactions influence the expression and secretion of cathepsin B. Not only

tumor cells, but also other cells present in the tumor microenvironment, such as inflammatory macrophages and fibroblasts, exhibit elevated levels of cathepsin B (Campo et al., 1994; McKerrow et al., 2000). Our laboratory determined that growth of human breast fibroblasts on collagen I alters cell morphology and increases cathepsin B expression and secretion of procathepsin B (Koblinski et al., 2002). In agreement with these findings Klose *et al* have observed that cathepsin B protein levels and cellular localization are affected when high-invasive melanoma cells were cultured with collagen I, (Klose et al., 2006). Increases in expression of uPA and MMPs are also observed when epithelial cells, malignant cells, and stromal cells are cultured on various extracellular matrices (Mauch et al., 1989; Khan and Falcone, 1997; Bafetti et al., 1998). Thus, findings from several studies suggest that cell-matrix interactions play a pivotal role in the regulation, localization, and activity of cathepsin B and many other proteinases.

Cathepsin B cleaves a plethora of targets in the tumor mircoenvironment. For example, cathepsin B is capable of degrading ECM components such as type IV collagen, fibronectin, and laminin. The activity of cathepsin B, like other tumor promoting proteases, has a more complex function in malignant progression than once thought. Mature active cathepsin B is capable of converting these zymogens into their active derivatives: pro-MMP-3 (Murphy et al., 1992), and pro-uPA (Kobayashi et al., 1991). On the other hand, procathepsin B activators include cathepsin D (van der Stappen et al., 1996),

cathepsin G, tPA, uPA, and the elastases (Dalet-Fumeron et al., 1993; Dalet-Fumeron et al., 1996). Cathepsin B can also undergo glycosaminoglycan facilitated autoactivation (Caglic et al., 2007). Finally, cathepsin B, by inactivation of endogenous protease inhibitors, indirectly increases the activity of other proteases. For example, TIMP-1 and TIMP-2, the tissue inhibitors of matrix metalloproteinases, and the serine protease inhibitor, antileukoproteinase, are degraded by cathepsin B (Kostoulas et al., 1999; Taggart et al., 2001).

Cathepsin B participates in a complex proteolytic network to regulate tumor progression [for review, see (Mason and Joyce, 2011)]. Moreover, pericellular proteolytic pathways and signaling pathways converge to specific regions on the cell surface, named caveolae. The annexin II tetramer, cathepsin B, uPAR, uPA, and β1 integrin all localize to caveolae on the cell surface [for review, see (Sloane et al., 2005)]. Not only do these proteins localize to caveolae, they also facilitate interactions of their binding partners. Associations between S100A10, the light chain of the AIIt, with both pro-cathepsin B and plasminogen have been reported (Kang et al., 1999; Mai et al., 2000). The heavy chain, annexin II, is a collagen I binding protein (Santoro et al., 1994). Also, the uPA:uPAR protein complex was shown to act as a ligand of β1 integrin in Chinese hamster ovary cells (Tarui et al., 2003). Secretion and cell surface association of both pro- and active cathepsin B observed in malignancy favor conditions for its involvement in tumor invasion as well.

Cathepsin B may play causal roles in tumor growth, not just invasion and metastasis. Growth factors, such IGFs, FGFs, and TGF-βs, associated with ECM components, control cell proliferation, differentiation, and synthesis of the extracellular matrix. Cathepsin B remodeling of the extracellular matrix (ECM) could influence the release of growth factors from matrix storage and even their activation (Taipale and Keski-Oja, 1997). For example, cathepsin B proteolysis of thyroglobulin mediates thyroid hormone liberation in thyroid epithelial cells (Brix et al., 1996).

uPA and uPAR: Components of the Plasminogen Activation System. The urokinase plasminogen activating system is a serine protease family including uPA, its glycosyl phosphatidyl inositol-anchored receptor uPAR, soluble uPAR, uPAR associated protein, plasminogen and the two inhibitors of the serine proteinase inhibitor superfamily, plasminogen activator inhibitor-1 and -2. This system is important for wound healing, tissue regeneration, immune response and multiple aspects of neoplastic progression including cell adhesion, ECM degradation and remodeling, migration, metastasis, growth at secondary tumor site and neoangiogenesis [for reviews, see (Choong and Nadesapillai, 2003; Duffy, 2004; Ulisse et al., 2009)]. uPA is secreted as a zymogen or pro-uPA and binds to its receptor, uPAR, on the cell surface. Pro-uPA is processed to an active two-chain form consisting of the uPAR binding A chain and catalytically active B-chain (Robison and Collen, 1987; Gurewich, 2000). Biological activity of

uPA is highly dependent on its binding to uPAR. However, uPA-mediated activation of plasmin and MMPs occurs in uPAR-deficient mice (Carmeliet et al., 1998). uPAR-independent effects of uPA also include mitogenic stimulation of quiescent melanoma cells (Koopman et al., 1998). Proteolytic cleavage of plasminogen, the primary substrate of uPA, generates the serine protease plasmin (Rickli, 1975), which in turn activates uPA, creating a feedback activation loop between these proteases. The key physiological role of plasmin is fibrinolysis (Robison and Collen, 1987), but it also degrades ECM components and activates MMPs in processes of angiogenesis and metastasis (Pepper, 2001; Rabbani and Mazar, 2001).

The plasminogen activation system is directly involved in metastatic spread and reduced patient survival in breast cancer [for review, see (Han et al., 2005). More than 20 years ago uPA was first suggested as a marker of aggressive breast cancer (Duffy et al., 1988). Since then many studies have corroborated that uPA and uPAR are highly expressed in breast cancer patient samples and are predictive of poor outcome (Grondahl-Hansen et al., 1995; Grondahl-Hansen et al., 1997; Foekens et al., 2000). Plasminogen activation and cell surface binding is regulated by uPA in breast cancer cells of high invasive potential (Stillfried et al., 2007). In this study, the authors suggest that uPA is a therapeutic target for the treatment of aggressive breast cancer. In addition to malignant epithelial breast tissue, the plasminogen activation system is also associated with stromal components of the tumor microenvironment, such

as macrophages (Pyke et al., 1993), myofibroblasts (Nielsen et al., 1996) and endothelial cells (Nielsen et al., 2001). MMTV-PymT transgenic mice deficient in either uPA or plasminogen exhibit reductions in tumor cell spread to lymph nodes and decreased lung metastasis (Bugge et al., 1998; Almholt et al., 2005).

Significance and Overall Hypothesis. My focus was to identify factors that cause the aggressiveness and progression of IBC. Caveolae at the surface of IBC cells may be involved in initiation of proteolytic pathways as a result of the convergence of the plasminogen cascade with activation of the cysteine protease cathepsin B. My overall hypothesis was that cell surface association of the cysteine protease cathepsin B, the serine proteases of the plasminogen cascade and their binding partners in caveolae enhance cell surface proteolysis, and ultimately, the aggressiveness of IBC cells. To test this hypothesis, I proposed the following Specific Aims:

1: Determine whether there is active cathepsin B at the surface of IBC cells. Breast cancer invasion has been linked to proteolytic activity at the tumor cell surface. My working hypothesis is that active cathepsin B localized to specialized regions of the cell surface, caveolae, contributes to the aggressive IBC phenotype. We tested this hypothesis by treating IBC cells with a highly selective cell impermeable cathepsin B inhibitor and monitoring pericellular proteolysis by and invasion of IBC cells.

2: Determine whether targeting caveolae, a specialized lipid raft, by knockdown of the expression of caveolin-1 in IBC cells alters their aggressive phenotype. My working hypothesis is that caveolae are a functional component of the IBC phenotype. We tested this hypothesis by knocking down the expression of caveolin-1 in the SUM149 IBC cell line. We assessed how downregulation of caveolin-1 affected degradation of ECM proteins, invasion through rBM and localization of proteins, including those of proteolytic pathways that are associated with caveolae in other cancer cells.

3: Determine whether targeting lipid rafts by treating IBC cells with lovastatin alters their aggressive phenotype. My working hypothesis is that lipid rafts are a functional component of the IBC phenotype. Therefore, cholesterol depletion by treatment of IBC cells with a statin drug (i.e., lovastatin) through the disruption of lipid microdomains, including caveolae, will affect the IBC phenotype. We tested this hypothesis by treating IBC cell lines with lovastatin and monitored degradation of ECM proteins, invasion through rBM and localization of proteins, including those of proteolytic pathways that are associated with caveolae in other cancer cells.

CHAPTER 2

MATERIALS AND METHODS

Materials and Reagents. *Tissue culture media and supplements:* Ham's F-12 medium was purchased from Mediatech (Manassas, VA); insulin, hydrocortisone, ethanolamine, HEPES, 3,3′,5-triiodo-L-thyronine sodium salt, sodium selenite, bovine serum albumin and antibiotics (penicillin/streptomycin) from Sigma (St. Louis, MO); fetal bovine serum (FBS) from HyClone (Logan, UT); trypsin-EDTA from GIBCO (Grand Island, NY); and the reconstituted basement membrane Cultrex from Trevigen (Gaithersburg, MD). *Antibodies:* Monoclonal antibodies: β1-integrin was a kind gift from Dr. Kenneth Yamada (National Institute of Dental and Craniofacial Research, National Institutes of Health, Bethesda, MD); uPA and uPAR from American Diagnostica Inc. (Stamford, CT); transferrin receptor from Invitrogen (Carlsbad, CA); β-tubulin from the Developmental Studies Hybridoma Bank (National Institute of Child Health and Human Development, University of Iowa, Iowa City, IA); and p36 and p11 from BD Biosciences (Bedford, MA). Polyclonal antibodies: uPA and uPAR were purchased from Abcam (Cambridge, MA) and caveolin-1 from BD Biosciences. The polyclonal antibody to cathepsin B was developed and characterized in our laboratory (Moin et al., 1992). Horseradish-peroxidase-labeled goat anti-mouse and goat anti-rabbit IgG secondary antibodies were from Pierce (Rockford, IL). The anti-rabbit Alexa Fluor 488 and donkey anti-mouse

Alexa Fluor 555 were from Invitrogen. *Other:* Normal donkey serum, saponin, doxycycline, Triton X-100, octylglucoside, dimethyl sulfoxide (DMSO), puromycin, hexadimethrine bromide (polybrene), filipin III, lovastatin and all other chemicals unless otherwise stated were from Sigma; (3-(4,5-Dimethylthiazol-2-yl)-2,5-diphenyltetrazolium bromide (MTT), 4',6-diamidino-2-phenylindole-dihydrochloride (DAPI), Hoechst 33342 and DQ-collagen IV were from Invitrogen; benzyloxy-carbonyl-L-arginyl-L-arginine-4-methyl-7-coumarylamide (Z-Arg-Arg-NHMec) was from Bachem (Torrance, CA); the cathepsin B inhibitor, N-(l-3-trans-propyl-carbamoyloxir-ane-2-carbonyl)-L-isoleucyl-L-proline (CA074), was from Peptides International (Louisville, KY); formaldehyde from Polysciences, Inc. (Warrington, PA); acrylamide and nitrocellulose membranes were from BioRad (Hercules, CA); Ultrafree-0.5 PBGC Centrifugal Filter Units with 5 kDa molecular weight cut off Biomax Membranes (Millipore, Billerica, MA); micro-bicinchoninic acid (BCA) reagents were from Pierce (Rockford, IL); enhanced chemiluminescent immunoblotting detection kit was from PerkinElmer (Waltham, MA); OpenBiosystems TRIPZ shRNAmir Lentiviral Packaging system and Non-silencing TRIPZ Lentiviral Inducible shRNAmir control particles were from Open Biosystems, Thermo Fisher Scientific (Huntsville, AL); 8.0 μm transparent PET membranes from BD Biosciences (Franklin Lakes, NJ); DakoCytomation EnVision + Dual Link System-HRP (DAB +) were from Dako (Carpinteria, CA); Permount® from Fisher Scientific (Pittsburgh, PA); and Diff-Quik Stain Set was from Dade Behring (Newark, DE).

Cell Lines and Tissue Culture. SUM149 and SUM190 human IBC cell lines (a kind gift of Dr. Stephen Ethier, Wayne State University, Detroit, MI) and the human IBC cell line, MDA-IBC-3 (provided by Dr. Wendy A. Woodward, The University of Texas MD Anderson Cancer Center, Houston, TX), were cultured as originally specified (Neve et al., 2006; Klopp et al., 2010) in Hams F-12 media containing 5 mg/ml insulin, 1 mg/ml hydrocortisone, antibiotics (penicillin/streptomycin) and 5% (SUM149), 2% (SUM190) or 10% (MDA-IBC-3) FBS. Media for SUM190 cells were further supplemented with 5 mM ethanolamine, 10 mM HEPES, 5 mg/ml transferrin, 6.6 ng/ml 3,3′,5-triiodo-L-thyronine sodium salt, 8.7 ng/ml sodium selenite and 1 mg/ml bovine serum albumin. All cells were maintained in 5% CO_2/humidified atmosphere at 37°C with the media changed every two days.

All IBC cell lines were maintained and grown as a monolayer in tissue culture flasks. During log phase growth, cells were first washed twice with phosphate buffered saline (PBS). For dissociation of cells from the culture flask, 0.25% trypsin-EDTA was added and cells were incubated at 37°C for either 2 minutes (SUM190 and MDA-IBC-3 cells) or 4 minutes (SUM149 cells). The cells were then washed with 4 volumes of growth medium, transferred to a 15-ml conical tube and centrifuged at 100 x *g* for 5 min. The media were aspirated and the cell pellet resuspended in an appropriate amount of fresh growth media. Cells were seeded in a new tissue culture flask. IBC cells were typically split at a ratio of 1:3.

Preparation of cell lysates and conditioned media. IBC cells were grown on plastic to 70% confluency and then serum-starved overnight. Conditioned media were collected and centrifuged at 100 x *g* at 4 °C to remove whole cells, and then re-centrifuged at 800 x *g* at 4 °C to remove cell debris. All conditioned media samples were concentrated to equal volumes in Ultrafree-0.5 PBGC Centrifugal Filter Units with 5 kDa molecular weight cut-off Biomax Membranes. Cells were harvested in lysis buffer (10 mM Tris, pH 7.5, 150 mM NaCl, 1% Triton X-100, 60 mM octylglucoside) and then passed ten times through a syringe with a 20-gauge needle and centrifuged for 5 minutes at 10,000 x *g* at 4°C. Supernatants were recovered and protein concentrations were quantified using micro-BCA reagents according to the manufacturer's instructions.

Preparation of 3D reconstituted basement membrane (rBM) overlay cultures. Sixty-mm dishes were coated with 300 μl of rBM (Cultrex) and allowed to solidify for 15 min at 37 °C. Suspensions of single cells (1 x 10^6) were seeded on top of solidified rBM and grown in complete media containing 2% rBM. Within 24 hours, cells formed 3D spheroid structures.

Subcellular fractionation. Non-detergent and detergent based protocols were used to prepare caveolae-enriched membrane fractions of IBC cells (Cavallo-Medved et al., 2009). In the non-detergent based method, cells grown

as a 2-dimensional (2D) monolayer on plastic (4 x 100-mm dishes) and in 3-dimensions (3D) on rBM (4 x 60-mm dishes) for 2 and 5 days, respectively, were washed with PBS and collected into 500 mM sodium carbonate buffer, pH 11.0. Cells were homogenized in a Dounce homogenizer on ice and sonicated three times for 10 seconds each. A discontinuous sucrose gradient was prepared as previously detailed (Cavallo-Medved et al., 2009). Briefly, the cell homogenate was mixed thoroughly with an equal volume of 90% (w/v) sucrose, then overlaid with 35% (w/v) sucrose and 5% (w/v) sucrose and subsequently centrifuged (185,000 x *g*) for 19 hours at 4 °C. One ml fractions were collected and equal volumes of fractions 3-11 were analyzed by SDS-PAGE and immunoblotting (Figure 2.1).

A successive detergent based method of cell fractionation was also employed to separate Triton X-100-soluble (TS) and –insoluble (TI) membrane fractions (Solomon et al., 1998). 3D cultures were prepared and grown, as described above, for 2 days and thereafter washed with cold PBS, incubated with 300 μl of lysis buffer containing 1% Triton X-100 for 20 minutes on ice, and collected and centrifuged at 14,000 x *g* for 10 min at 4 °C. The supernatant (TS fraction) was collected and the pellet was resuspended in 300 μl of lysis buffer containing 1% Triton X-100 plus 60 mM octylglucoside, incubated on ice for 20 minutes, passed through a syringe with a 21.5-gauge needle and centrifuged at 14,000 x *g* for 10 min at 4 °C. The supernatant (TI fraction) was recovered (Figure 2.2.).

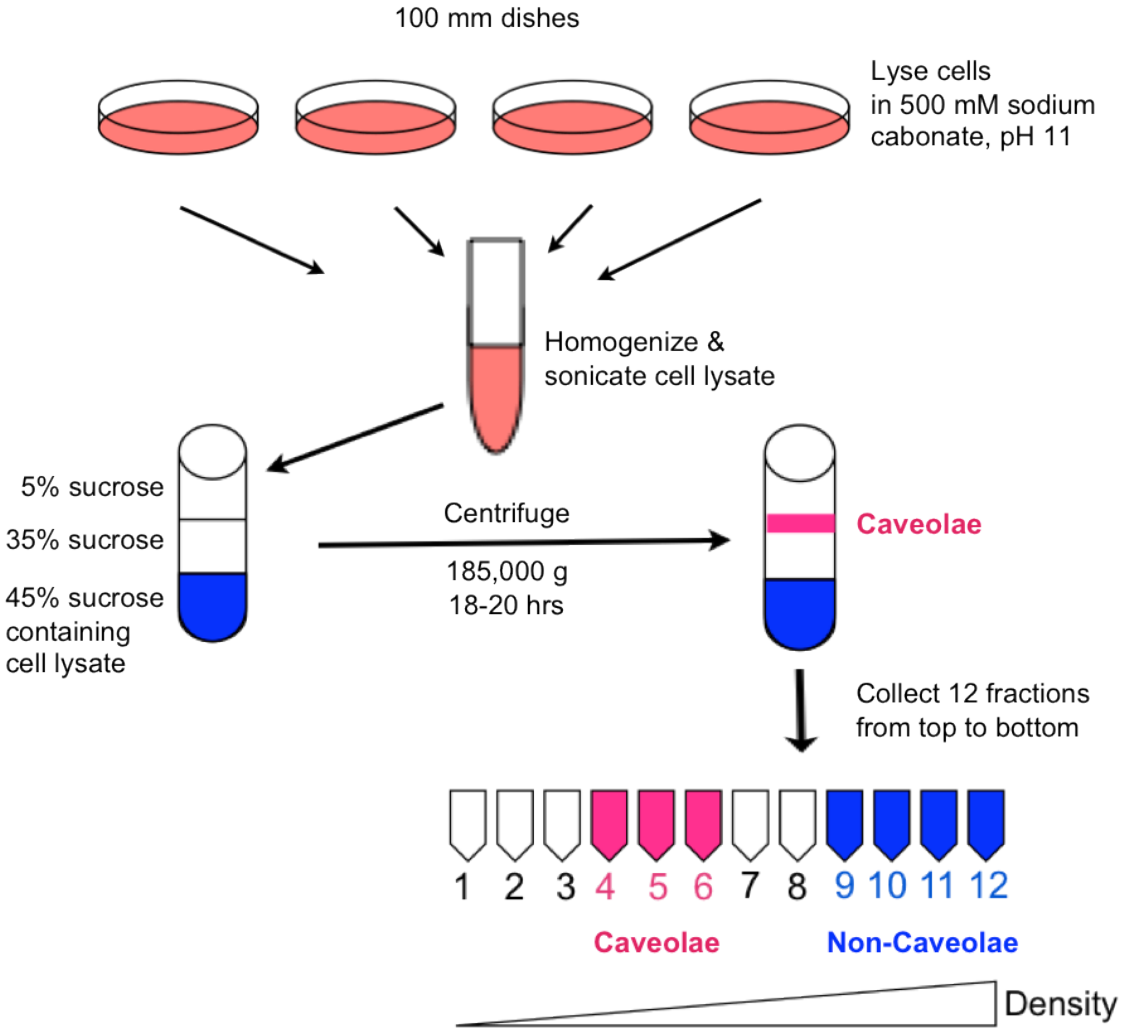

Figure 2.1. Schematic for isolation of caveolae enriched fractions from IBC cells, using non-detergent based lysis followed by subcellular fractionation on a sucrose gradient.

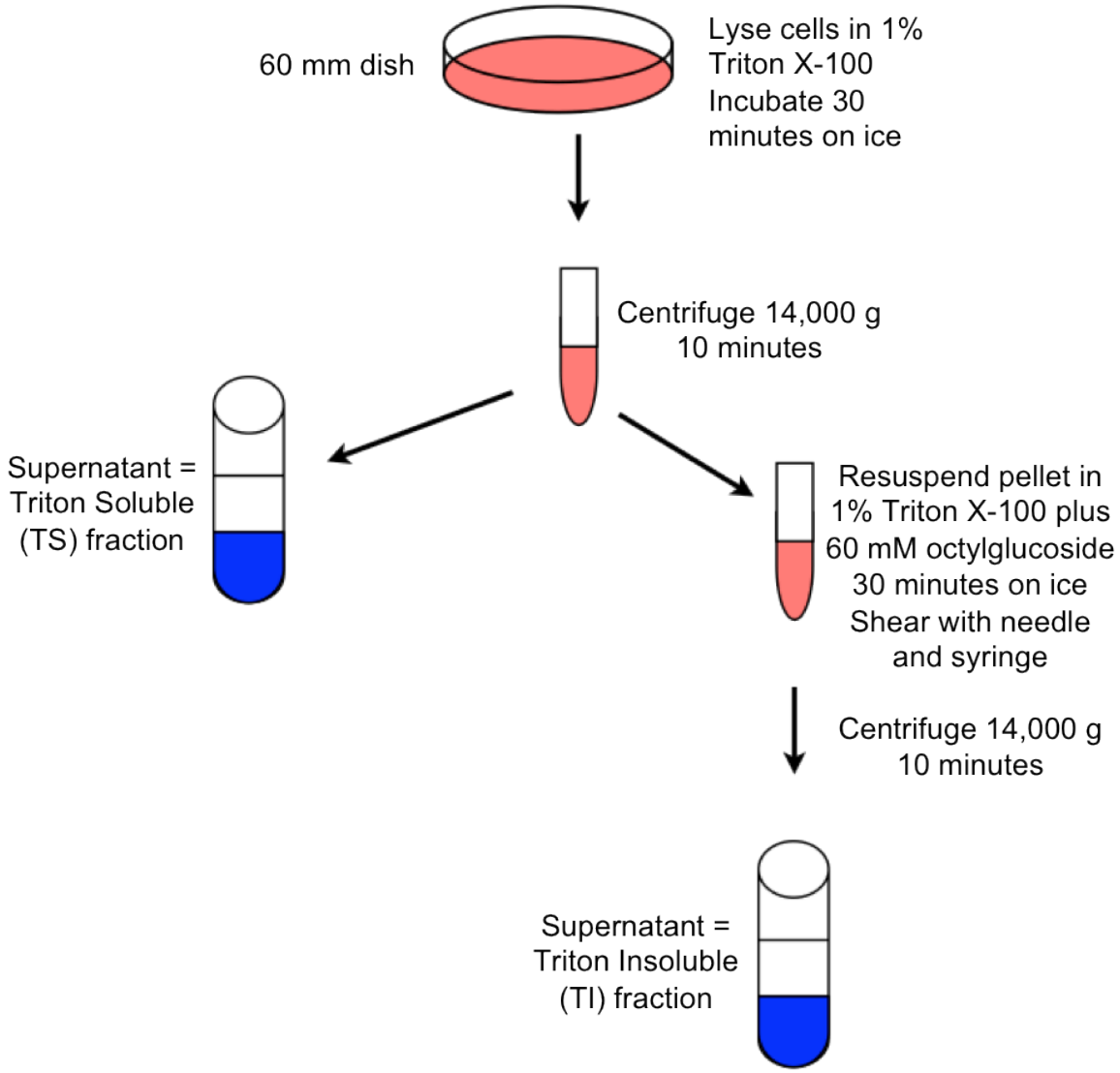

Figure 2.2. Schematic for isolation of caveolae-enriched fractions from IBC cells, using detergent based lysis followed by subcellular fractionation.

SDS-PAGE and immunoblotting. Samples were equally loaded and separated by SDS-PAGE (10 or 12%) under either reducing or non-reducing conditions, transferred to a nitrocellulose membrane, blocked and immunoblotted with primary antibodies against human cathepsin B (1:4000), β1-integrin (1:3000), uPA (1:2000), uPAR (1:2000), caveolin-1 (1:4000) or β-tubulin (1:1500) in TBS buffer (20 mM Tris, pH 7.5, 0.5 M NaCl) containing 0.5% Tween 20 and 5% (w/v) non-fat dry milk. After washing, membranes were immunoblotted with secondary antibodies conjugated with horseradish peroxidase (1:10,000). After washing, bound antibodies were detected by enhanced chemiluminescence according to the manufacturer's instructions.

Cathepsin B activity assay. Cathepsin B activity was measured using the synthetic fluorometric substrate Z-Arg-Arg-NHMec, as previously described (Cavallo-Medved et al., 2003). Briefly, equal-volume aliquots of TS and TI fractions were incubated with activator buffer for 15 minutes at 37 °C. Following this activation step, 150 mM Z-Arg-Arg-NHMec (pH 6.0) was added to the assay buffer and fluorescence was measured in triplicate, at one-minute intervals over a 30 minutes period, at an excitation of 360 nm and an emission of 465 nm.

Live-cell proteolysis assay. Proteolytic cleavage of DQ-collagen IV by live IBC cells was imaged in real time and quantified, as previously described (Jedeszko et al., 2008; Sameni et al., 2009). Briefly, IBC cells (2.5×10^4) were

seeded on round glass coverslips coated with rBM containing 25 mg/ml DQ-collagen IV substrate and incubated at 37 °C for 40 minutes to allow for cell attachment. Complete media containing 2% rBM was then added to the cultures and grown for 24 to 48 hours. Live cells were pretreated with Hoechst 33342 nucleic acid stain and imaged with a Zeiss LSM 510 META NLO confocal microscope, equipped with an incubator (37 °C and 5% CO_2) surrounding the microscope stage, using a 40X Plan neofluar (N.A., 0.7) objective. DQ-collagen IV cleavage products were observed as green fluorescence (Figure 2.3). Where specified, the assay was performed in the presence of 10 mM CA074, a highly selective cathepsin B inhibitor (Murata et al., 1991).

Invasion assay. Cell culture inserts [8.0 µm transparent PET membranes], were coated with 2 mg/ml rBM and incubated in a 24-well plate at room temperature to permit rBM solidification. Complete media, the stimulant for invasion, was added to the bottom of each well. SUM149 cells (5.0×10^4) in serum-free media were seeded onto the rBM-coated inserts and incubated for 24 h at 37 °C in the presence of DMSO (vehicle control) or 10 µM CA074. Cells that had not invaded were removed with a cotton swab. Cells that had invaded were fixed with 3.7% formaldehyde, stained with DAPI and imaged at 20X magnification with a Zeiss Axiophot conventional epifluorescent microscope. Ten random microscopic fields per filter were analyzed. The number of cells that

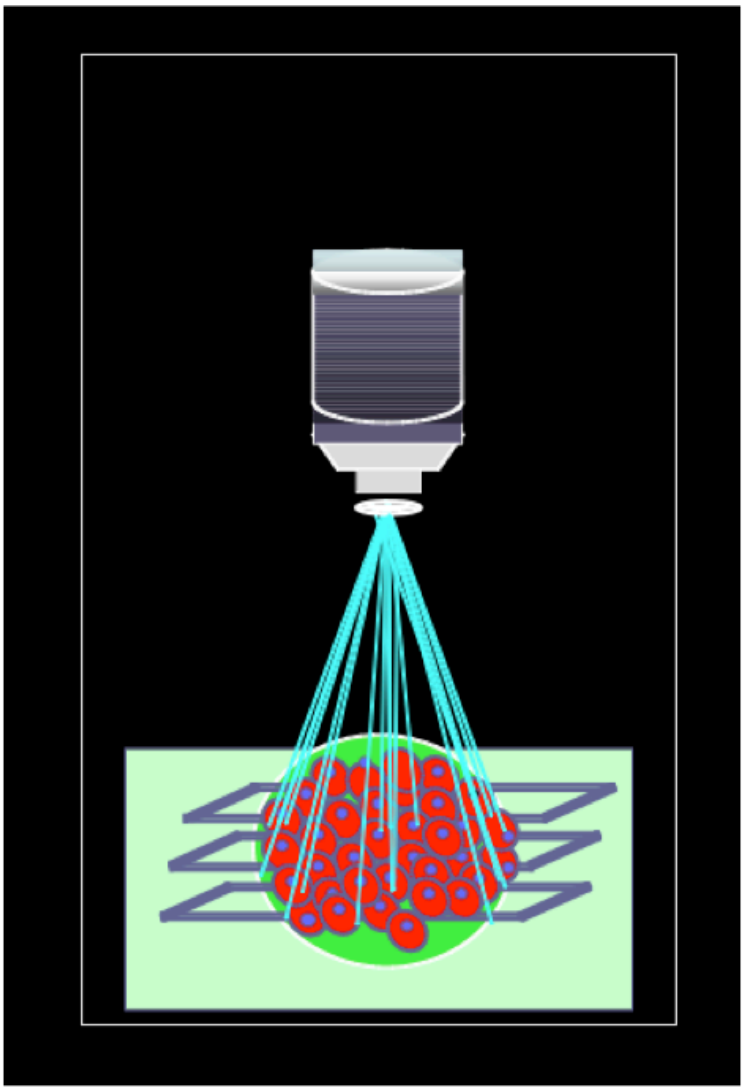

Figure 2.3. Cartoon depicting imaging of live cell proteolysis by confocal microscopy. IBC cells are grown in rBM containing DQ-collagen IV. Using a water-immersion dipping objective, optical sections as depicted by the gray rectangles are acquired throughout the entire volume of the 3D cellular structures.

invaded was assessed by counting nuclei with MetaMorph™ image analysis software (Molecular Devices, Sunnyvile, CA).

Immunocytochemical staining. Intracellular co-staining was performed at room temperature on 2D (permeabilized with 0.1 % saponin) and 3D cultures (permeabilized with 0.2% Triton X-100). In our experience, Triton X-100, a mild detergent, is better than saponin for permeabilizing cells grown in 3D cultures. The cultures were fixed with 3.7% formaldehyde and incubated with the following primary antibodies diluted in 0.2% Triton X-100/PBS: rabbit anti-caveolin-1 (1:50), mouse anti-uPA (1:25), and mouse anti-uPAR (1:12.5). Secondary antibodies [donkey anti-rabbit Alexa Fluor 488 and donkey anti-mouse Alexa Fluor 555] were diluted (1:5000) in 0.2% Triton X-100/PBS plus 5% normal donkey serum. All immunocytochemical staining was imaged on a Zeiss LSM 510 META NLO confocal microscope using either a 100X oil Plan neofluar (N.A., 1.3) objective (2D cultures) or 40X Plan apofluar (N.A., 0.7) objective (3D cultures).

Immunohistochemical (IHC) staining of patient samples. Institutional review board approval from Ain Shams University ethics committee and the National Cancer Institute, Cairo University along with patient consent forms were obtained for the purpose of patient enrollment in this study. Inclusion criteria for patients included clinical, mammographic, ultrasound and pathological diagnosis

according to the American Joint Committee on Cancer T4 d designation for IBC (Dawood et al., 2011). Pre-treated formalin fixed paraffin embedded IBC (*n* = 23) and non-IBC (stage II-III, *n* = 27) patient tissue samples were subjected to IHC analysis (Nouh et al., 2011). Briefly, tissue sections were incubated for one hour at room temperature with either monoclonal anti-caveolin-1 (1:150) or polyclonal anti-cathepsin B (1:500) primary antibodies. A second incubation was performed with HRP rabbit/mouse [EnVision + Dual Link System-HRP (DAB +)] for 45 minutes. Nuclei were counterstained with hematoxylin, sections were mounted with Permount® and imaged with an Olympus, CX41 light microscope. Patient's pathological evaluation, IHC and scoring analysis were done in collaboration with a group at Cairo University. We performed the statistical analysis for this study.

MTT proliferation assay. IBC cells were seeded (5,000 per well) in 96-well plates and cultured overnight. On day one, cells were treated with 3 μM lovastatin or vehicle (DMSO) containing 200 μl of growth media and cultured for 24, 48 and 72 h. Fifty microliters of MTT stock solution (5 mg/ml) was added to each well and incubated for 3 h at 37 °C allowing the production of formazan by living cells. The media was subsequently removed and 150 μl of DMSO was added to each well and plates were placed on a shaker to dissolve the formazan for 40 minutes at room temperature. Absorbance values were measured in triplicate at a 485 nm wavelength using a SpectraFluor Plus (Teccan, Salzburg, Austria).

Filipin III staining. Cells grown in monolayer on round glass coverslips and treated for 24 h with 3 μM lovastatin or vehicle were washed 3 times with PBS. Cells were fixed with 3.7% formaldehyde solution for 15 minutes at room temperature. After washing, the fixed cells were incubated with Filipin III (stock solution of 5 mg/ml diluted 1:150 in 4% bovine serum albumin/PBS) for 2 hours. Stained cells were imaged on a Zeiss LSM 510 META NLO confocal microscope using a 63X oil Plan neofluar (N.A., 1.3) objective.

Lentiviral Transduction of SUM149 cells. Knockdown of caveolin-1 gene expression was carried out using the OpenBiosystems TRIPZ shRNAmir Lentiviral Packaging system. For lentivirus production, HEK293T (Open Biosystems) cells were cultured in Dulbecco's modified Eagles medium containing 10% FBS without antibiotics in 35-mm dishes to 100% confluence. The cells were then transfected with 5.7 μg of TransLenti Viral Packaging Mix (pTLA1-Pak, pTLA1-Enz, pTLA1-Env, PTLA1-Rev and pTLA1-TOFF) and 1.8 μg of each pTRIPZ CAV1 shRNA transfer vector with 37.5 μg of Arrest-In transfection reagent. HEK293T cells were incubated for 6 hours at 37 °C and 5% CO_2 and the medium was changed to fresh culture medium without antibiotics and placed in an incubator set at 32 °C and 5% CO_2 for 24 hours to produce viruses. Subsequently the viral broth was harvested and centrifuged at 1000 rpm for 5 minutes. SUM149 cells (25,000 per well) were seeded in a 12-well plate, treated with 6 μg/ml polybrene and infected with virus collected from HEK293T

cells 24, 48 and 72 h post-transfection for 3 rounds of infection. Media was then changed to complete growth medium of SUM149 cells containing 1 μg/ml puromycin and 500 ng/ml doxycycline.

Statistical Analysis. A two-tailed, assuming equal variance, Student's t-test was executed to determine the statistical significance of differences in live cell proteolysis and invasion assays. *P* values for the relationship between cathepsin B expressing breast carcinoma cells, of both IBC and non-IBC, and caveolin-1 protein expression were assessed with a chi-square test.

CHAPTER 3

RESULTS

Caveolin-1, β1-integrin and uPAR expression are higher in SUM149 than in SUM190 cells. Caveolin-1 and β1-integrin form a trimeric complex with uPAR within caveolae (Schwab et al., 2001), a complex that mediates cell adhesion and migration. Therefore, we compared expression of caveolin-1 and β1-integrin in SUM149 and SUM190 cells. There was a striking dissimilarity in levels of the two proteins (Figure 3.1A), The cell surface receptor for uPA is uPAR (Vassalli et al., 1985; Cubellis et al., 1986), a GPI-anchored membrane glycoprotein that has been localized to caveolae in a wide variety of cells (Wei et al., 1999; Schwab et al., 2001; Cavallo-Medved et al., 2005). We found that SUM149 cells expressed more receptor than did SUM190 cells (Figure 3.1A), paralleling the difference in expression of caveolin-1 and β1-integrin. These data suggest that pericellular proteolysis by the two cell lines may not be the same due to the observed differences in cav-1, uPAR and β1-integrin expression and thus the potential to localize pro-uPA and a caveolae-associated protease known to activate pro-uPA, i.e., cathepsin B, at the cell surface.

Cathepsin B and uPA expression and secretion are similar in SUM149 and SUM190 cells. Cathepsin B has been linked to both pericellular and intracellular proteolysis in breast cancer cells (Sameni et al., 2000). Our

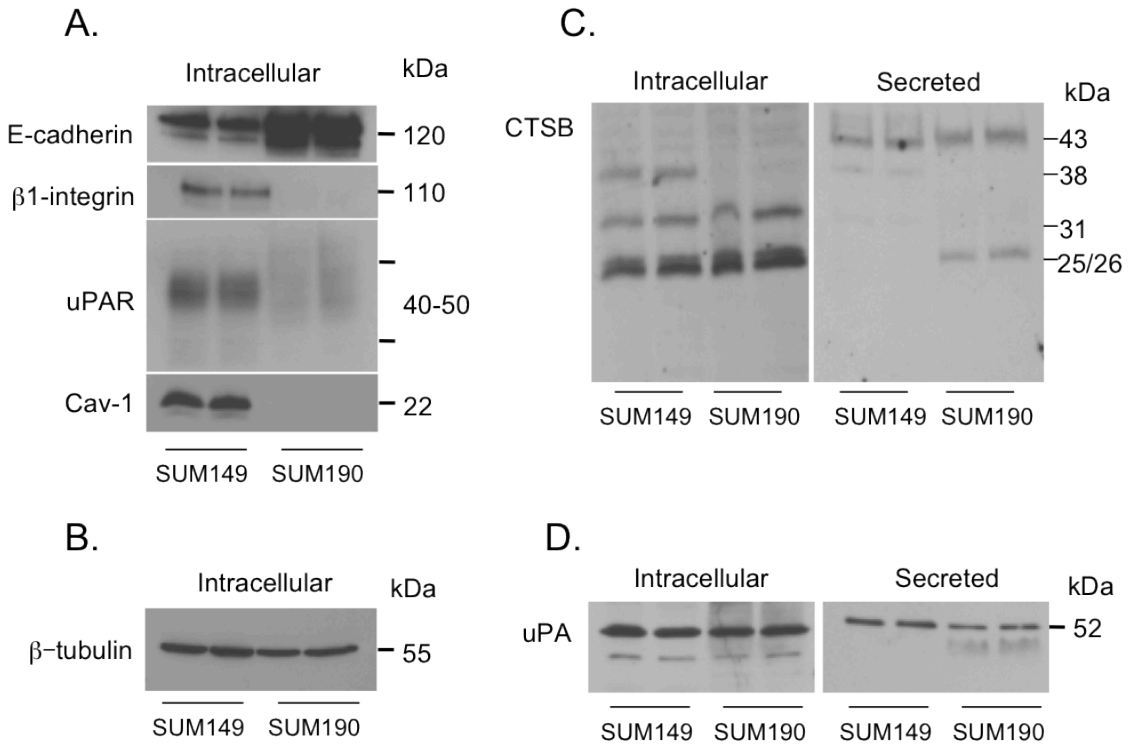

Figure 3.1. Expression of cathepsin B, uPA, uPAR, β1-integrin and caveolin-1 in SUM149 and SUM190 IBC cells. Duplicate samples of cell lysates (intracellular) and conditioned media (secreted) from 2D cultures of SUM149 and SUM190 cells were resolved by SDS-PAGE. Proteins were transferred to a nitrocellulose membrane and immunoblotted with (A) anti-E cadherin, anti-uPAR, anti-β1-integrin, anti-caveolin-1 (cav-1) antibodies; (B) anti-β-tubulin antibody as a loading control; (C) an anti-cathepsin B (CTSB) antibody [bands represent proform (43 kDa), intermediate (38 kDa), single chain mature (31 kDa), and heavy chain of double chain mature (25/26 kDa) cathepsin B] and (D) an anti-uPA antibody.

previous *in vitro* findings demonstrate that monocytes, an inflammatory component associated with IBC, stimulate the invasive potential and degradation of ECM proteins by SUM149 IBC cells (Mohamed et al., 2008). These results correlate with increased cathepsin B expression and activity in the SUM149 cells. Recent *in vivo* studies have also identified cathepsin B as a potential prognostic marker for IBC (Nouh et al., 2011). Here we examined two IBC cell lines, SUM149 and SUM190, for expression of cathepsin B protein. We found that the two cell lines express comparable levels of the mature single chain (31 kDa) and double chain (25/26 kDa heavy chain + 5 kDa light chain) forms of cathepsin B in cell lysates and secrete comparable levels of procathepsin B (43 kDa) into the media (Figure 3.1C). A 38 kDa intermediate form of the enzyme was present only in lysates of the SUM149 cells and mature double chain cathepsin B was secreted only from SUM190 cells (Figure 3.1C); these differences between the two cell lines are likely due to variations in the extent of processing of the proenzyme into the various mature forms. We have observed similar differences in a variety of human tumor tissues (Moin et al., 1992). Since cathepsin B activates both soluble and cell surface bound pro-uPA (Kobayashi et al., 1991; Kobayashi et al., 1992; Kobayashi et al., 1993; Guo et al., 2002), we also compared the expression of uPA in the two IBC cell lines. Both expressed similar levels of intracellular pro-uPA; however, secretion of pro-uPA from the SUM149 cell line was slightly higher (Figure 3.1D).

IBC cells express E-cadherin. Normal epithelium is highly organized and exhibits polarity due largely to E-cadherin-mediated cell:cell interactions called adherens junctions. Deregulation of E-cadherin is a criterion for epithelial-mesenchymal transition (EMT), which often accompanies malignant initiation and progression (Hirohashi, 1998). Inactivation of adherens junctions in human cancer is mediated by genetic modification of adherens associated proteins, e.g., E-cadherin and catenins (Oda et al., 1994; Oyama et al., 1994), decreased expression of E-cadherin (Birchmeier and Behrens, 1994) and aberrant phosphorylation of β-catenin resulting in activation of cancer promoting signaling pathways (Schmalhofer et al., 2009). In addition, E-cadherin ectodomain shedding by proteases is an alternative mechanism of E-cadherin loss of function. For example, cathepsin B is capable of cleaving the extracellular domain of E-cadherin *in vitro and in vivo* [Roshy, doctoral thesis and (Gocheva et al., 2006)]. Generally, downregulation or complete loss of E-cadherin expression correlates with breast cancer that is invasive, higher grade and metastatic (Berx and Van Roy, 2001; Vincent-Salomon and Thiery, 2003). Elevated levels of E-cadherin are strongly associated with IBC (Kleer et al., 2001). In contrast, invasive ductal and lobular carcinomas exhibit significantly reduced expression of E-cadherin (Moll et al., 1993). Kleer and colleagues suggest that expression of E-cadherin may facilitate the formation of IBC tumor emboli after intravasation into lymphatic vessels *in vivo*. As expected, we found that both IBC cell lines expressed E-cadherin (Figure 3.1).

SUM149 and SUM190 cells exhibit different patterns of proteolysis of type IV collagen. We used a functional live-cell proteolysis assay to assess in real time degradation of DQ-collagen IV by SUM149 and SUM190 cells. DQ-collagen IV cleavage products (green fluorescence) were present in cultures of both cell lines; however, there were distinct differences in localization of the fluorescent cleavage products (Figure 3.2). Cleavage products were found adjacent to the external cell surface of the SUM149 cells, i.e., pericellularly. In contrast, in the SUM190 cells a distinct punctate fluorescence pattern was present intracellularly, consistent with the cleavage products being in vesicles. This may reflect proteolysis that occurs either intracellularly in the vesicles or extracellularly with the degradation fragments taken up into the vesicular compartment by endocytosis.

uPA and uPAR colocalize in caveolae-enriched fractions of SUM149 cells. Our laboratory utilizes two methods for purification of caveolae-enriched membranes, a non-detergent and a detergent based protocol. These methods are employed based on the biochemical properties of caveolae: they have a light buoyant density and are resistant to detergent solubilization. Since non-caveolae lipid rafts have similar characteristics, there is controversy over purification methods, however the sodium carbonate method is considered preferable (Song et al., 1996). Since expression levels of caveolin-1 and uPAR were high in SUM149 cells and we have previously shown that uPA and uPAR colocalize in

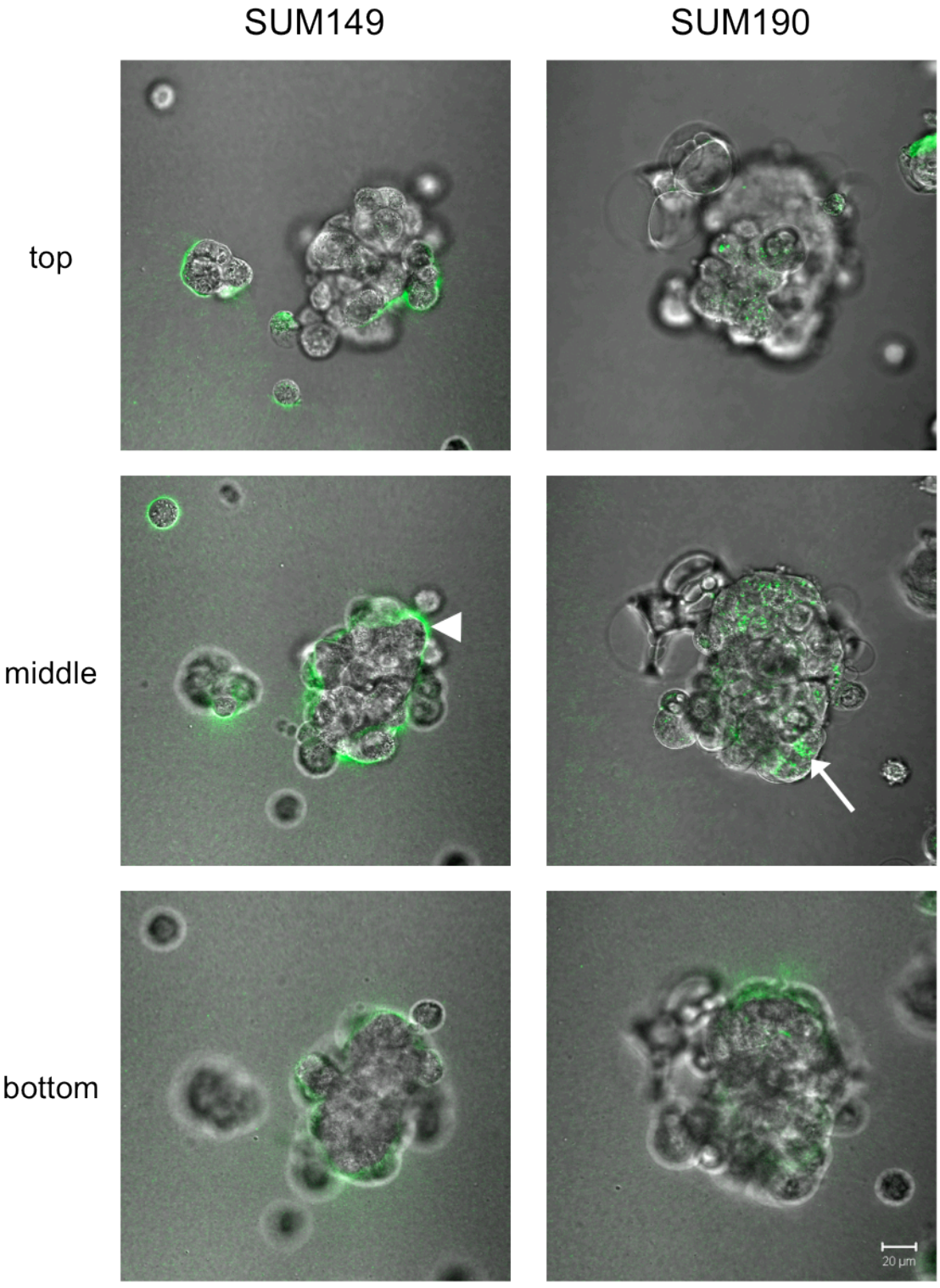
SUM149
SUM190
top
middle
bottom
20 µm

Figure 3.2. Live-cell proteolysis assay revealed disparate proteolytic patterns in 3D cultures of SUM149 and SUM190 cells. SUM149 and SUM190 cells were seeded onto glass-coverslips coated with rBM containing DQ-collagen IV. Following overnight incubation at 37 °C, cells and DQ-collagen IV cleavage products (green) were imaged using confocal microscopy (see Materials and Methods). Live SUM149 and SUM190 cells grown in 3D degraded DQ-collagen IV pericellularly (arrowhead) and predominantly intracellularly (arrow), respectively. Confocal Z stack images were reconstructed in 3D utilizing Volocity™ software (PerkinElmer, Waltham, MA). Representative merged images of DIC and green channels of the equatorial plane (middle) and two planes equidistant, 20 μm, from the equatorial plane (top and bottom) are also shown. Bar, 20 μm.

caveolar fractions of colorectal carcinoma cells (Cavallo-Medved et al., 2005), we isolated caveolae-enriched fractions from SUM149 cells. We used a method that employs a sodium carbonate buffer for cell lysis followed by subcellular fractionation in a sucrose density gradient (Cavallo-Medved et al., 2009). Analysis of caveolae-enriched fractions (i.e., fractions in which caveolin-1 was primarily distributed) revealed that uPA and its receptor uPAR were both present in these fractions (Figure 3.3A-B). This was observed for SUM149 cells grown either as 2D or 3D cultures. For cell fractionation studies, sufficient starting material is more readily obtained from 2D cultures. We prefer, however, to analyze 3D cultures as they more closely resemble the *in vivo* phenotype (Debnath and Brugge, 2005) and have been shown to be predictive of drug responses *in vivo* (Weigelt and Bissell, 2008; Li et al., 2010). In agreement with our fractionation studies, immunostaining of 2D (Figure 3.3C) and 3D (Figure 3.3D) cultures of SUM149 cells showed that uPA and uPAR colocalized with caveolin-1, consistent with a role for caveolin-1 in the distribution of these proteins to the cell surface.

Active cathepsin B is present in caveolae-enriched fractions of SUM149 cells. We have previously shown, using both detergent and non-detergent methods, that cathepsin B localizes to caveolae-enriched fractions of colon carcinoma and endothelial cells (Cavallo-Medved et al., 2003; Cavallo-Medved et al., 2005; Cavallo-Medved et al., 2009). Cathepsin B is denatured

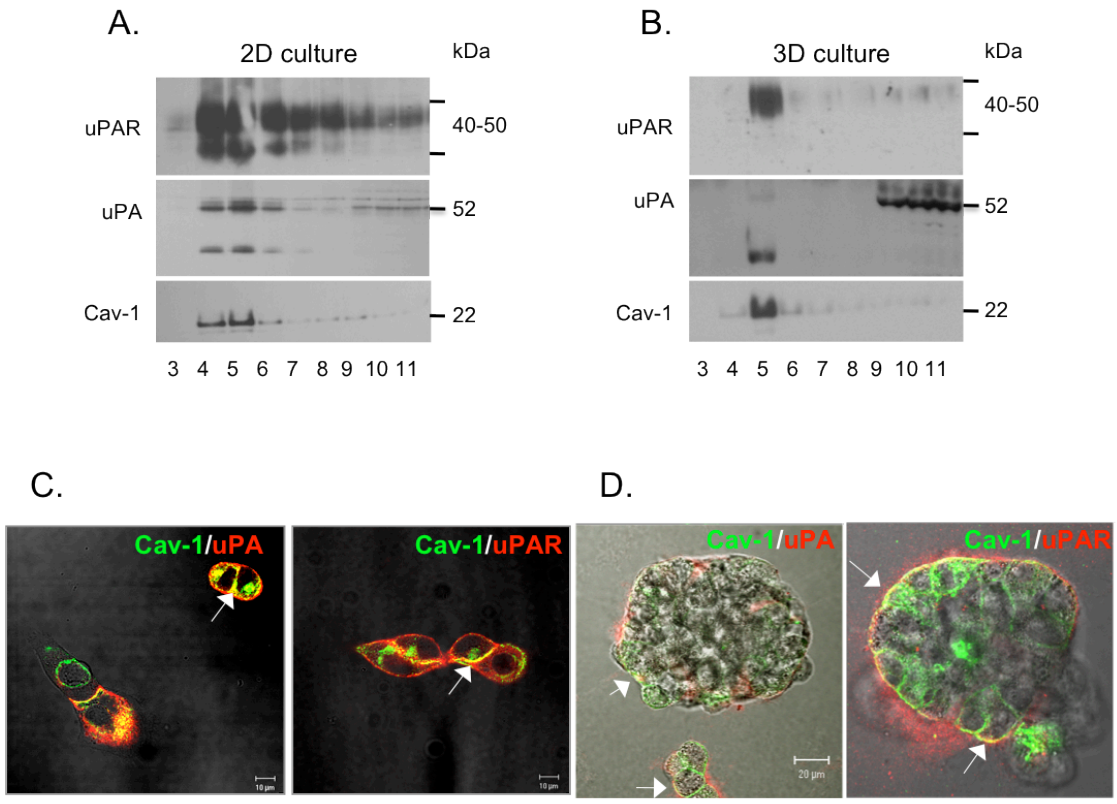

Figure 3.3. uPA and uPAR codistributed with caveolin-1 in subcellular fractions of SUM149 cells. Isolation of caveolae from SUM149 cells grown in 2D (A) or in 3D culture (B) was performed using a non-detergent method as described in Materials and Methods. Equal-volume aliquots of fractions 3-11 were analyzed by SDS-PAGE and immunoblotted with antibodies against uPA, uPAR or caveolin-1. Merged DIC and fluorescent images are representative images of SUM149 2D (C) or 3D (D) cultures immunostained for caveolin-1 (green) and uPA (red) or uPAR (red). Colocalization of the two proteins appears yellow (arrows). Confocal microscopy was performed as described in Materials and Methods. Bar, 10 μm for 2D cultures; 20 μm for 3D cultures.

and thus is inactive in the non-detergent based method as the cells are lysed in sodium carbonate buffer at pH 11. Therefore, to further assess localization of cathepsin B to caveolae-enriched fractions of SUM149 3D cultures, we utilized a detergent-based method that separates Triton X-100-soluble (TS) from –insoluble (TI) membrane components. Since caveolae are insoluble in 1% Triton X-100, the TI fraction contains caveolae and associated proteins and the TS fraction contains proteins from cellular components that are solubilized by the detergent including lysosomes. As expected more caveolin-1 was observed in the TI fraction than the TS fraction (Figure 3.4A). Caveolin-1 subcellular localization is not exclusive to caveolae, but is also present in the endoplasmic reticulum, Golgi and cytosolic where it is presumed to complex with chaperones or embedded in lipoprotein-like particles (Liu et al., 2002a). Mature forms of cathepsin B were present in the TI fractions (Figure 3.4A). Substantially higher levels of mature cathepsin B were present in the TS fractions containing lysosomes, the predominant subcellular localization of cathepsin B. Cathepsin B activity was observed in both TS and TI fractions (Figure 3.4B), at levels comparable to the levels of mature cathepsin B detected by immunoblotting (Figure 3.4A). The enzymatic activity in the isolated TS and TI fractions was completely abrogated by CA074, a highly selective inhibitor for cathepsin B (Murata et al., 1991). The presence of cathepsin B activity in the TI fractions might be consistent with a functional role for cathepsin B at the cell surface. We showed that uPA and uPAR colocalize to caveolae-enriched fractions using a

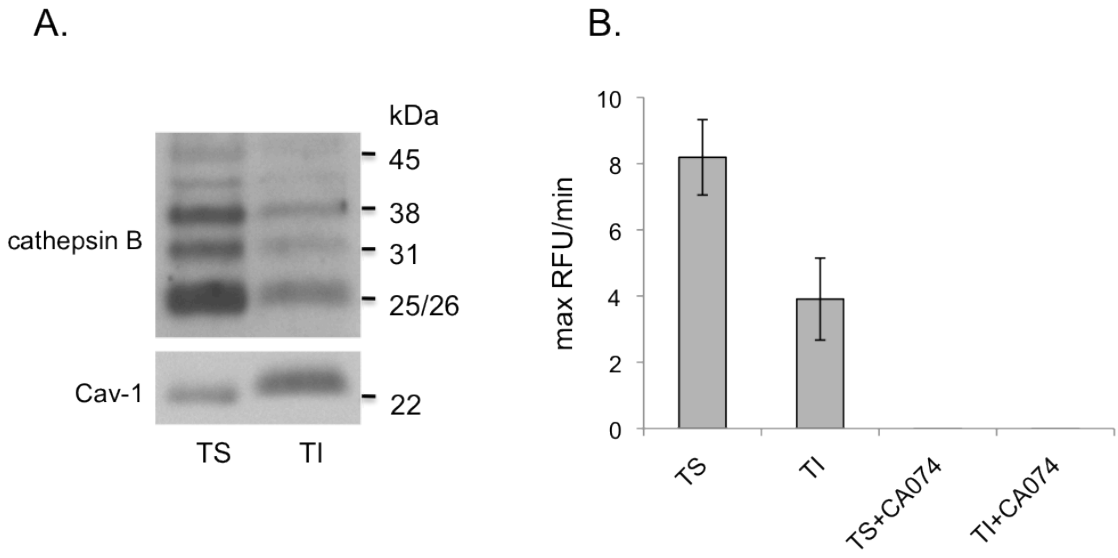

Figure 3.4. Active cathepsin B is present in caveolae-enriched fractions of SUM149 3D cultures. Caveolae from SUM149 3D cultures were isolated by a detergent-based method, as described in Materials and Methods, that separate Triton X-100-soluble (TS; non-caveolae) from Triton X-100–insoluble (TI; caveolae-enriched) cellular fractions. (A) Equal volume aliquots of each fraction were analyzed by SDS-PAGE and immunoblotted with antibodies against cathepsin B or caveolin-1. (B) TS and TI fractions were assayed for enzymatic activity against the synthetic cathepsin B substrate Z-Arg-Arg-NHMec. Cathepsin B activity in both TS and TI fractions was inhibited by 10 μM CA074.

non-detergent based sucrose fractionation method (Figure 3.3A-B) and obtained similar results by the detergent based method as well (Figure 3.5). In addition, we also observed E-cadherin and β1-integrin localized to TI fractions (Figure 3.5).

Our laboratory identified p11, the light chain of the annexin II tetramer, as a binding partner for procathepsin B *in vitro* (Mai et al., 2000). Procathepsin B via its interaction with the light chain of the annexin II tetramer is bound to the surface of tumor cells. Cathepsin B, p11, and p36 have all been identified in caveolae-enriched membrane fractions of the human colon carcinoma cell line HCT 116 (Cavallo-Medved et al., 2003). Using SUM149 cells, we were also able to show that p36 and p11, the cathepsin B binding partner, localized to caveolae-enriched fractions in these cells (Figure 3.5).

Inhibition of cathepsin B reduces type IV collagen degradation and invasion by IBC cells. The live-cell proteolysis assays indicated that SUM149 cells degrade DQ-collagen IV pericellularly. Our subcellular fractionation and enzymatic assays indicated that active cathepsin B is associated with caveolae-enriched fractions and therefore on the surface of SUM149 cells. Thus, we examined whether inhibiting cathepsin B would reduce pericellular degradation of DQ-collagen IV. For these cell-based assays, we used CA074, the highly selective cathepsin B inhibitor that is cell-impermeant (Murata et al., 1991) and thus would only reduce cathepsin B activity outside the SUM149 cells. We used

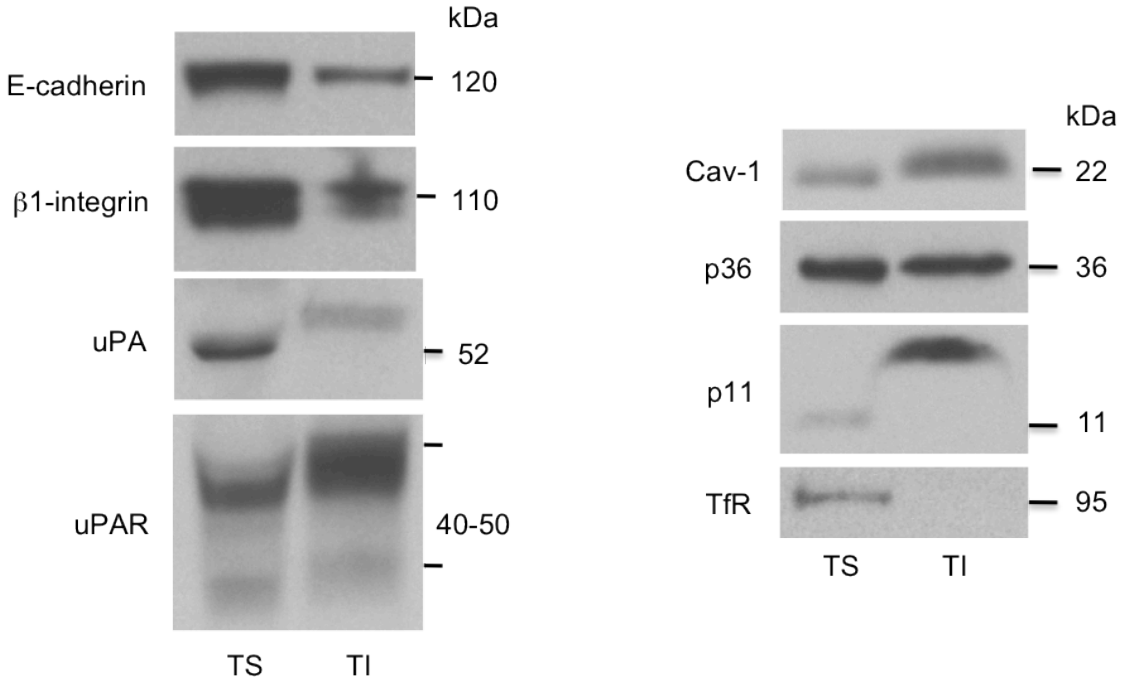

Figure 3.5. E-cadherin, β1-integrin, uPA, uPAR, p36 and p11 are localized to caveolae-enriched fractions of SUM149 3D cultures. Caveolae enriched fractions were isolated by a detergent based method that separates Triton X-100-soluble (TS) from –insoluble (TI) membrane components. TS indicates non-caveolae fractions and TI indicates caveolae-enriched fractions. Equal volumes of each fraction were analyzed by SDS-PAGE and immunoblotted with anti-E-cadherin, anti-β1-integrin, anti-uPA, anti-uPAR, anti-caveolin-1, anti-p36, anti-p11 and anti-transferrin receptor (TfR) antibodies. TfR is a negative control as it is not associated with lipid rafts.

our previously established methods to quantify degradation of DQ-collagen IV on a per cell basis throughout the entire volume of SUM149 3D cultures (Jedeszko et al., 2008). We demonstrated that CA074 significantly attenuated degradation of DQ-collagen IV (Figure 3.6) and invasion (Figure 3.7), suggesting that cathepsin B contributes to pericellular degradation and invasion by SUM149 cells.

Cathepsin B and caveolin-1 are co-expressed in IBC tissues in vivo. To determine whether there is an association between cathepsin B and caveolin-1 *in vivo,* we immunostained paraffin-embedded tissue samples from IBC and non-IBC patients for cathepsin B and caveolin-1. IBC patients in this study ranged in age from 29 to 60 years (mean ± SD = 41 ± 8); non-IBC patients ranged in age from 33 to 67 years (mean ± SD = 50 ± 9). Tumor grade analysis revealed that 65% and 78% of the IBC and non-IBC samples, respectively, were grade I or II and 35% and 22% of the IBC and non-IBC samples, respectively, were grade III. For further clinical and pathological characterization of the IBC and non-IBC samples, see Nouh et al. (Nouh et al., 2011). In the IBC tissues, we observed strong expression of cathepsin B in tumor cells and in tumor emboli within dermal lymphatics and moderate expression in stromal cells (Figure 3.8A and B). There was heterogeneous staining for caveolin-1 in tumor emboli (Figure 3.8C). Endothelial cells of dermal lymphatics containing tumor emboli stained strongly for caveolin-1, consistent with the known high levels of caveolae in

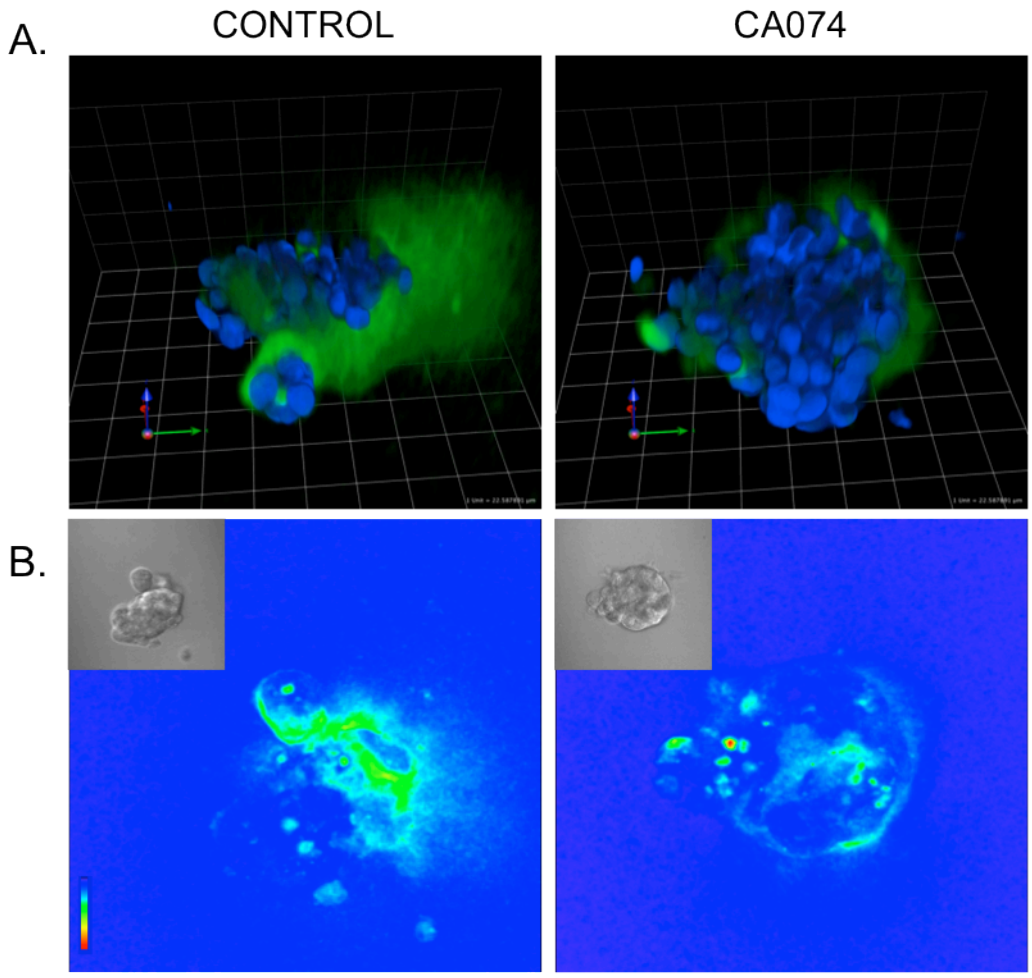
A.
CONTROL
CA074
B.

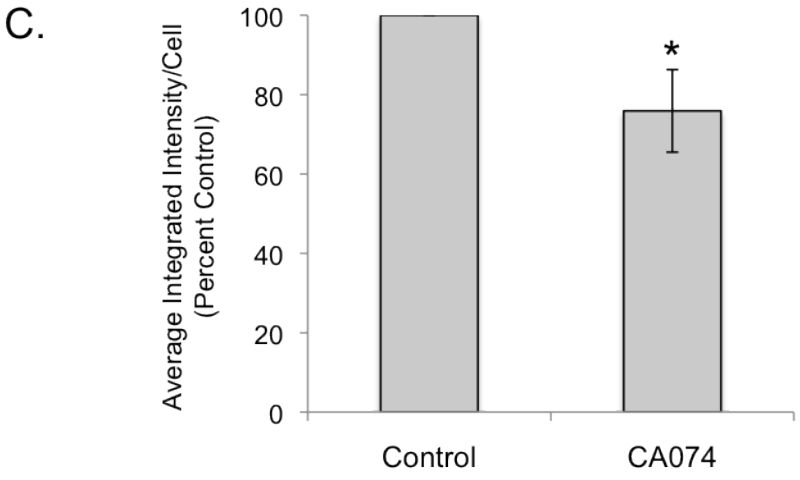
C.
Average Integrated Intensity/Cell
(Percent Control)
100
80
60
40
20
0
*
Control
CA074

Figure 3.6. Inhibition of cathepsin B activity modestly, but significantly, reduced degradation of DQ-collagen IV by SUM149 3D cultures. SUM149 cells were grown as 3D rBM overlay cultures containing DQ-collagen IV in the presence of either DMSO (control) or 10 μM CA074. Confocal Z stack images were captured and used to generate 3D reconstructions. (A) Representative 3D reconstructions of DQ-collagen IV degradation products (green), SUM149 nuclei (stained with Hoechst 33342, blue). (B) Corresponding intensity map (red being most intense and blue least intense) of DQ-collagen IV degradation products and corresponding DIC images (insets). Magnification, 40X. (C) Quantification of proteolysis in the entire volume of three-dimensional structures measured as the average integrated intensity of fluorescence per cell and expressed as percent control. Results from three independent experiments are presented as mean ± SD; *, $P < 0.02$.

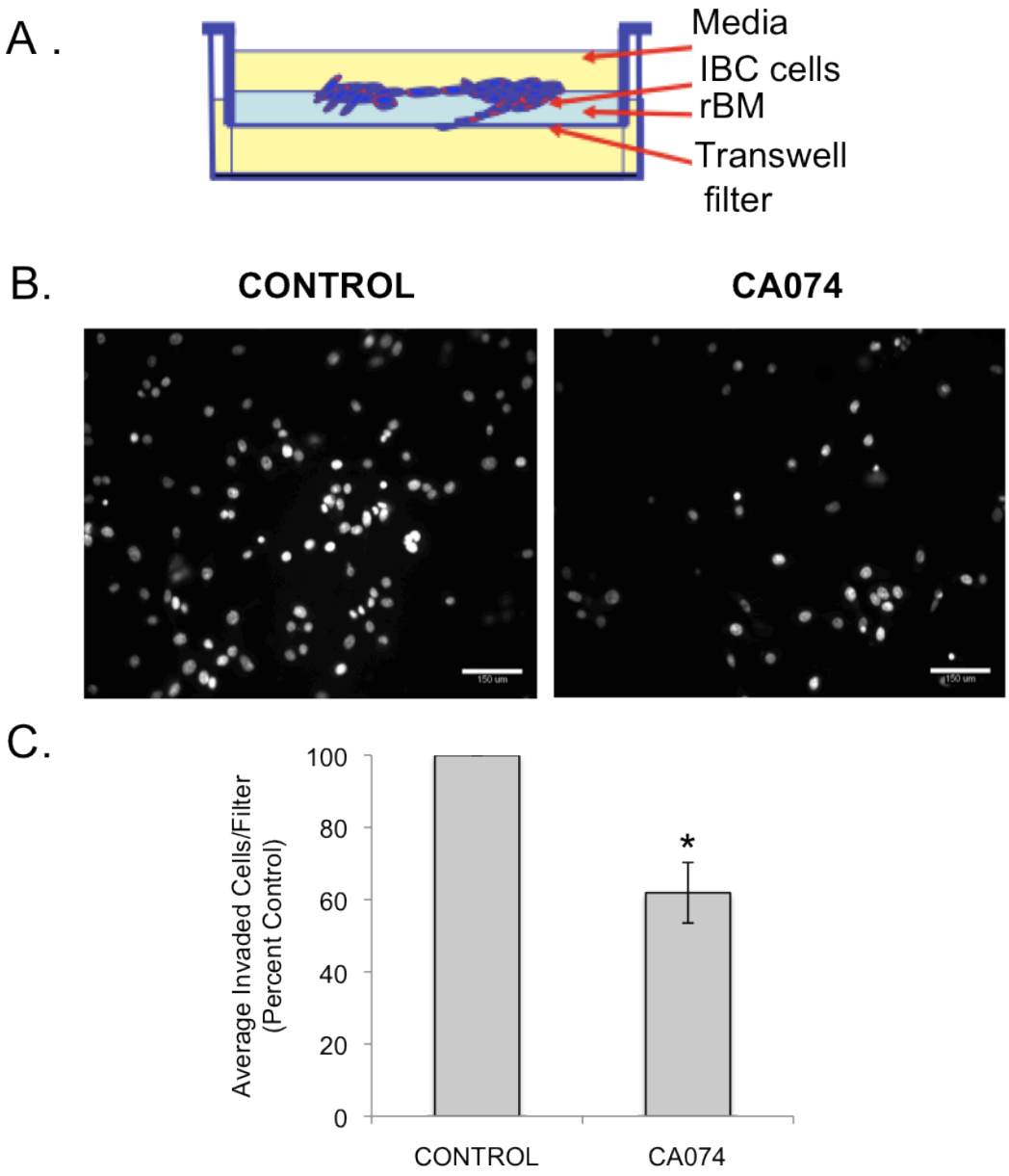

Figure 3.7. Inhibition of cathepsin B activity significantly reduces invasiveness of SUM149 cells. SUM149 cells were subjected to transwell invasion assays in the presence of DMSO (vehicle control) or 10 μM CA074. (A) Cartoon representing setup of invasion assay. (B) Images are SUM149 cells that have invaded through rBM-coated filters; bar, 150 μm. (C) Quantification of invaded cells was performed by counting the number of nuclei from 10 fields of view per filter (using Metamorph software) and expressed as percent control. Results from three independent experiments are presented as mean ± SD; *, $P < 0.05$.

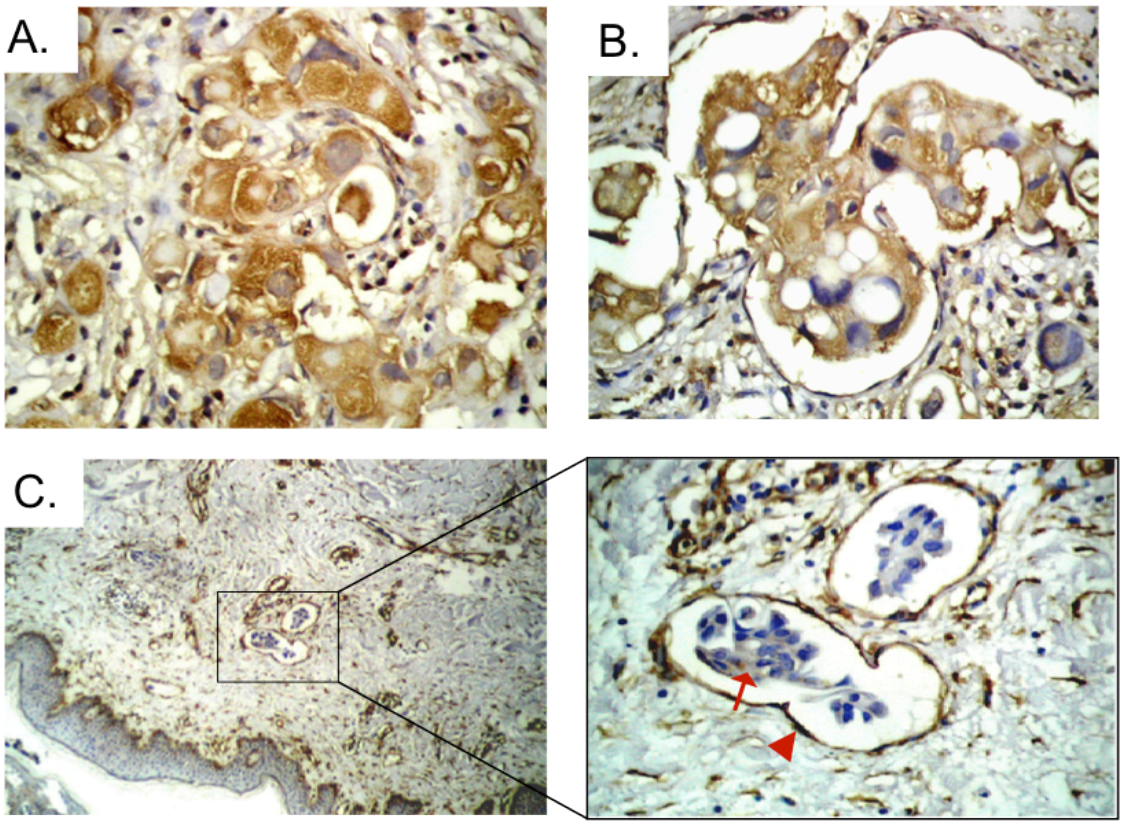

Figure 3.8. Immunohistochemical staining for cathepsin B and caveolin-1 in paraffin sections of IBC tissues. Diffuse cytoplasmic staining for cathepsin B is present in tumor and stromal cells (A) and tumor emboli (B); magnification, 40x. (C) Caveolin-1 staining is present in tumor emboli (arrow) within dermal lymphatics and on the surface of dermal lymphatic endothelial cells (arrowhead); magnification: left panel, 10x and right panel, 40x.

endothelial cells (Couet et al., 2001). Furthermore, there was a difference between IBC and non-IBC carcinoma cells in regard to co-expression of cathepsin B and caveolin-1. Seventy percent of IBC tumor cells that express cathepsin B (score of ++ or +++) also expressed caveolin-1 (score of ++ or +++), whereas only 19% of non-IBC tumor cells showed this co-expression (P = 0.001; Table 3.1).

Downregulation of caveolin-1 expression in IBC cells. We hypothesize that downregulation of caveolin-1 will disrupt caveolae, decrease the cell surface association of cathepsin B and also reduce both invasion and degradation of extracellular matrix (ECM). The role of caveolae and their structural protein caveolin-1 in breast cancer and other cancers is controversial. Some studies, both *in vitro* and *in vivo*, conclude that caveolin-1 functions as a tumor suppressor whereas others strongly support an oncogenic and prometastatic function for caveolin-1 [for review, see (Goetz et al., 2008)]. To reconcile these contradictory findings, Lloyd and Hardin (2011) have proposed a model in which the role played by caveolin-1 is dependent on both stage of disease and tumor type (Lloyd and Hardin, 2011). Lisanti and colleagues have suggested at early stages of breast cancer and in some ductal carcinomas of the breast, caveolin-1 is a tumor suppressor (Williams and Lisanti, 2005). On the other hand, in IBC, caveolin-1 is upregulated and promotes aggressiveness of these tumors (Perou et al., 2000; Pinilla et al., 2006).

	Caveolin-1		total
	negative	positive	
IBC	7 (30.4)	16 (69.6)	23
non-IBC	17 (81.0)	4 (19.0)	21
total	24	20	44
	P value = 0.001		

Table 3.1. Co-expression of caveolin-1 and cathepsin B in carcinoma cells of IBC versus non-IBC patient tissues. Immunohistochemical scores of 0 and + were considered negative and scores of ++ and +++ were considered positive. Data presented as number of patients (%). Chi-square = 11.3 (degrees of freedom = 1).

High expression of caveolin-1 is a characteristic of triple-negative and other basal-like breast cancers (Elsheikh et al., 2008). Triple-negative breast cancer (TNBC) refers to breast cancers that do not express estrogen receptor (ER), progesterone receptor (PR) and Her2/neu. In addition to increased caveolin-1, absence of both ER and PR has been reported to be higher in IBC than non-IBC patient samples (Nguyen et al., 2006); hormone receptor negative breast cancers are known to have a worse prognosis.

To test whether caveolae are a functional part of the IBC aggressive phenotype, our experimental approach was to downregulate expression of caveolin-1 in the SUM149 IBC cell line. Caveolin-1 is essential to caveolae biogenesis (Drab et al., 2001; Razani et al., 2001). We predict that caveolin-1 knockdown in IBC cells will result in decreased formation of caveolae and decrease cathepsin B localization at the cell surface. Knockdown of caveolin-1 in the SUM149 cells was carried out using the OpenBiosystems TRIPZ shRNAmir lentiviral packaging system. We chose lentiviral transduction due to the high efficiency and stability of this technique (Stegmeier et al., 2005; Matrai et al., 2010). A feature of the OpenBiosystems TRIPZ system is the Tet-inducible promoter that regulates expression of the shRNAmir (Figure 3.9). Therefore, knockdown is inducible in the presence of doxycycline, the tetracycline response element agonist. In addition, the marker TurboRFP tracks expression of the shRNAmirs, (control and experimental). In the absence of doxycycline the system is turned off thus allowing for an internal control. OpenBiosystems also

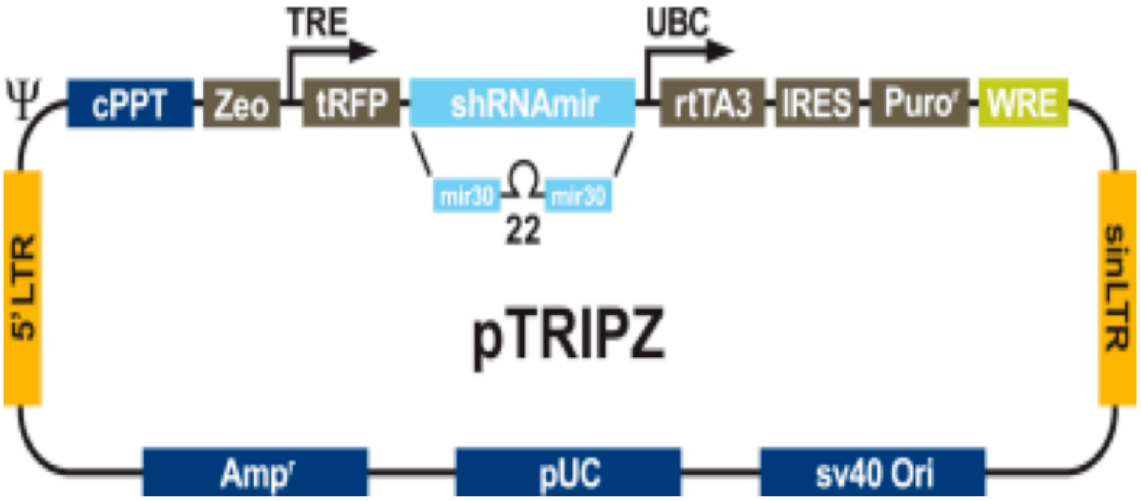

Figure 3.9. Map of TRIPZ plasmid illustrating vector elements: Tet-inducible promoter (TRE) for regulating expression of knockdown; TurboRFP marker (tRFP) to track inducible shRNAmir expression.

http://www.openbiosystems.com/RNAi/shRNAmirLibraries/TRIPZlentiviralinducibleshR/

offers a GIPZ Lentiviral shRNAmir system utilizing TurboGFP tracking shRNAmir expression. This system is not compatible withour live cell proteolysis assay given that DQ-collagen IV degradation products fluoresce green upon proteolytic cleavage. For this reason we chose to utilize the TRIPZ rather than the GIPZ system.

Using six pTRIPZ constructs specific to caveolin-1, we knocked-down the expression of caveolin-1 by transducing SUM149 cells with lentivirus. Figure 3.10 lists the sequences of each clone ID and the targeting site within the caveolin-1 mRNA. To produce the lentivirus, the HEK293T cells were transfected with each pTRIPZ construct and TransLenti viral packaging mix using the Arrest-In transfection reagent. The viral broth of the HEK293T cultures was harvested and used to infect the SUM149 cells. After three rounds of viral infection, transduced SUM149 cells were grown in media containing 1 µg/ml puromycin to selectively kill any non-infected cells. A one µg/ml concentration of puromycin for selection of SUM149 cells post-lentiviral transduction has been previously reported (Baillo et al., 2011). To confirm that the 1 µg/ml puromycin concentration was appropriate for selection in our hands, we monitored the growth of SUM149 cells in puromycin concentrations ranging from 0 – 5 µg/ml. Within 4 days, the 1 µg/ml concentration killed 100% of the cells, verifying that this concentration was appropriate for selection of SUM149 cells. Concentrations of puromycin below 1 µg/ml did not kill all cells, whereas concentrations above 1 µg/ml were toxic within 1 to 2 days.

A.

Clone ID	Mature Sense Sequence	Mature Anti-sense sequence
V2THS_279513_A6	CATCAACTTGCAGAAAGAA	TTCTTTCTGCAAGTTGATG
V2THS_150249_C8	GCAGTTGTACCATGCATTA	TATTGCATGGTACAACTGC
V2THS_150248_H1	CACCTTCACTGTGACGAAA	TTTCGTCACAGTGAAGGTG
V3THS_312899_F2	ACGATGACGTGGTCAAGAT	ATCTTGACCACGTCATCGT
V3THS_312895_B7	TGGTCAACCGCGACCCTAA	TTAGGGTCGCGGTTGACCA
V3THS_312896_F7	CGCATCAACTTGCAGAAAG	CTTTCTGCAAGTTGATGCG

B.

atgtctgggggcaaatacgtagactcggagggacatctctacaccgttcccatccggga
acagggcaacatctacaagcccaacaacaaggccatggcagacgagctgagcgagaagc
aagtgtacgacgcgcacaccaaggagatcgacctggtcaaccgcgaccctaaacacctc
aacgatgacgtggtcaagattgactttgaagatgtgattgcagaaccagaagggacaca
cagttttgacggcatttggaaggccagcttcaccaccttcactgtgacgaaatactggt
tttaccgcttgctgtctgccctctttgcatcccgatggcactcatctggggcatttact
tcgccattctctctttcctgcacatctgggcagttgtaccatgcattaagagcttcctg
attgagattcagtgcatcagccgtgtctattccatctacgtccacaccgtctgtgaccc
actctttgaagctgttgggaaaatattcagcaatgtc[cgcatcaacttgcagaaag]a
aatataa

clone ID V3THS_312899_F2

clone ID V2THS_150249_C8

clone ID V2THS_150248_H1

clone ID V3THS_312895_B7

clone ID V2THS_279513_A6

[clone ID V3THS_312896_F7]

Figure 3.10. shRNA target gene set for caveolin-1 gene. (A) Table of the 6 clone IDs and their respective sense and anti-sense sequences. (B) The coding sequence of the caveolin-1 gene. The clones are highlighted or underlined indicating their target site within the mRNA of caveolin-1.

Of the six constructs tested, two induced the greatest levels of caveolin-1 knockdown. To investigate the effect of shRNAmir on the protein expression of caveolin-1 in the transduced SUM149 cells, we performed immunoblot analysis of cellular lysates of knockdown SUM149 cells ± doxycycline and of the parental SUM149 cells (Figure 3.11A). Immunoblotting showed a large decrease in caveolin-1 protein levels in two clones: C8 and F2. Densitometric analysis of the protein bands revealed that when the shRNAmir expression is turned on (i.e., + doxycycline), caveolin-1 protein expression was decreased approximately 40% in clone C8 and 95% in clone F2 (Figure 3.11B). As a result of these findings, all future experiments were performed with clones C8 and F2 ± doxycycline. As a negative control, we also transduced SUM149 cells with a non-silencing-TRIPZ lentiviral shRNAmir control that does not target any mRNA sequence in the mammalian genome.

Knockdown of caveolin-1 does not affect morphology of IBC cells. As early as 1976, Rohlich and Allison described how the pattern of membrane-associated vesicles, now known to be caveolae, depended on intact microtubule bundles (Rohlich and Allison, 1976). Later studies demonstrated that the cellular distribution and dynamics of caveolae require an intact cytoskeleton (Parton et al., 1994) and that actin is detected in caveolae-enriched microdomains (Lisanti et al., 1994; Smart et al., 1995). Caveolae form a bridge between the extracellular matrix and the cytoplasm. For example, reducing expression of

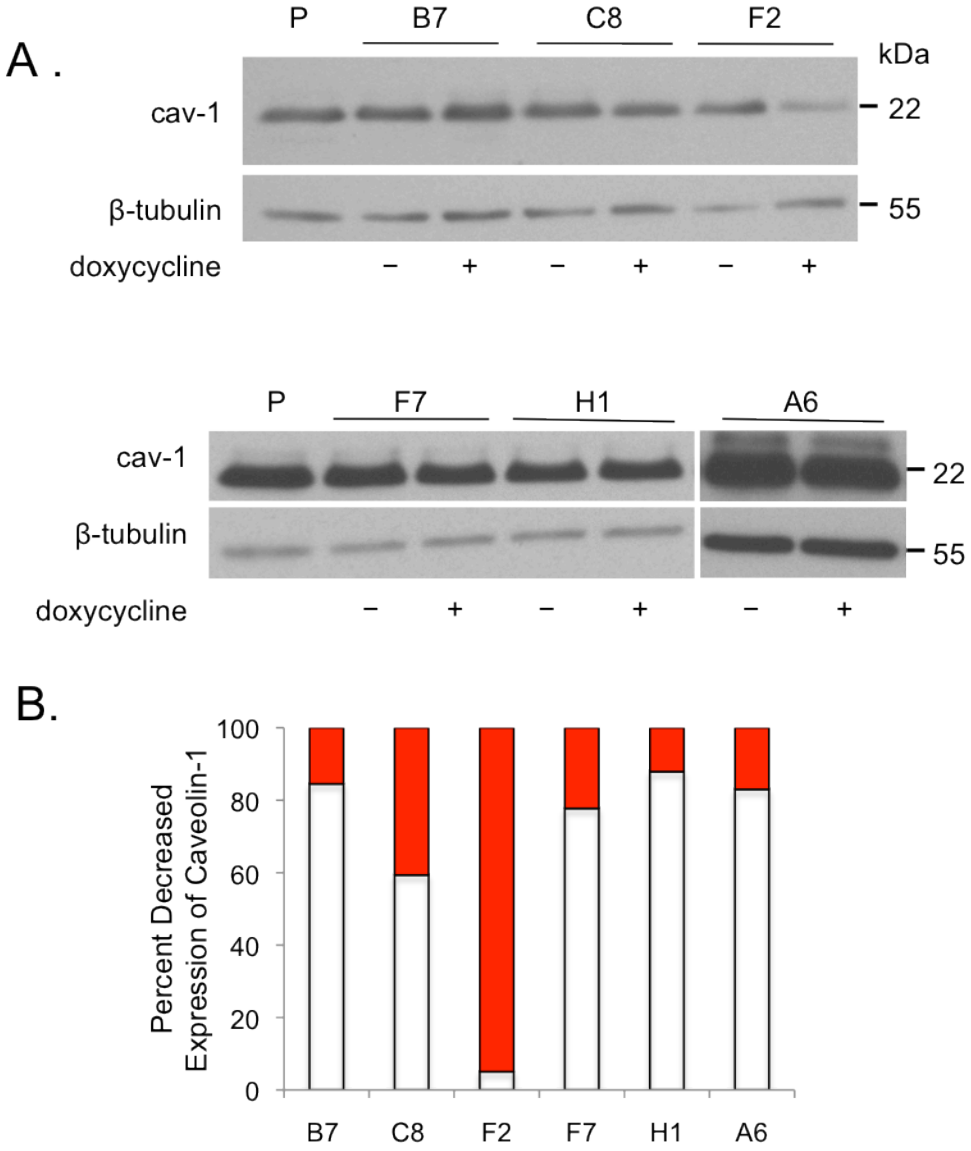

Figure 3.11. Caveolin-1 knockdown in SUM149 cells. (A) SUM149 cells stably infected with caveolin-1 shRNA lentiviral expression constructs were grown on plastic in either the presence or absence of doxycycline. P = parental SUM149. Cell lysate was harvested, separated by 12% SDS-PAGE under reducing conditions and transferred to nitrocellulose. Membranes were blotted for antibodies against caveolin-1 and β-tubulin as a loading control. (B) Quantification of densitometric analysis of caveolin-1 signal. Red bar indicates the decrease in caveolin-1 protein level for each clone.

caveolin-1 by an antisense approach disrupts β-1 integrin signaling leading to reduced focal adhesions, phosphorylation of focal adhesion kinase and cell adhesion (Wei et al., 1999). To test the effect of caveolin-1 knockdown on the morphology of IBC cells, we cultured control and knockdown populations in 3D rBM overlay cultures. Parental SUM149 cells grown in three-dimensional rBM overlay cultures form spheroid-like multicellular structures (Mohamed et al., 2008). Here, a single cell suspension of 25,000 transduced SUM149 cells was seeded onto round glass coverslips coated with solidified rBM. The cells were allowed to adhere to the rBM for 45 minutes. Growth medium containing 2% rBM was then overlaid onto the cultures. After 48 hours in culture we assessed morphology, in 3 independent experiments by confocal microscopy by examining a tile of 12 fields of vew of cells grown in 3D. With regard to structure complexity an shape, there were no obvious differences of the 3D structures when control shRNAmir cells and knockdown clones were cultured in either the presence or absence of doxycycline (Figure 3.12). These data suggest that the absence of caveolin-1 does not affect the morphology of IBC cells.

Caveolin-1 knockdown does not affect proliferation of SUM149 cells.

Caveolin-1 negatively regulates cell proliferation. For example, serum starvation of NIH 3T3 cells increases endogenous levels of caveolin-1 expression and induces cell cycle arrest in the G_0/G_1 phase (Galbiati et al., 2001). In addition to these findings, mouse embryonic fibroblasts isolated from caveolin-1 transgenic

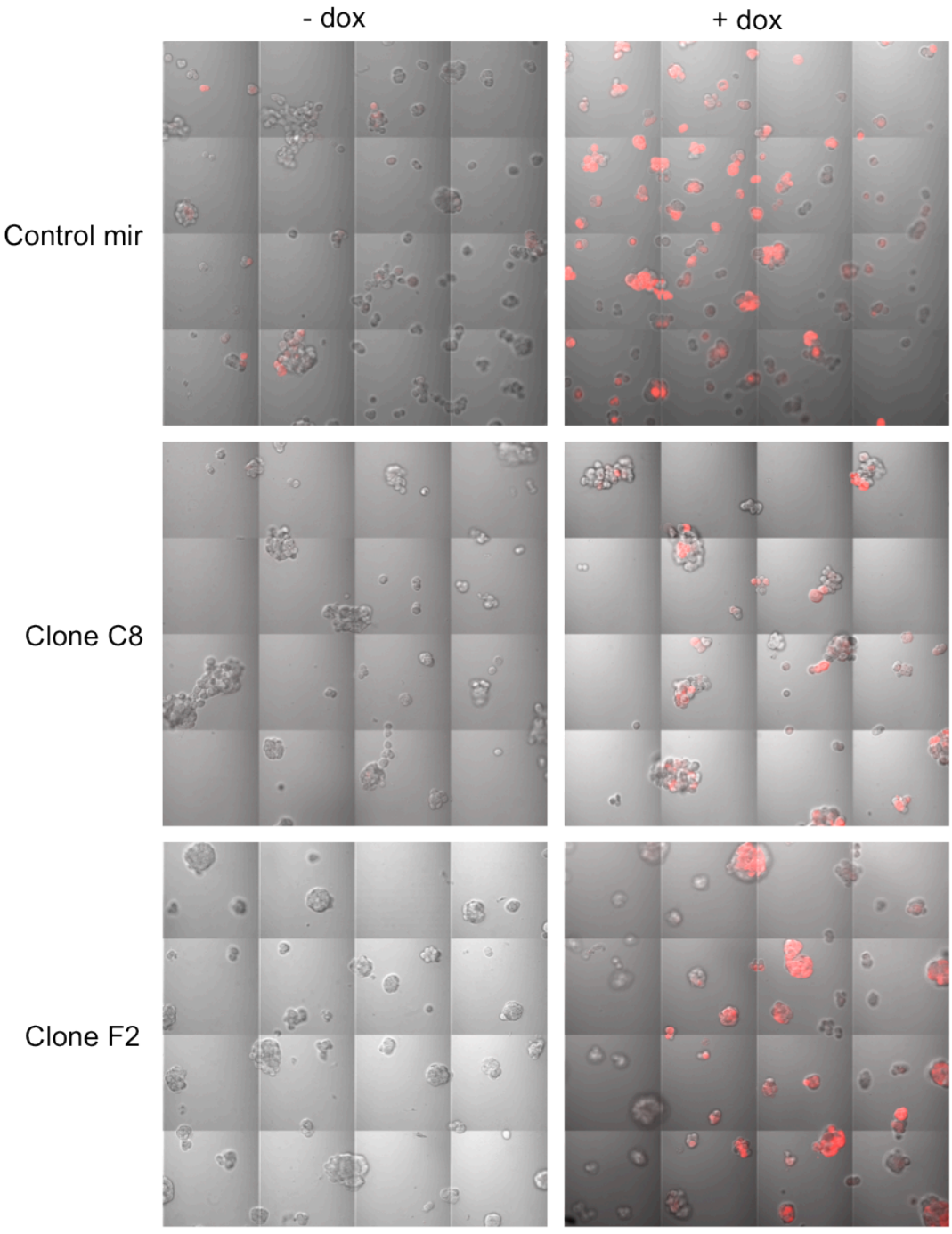
- dox
+ dox
Control mir
Clone C8
Clone F2

Figure 3.12. Comparitive growth and morphology of 3D rBM cultures of caveolin-1 knockdown SUM149 cells. SUM149 cells stably infected with caveolin-1 shRNA lentiviral expression constructs were grown in 3D rBM culture either the presence or absence of doxycycline. Cultrex coated glass coverslips were seeded with 25,000 cells and grown for 2 days. Merged DIC and fluorescent tile images of the cultures were imaged using confocal microscopy. Magnification, 40X.

mice exhibit a p53/p21-mediated reduction in cellular proliferation. A growth regulating function of caveolin-1 has also been demonstrated in a panel of non-IBC human breast cancer cell lines (Lee et al., 1998). To evaluate whether knockdown of caveolin-1 affects proliferation of IBC cells, we performed MTT assays over a 72 h period. Cultures of control shRNAmir cells, clones C8 and F2 were grown in the presence of 500 ng/ml of doxycycline or absence. Interestingly knockdown of caveolin-1 expression did not change the proliferation of IBC cells as measured by the ability of cells to reduce the MTT substrate (Figure 3.13).

Knockdown SUM149 cells exhibit altered distribution of caveolin-1. Analysis of whole cell lysates demonstrated that shRNAmir sequences resulted in decreased caveolin-1 protein (Figure 3.11). In addition we analyzed the subcellular localization of caveolin-1 in both control and knockdown populations. Transduced SUM149 cells were grown in the absence or presence of doxycycline to induce expression of the shRNAmir. These cultures were then subjected to the detergent-based method of subcellular fractionation separating Triton X-100-soluble (TS) from –insoluble (TI) membrane components. Equal volume aliquots of each fraction were separated by 12% SDS-PAGE under reducing conditions, transferred to nitrocellulose and probed for caveolin-1. In comparison to untreated samples (no doxycycline), caveolin-1 protein levels were clearly reduced in both fractions of clones C8 and F2 treated with

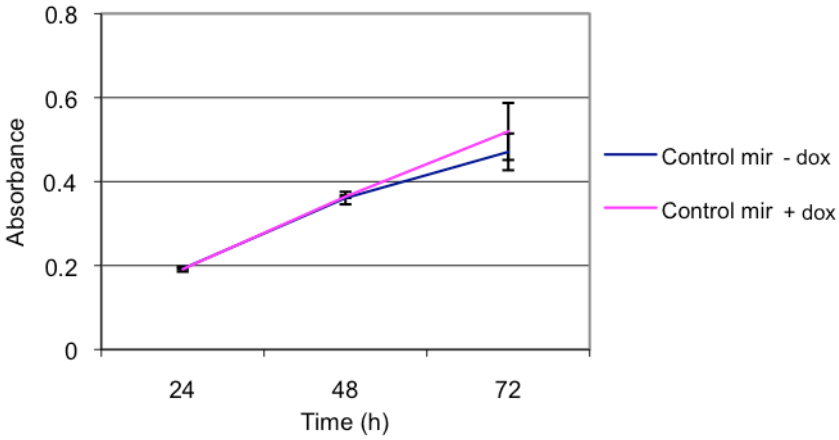
0.8
0.6
0.4
0.2
0
Absorbance
24
48
72
Time (h)
Control mir - dox
Control mir + dox

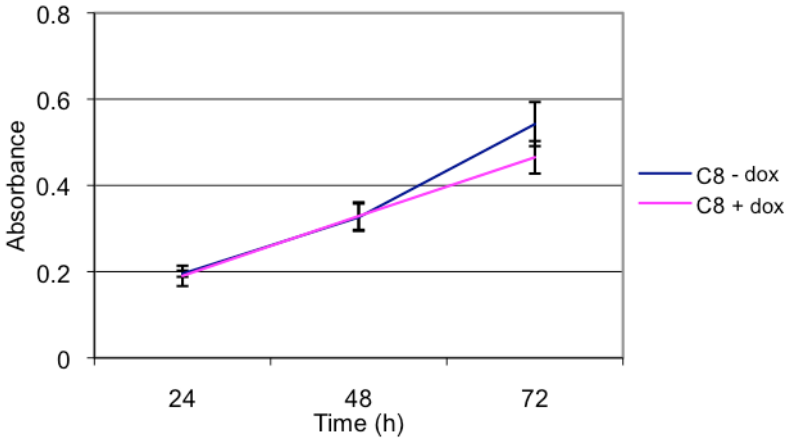
0.8
0.6
0.4
0.2
0
Absorbance
24
48
72
Time (h)
C8 - dox
C8 + dox

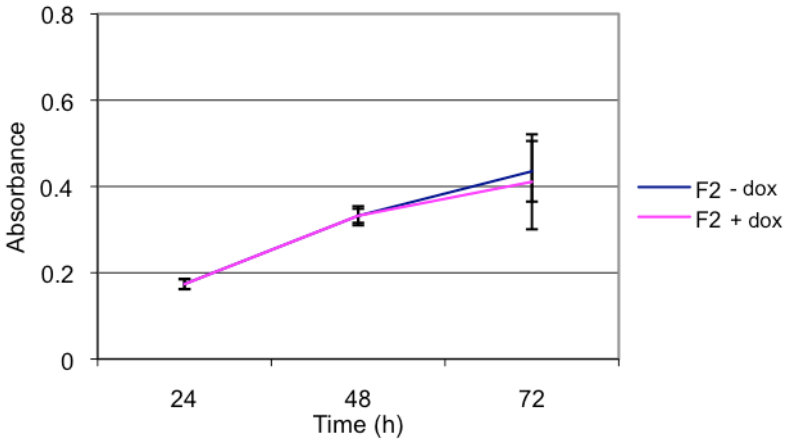
0.8
0.6
0.4
0.2
0
Absorbance
24
48
72
Time (h)
F2 - dox
F2 + dox

Figure 3.13. Knockdown of caveolin-1 does not alter proliferation of IBC cells as assessed by MTT assays. Control shRNAmir, clone C8 and clone F2 were seeded in 96-well plates (5,000 per well) ± doxycycline. At 24, 48 and 72 h time points, 50 µl of MTT stock solution was added to each well and incubated at 37°C for 3 hours. Media was removed and 150 µl of DMSO added to each well dissolving the formazan precipitate. Absorbance values were measured at a 485-nm wavelength.

doxycycline (Figure 3.14). As expected, no discernable difference was observed in the control shRNAmir cells ± doxycycline.

Knockdown of caveolin-1 decreases degradation of DQ-collagen IV by SUM149 3D cultures. We have previously shown that caveolin-1 expression affects the degradation of collagen type IV (Cavallo-Medved et al., 2005). When antisense was used as a method to target caveolin-1 expression in human colorectal carcinoma cells, they degraded less collagen IV than control cells. Therefore, we investigated whether downregulation of caveolin-1 can affect the ability of IBC cells to degrade type IV collagen. Using our live-cell proteolysis assay we demonstrated that cleavage products of type IV collagen were found adjacent to the external cell surface of parental SUM149 cells (Figure 3.2). We seeded individual cells of knockdown populations and control shRNAmir cells onto rBM containing DQ-collagen IV and grew them for 48 hours ± 500 ng/ml doxycycline. We then imaged DQ-collagen IV degradation in live cultures of IBC cells using confocal microscopy. Both caveolin-1 knockdown and control shRNAmir cells exhibited a pericellular pattern of proteolysis similar to that of the parental SUM149 cells. Confocal Z stack images were captured throughout the three-dimensional volume and used to generate 3D reconstructions (Figures 3.15-3.17). Quantitative analysis with Metamorph software revealed that control shRNAmir cells and clone C8 cultures exhibited no significant difference in the intensity of degradation products ± doxycycline treatment (Figure 3.18).

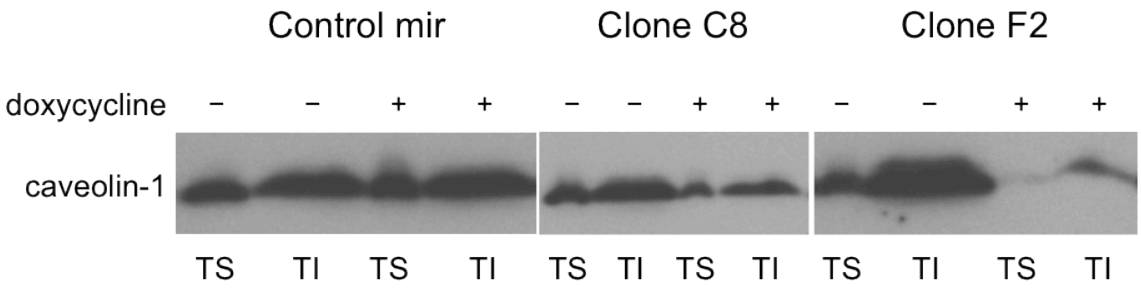

Figure 3.14. Distribution of caveolin-1 to lipid enriched fractions is decreased in knockdown SUM149 cells. Caveolae-enriched fractions from transduced SUM149 grown ± 500 ng/ml doxycycline were isolated by a detergent-based method that separates Triton X-100-soluble (TS) from Triton X-100–insoluble (TI) cellular fractions. Equal volumes of each fraction were analyzed by SDS-PAGE and immunoblotted with antibodies against caveolin-1.

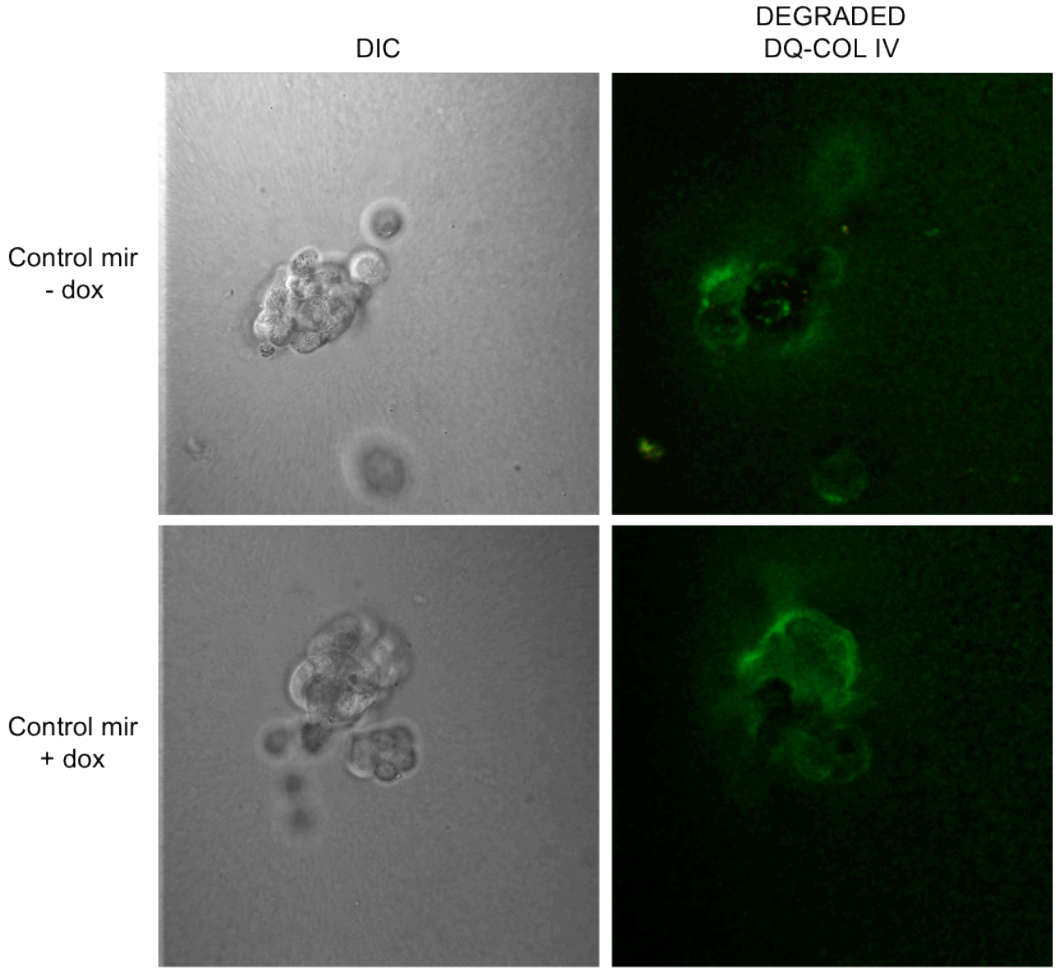

Figure 3.15. Degradation of DQ-collagen IV by control shRNAmir cells. Control shRNA mir cells were grown as 3D cultures in rBM containing DQ-collagen IV in the presence (+ dox) or absence (- dox) of 500 ng/ml doxycycline. Representative 3D reconstructions of DQ-collagen IV degradation products (green) and corresponding DIC images shown. Magnification, 40X.

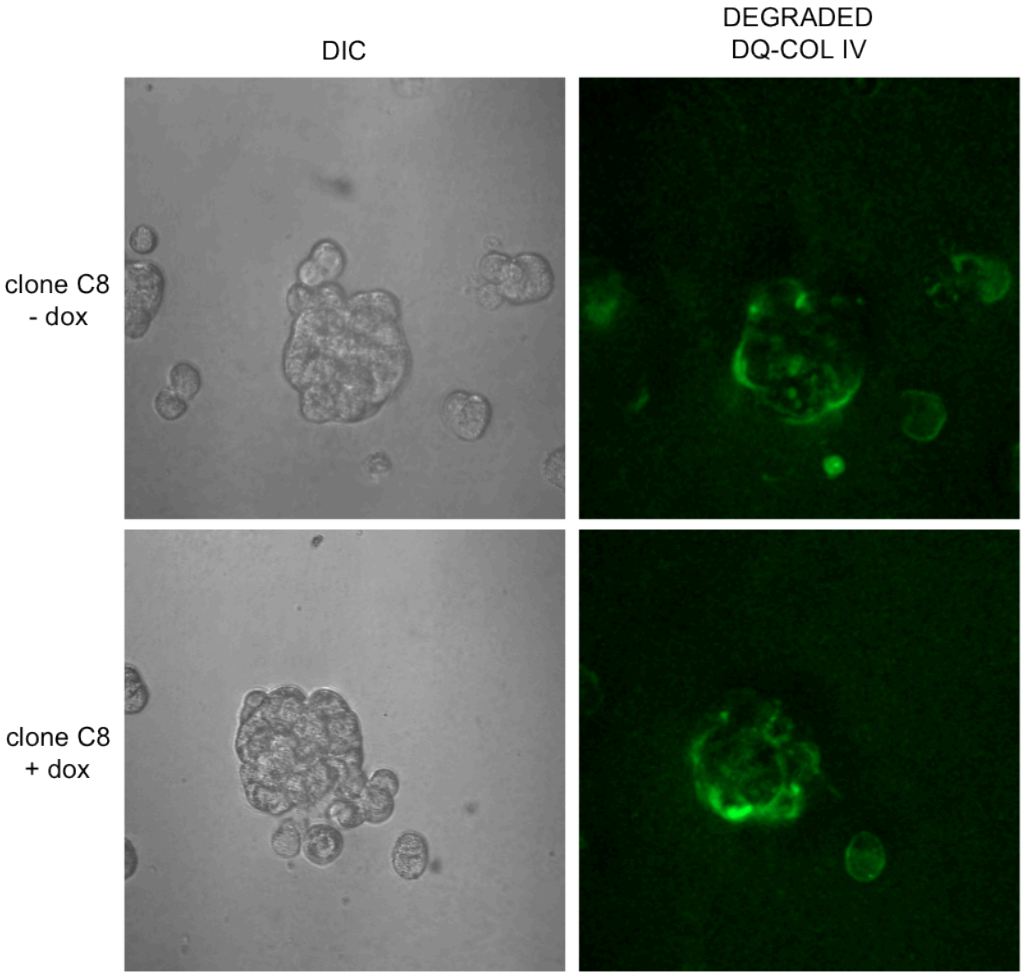

Figure 3.16. Degradation of DQ-collagen IV by caveolin knockdown cells. Clone C8 cells were grown as 3D cultures in rBM containing DQ-collagen IV in the presence (+ dox) or absence (- dox) of 500 ng/ml doxycycline. Representative 3D reconstructions of DQ-collagen IV degradation products (green) and corresponding DIC images shown. Magnification, 40X.

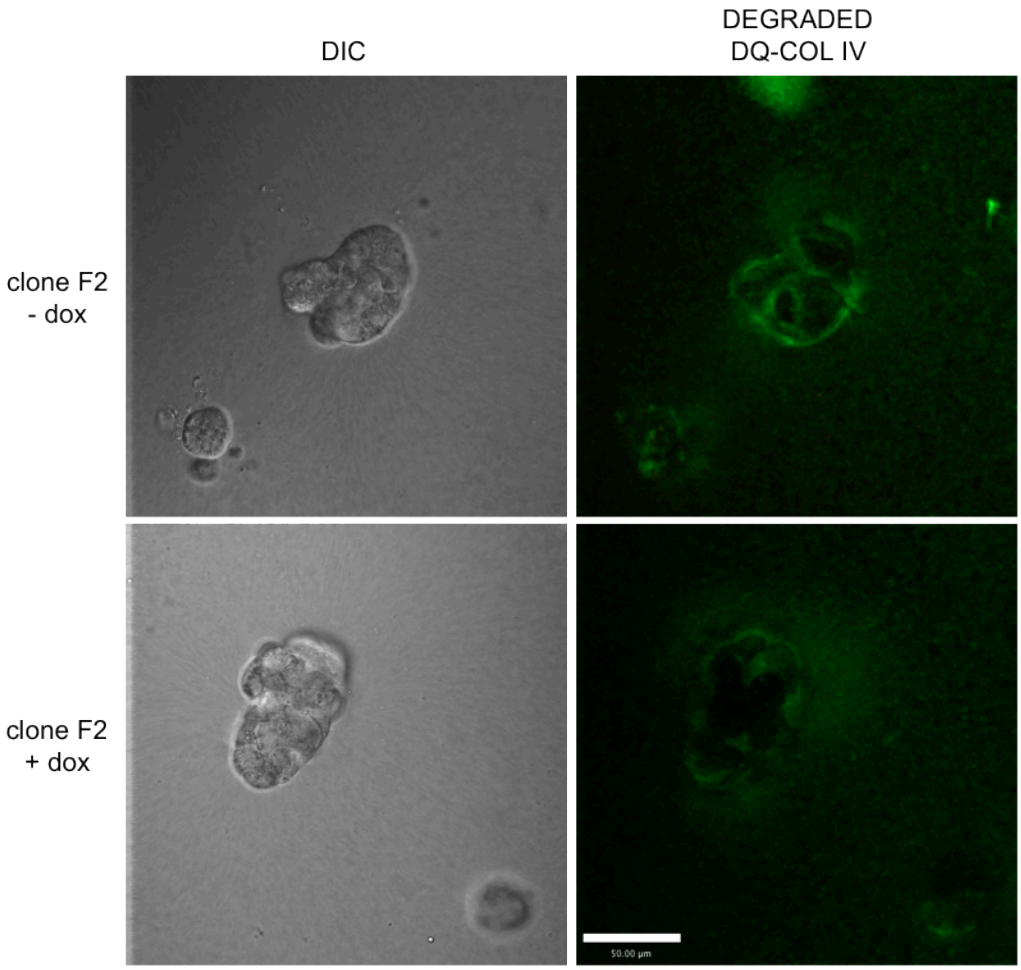

Figure 3.17. Degradation of DQ-collagen IV by caveolin knockdown cells. Clone F2 cells were grown as 3D cultures in rBM containing DQ-collagen IV in the presence (+ dox) or absence (- dox) of 500 ng/ml doxycycline. Representative 3D reconstructions of DQ-collagen IV degradation products (green) and corresponding DIC images shown. Magnification, 40X. Bar, 50 µm.

In contrast, a significant reduction in degradation of DQ-collagen IV by clone F2 cells was observed. Thus, in the F2 clone cells, when expression of the caveolin-1 targeting shRNAmir is induced, i.e. + doxycycline, and expression of caveolin-1 is knocked down, degradation by IBC cells of collagen IV is reduced.

Caveolin-1 knockdown results in reduced invasion by IBC cells. An abundance of tumor emboli in lymphatic vessels is one pathological feature distinguishing IBC from non-IBC (Bonnier et al., 1995). Therefore, we studied the role of caveolin-1 in the invasive phenotype of IBC. Invasion through transwell filters coated with rBM is a commonly used assay to test the invasive capacity of cells *in vitro*. In these experiments, we seeded equal numbers of control shRNAmir, clone C8 or clone F2 cells on rBM-coated transwell filters with or without 500 ng/ml of doxycycline. The cells were incubated with serum free media and complete media (Ham's F12 media with 5% FBS) below the rBM-coated transwell filter to stimulate invasion. Following 24 hours rBM and non-invasive cells were removed from the top of filter. The cells that had invaded, i.e., the cells attached to the bottom of the filter insert, were fixed and stained using Diff-Quik Stain Set. Filters were cut from the insert, mounted on a slide and invaded cells were imaged for counting by two independent observers. Only the clone F2 exhibited a decrease in the number of invaded cells when treated with 500 ng/ml doxycycline relative to untreated (Figure 3.19).

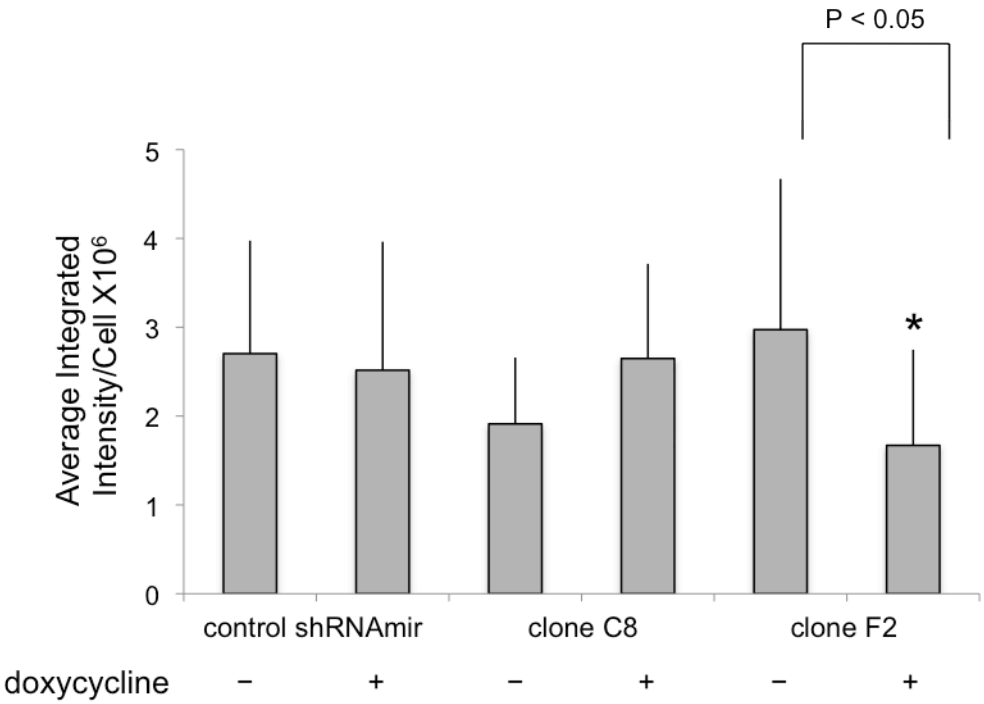

Figure 3.18. Knockdown of caveolin-1 decreases degradation of DQ-collagen IV by IBC cells. Quantification of proteolysis in the entire volume of three-dimensional structures measured as the average integrated intensity of fluorescence was normalized to the number of cells. Results from at least three independent experiments are presented as mean ± SD; *, P< 0.05.

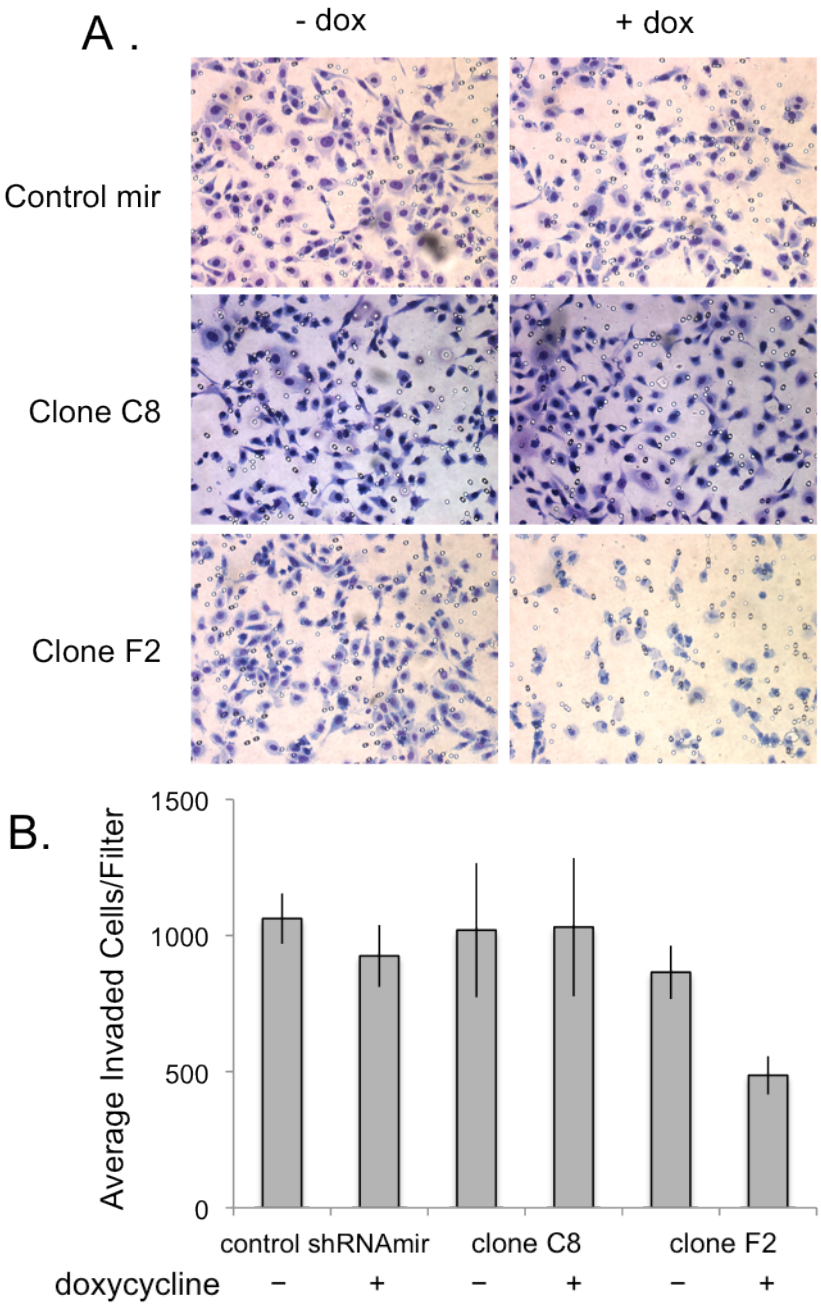

Figure 3.19. Knockdown of caveolin-1 expression decreases the invasiveness of IBC cells. Transduced SUM149 cells were subjected to transwell invasion assays in the presence of 500 ng/ml of doxycycline (+ dox) or untreated (- dox). (A) Images are cells that have invaded through rBM-coated filters. Magnification, 20X. (B) Quantification of invaded cells was performed by counting the number of cells that invaded through rBM-coated transwell filters. Bars represent mean ± SD; n=3.

Cathepsin B distributes to lipid microdomains in caveolin-1 knockdown IBC cells. Active cathepsin B localized to caveolae-enriched microdomains of SUM149 parental cells (Figure 3.4). We also demonstrated that inhibition of pericellular cathepsin B activity reduced extracellular matrix degradation and invasion of SUM149 parental cells (Figures 3.6 and 3.7). Caveolin-1 knockdown studies (Figures 3.15-17) revealed similar decreases in degradation and invasion by the F2 clone. To determine if caveolin-1 mediates cell surface localization of cathepsin B, we examined the subcellular distribution of cathepsin B in control shRNAmir cells and caveolin-1 knockdown populations. Three-dimensional rBM overlay cultures of control shRNAmir cells and caveolin-1 knockdown cells ± 500 ng/ml of doxycycline were subjected to detergent-based subcellular fractionation. Interestingly, we observed no change in the distribution of cathepsin B in caveolin-1 knockdown (doxycycline treated) cells as compared to untreated cells (Figure 3.20A). As expected, no changes in the distribution of cathepsin B were observed in control shRNAmir transduced cells ± doxycycline treatment (Figure 3.20A). The TS and TI fractions of control shRNAmir and clone F2 were also assayed for cathepsin B activity. We detected no differences in the activity of cathepsin B in doxycycline treated caveolin-1 knockdown (Figure 3.20C) and control shRNAmir cells (Figure 3.20B). These findings correspond to those of our immunoblotting studies and suggest that decreased caveolin-1 in the TI fraction and more specifically in the lipid microdomain fractions of IBC cells has no effect on the subcellular distribution of cathepsin B. We also investigated

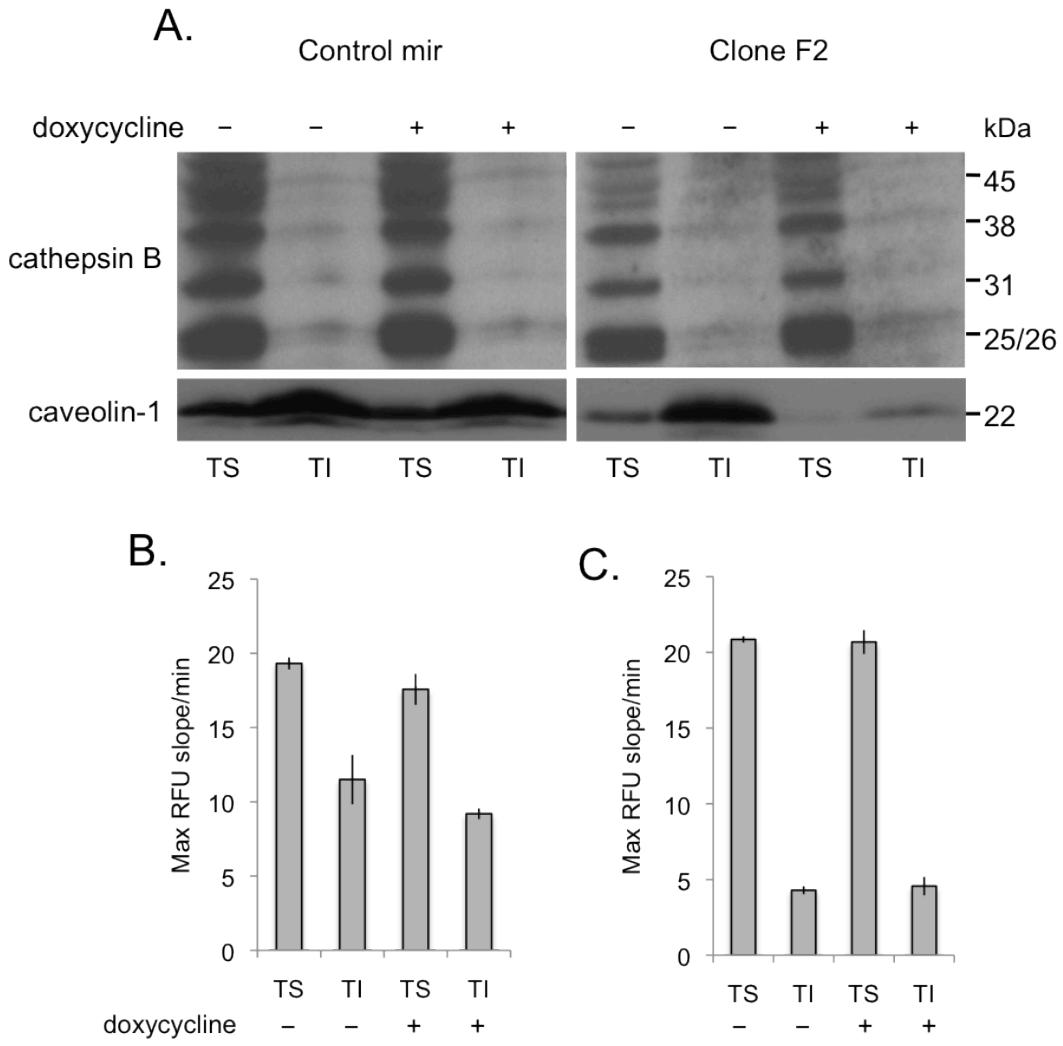

Figure 3.20. Active cathepsin B is present in caveolae-enriched fractions of caveolin-1 knockdown SUM149 cells in 3D cultures. Control shRNAmir and clone F2 3D cultures were subjected to detergent-based cellular fractionation method, as described in Materials and Methods, that separate Triton X-100-soluble (TS; non-caveolae) from Triton X-100–insoluble (TI; caveolae-enriched) cellular fractions. (A) Equal volume aliquots of each fraction were analyzed by SDS-PAGE and immunoblotted with antibodies against cathepsin B and caveolin-1. (B) Equal volume aliquots of (B) control mir and (C) clone F2 TS and TI fractions were assayed for enzymatic activity against the synthetic cathepsin B substrate Z-Arg-Arg-NHMec.

the localization of uPA and other proteins known to be associated with caveolae. In human colorectal carcinoma cells, we have established that the cell surface association of cathepsin B, uPA and their binding partners is caveolin-1 dependent (Cavallo-Medved et al., 2005). We observed no changes in the distribution to TI fractions of uPA, E-cadherin, β1-integrin, p36 and p11 in control shRNAmir cells when treated with doxycycline as compared to untreated cells (Figure 3.21). In contrast, knockdown caveolin-1 cells exhibited decreased distribution of uPA to the TI fraction when treated with doxycycline as compared to untreated cells (Figure 3.22).

Inhibiting cathepsin B activity reduced both type IV collagen degradation and invasion by IBC cells. Downregulation of caveolin-1 in IBC cells did not change the distribution of cathepsin B at the cell surface. Knockdown of caveolin-1 in clone F2 cells did, however, cause a decrease in both the degradation of collagen IV and invasion, consistent with a mechanism other than cathepsin B activity may be responsible for these findings. Signaling pathways mediated by EGFR have been thoroughly studied especially in TNBC [for review, see (Foley et al., 2010)]. Overexpression of EGFR and caveolin-1 are associated with triple negative breast cancers (Pinilla et al., 2006; Rastelli et al., 2010). This includes SUM149, a triple negative breast cancer cell line that also expresses EGFR, and in which EGFR localizes to lipid microdomains (Irwin et al., 2011). To determine if caveolin-1 mediates the association of EGFR with lipid microdomains, we assessed the subcellular distribution of EGFR in caveolin-

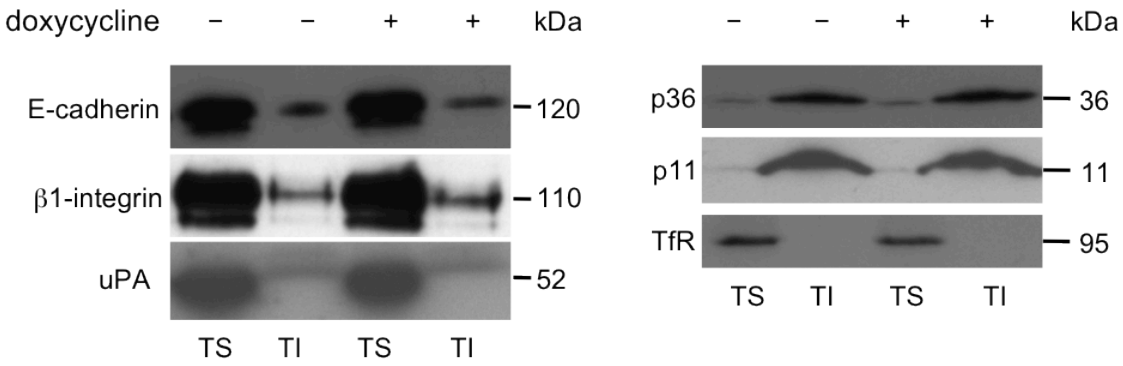

Figure 3.21. Subcellular distribution of E-cadherin, β1-integrin, uPA, p36 and p11 is unchanged in control shRNAmir transduced IBC cells. Caveolae enriched fractions were isolated from control shRNAmir cells ± doxycycline by a detergent based method that separates Triton X-100-soluble (TS) from –insoluble (TI) membrane components. TS indicates non-caveolae fractions and TI indicates caveolae-enriched fractions. Equal volumes of each fraction were analyzed by SDS-PAGE and immunoblotted with anti-E-cadherin, anti-β1-integrin, anti-uPA, anti-p36, anti-p11 and anti-transferrin receptor (TfR) antibodies. TfR is a negative control for lipid rafts.

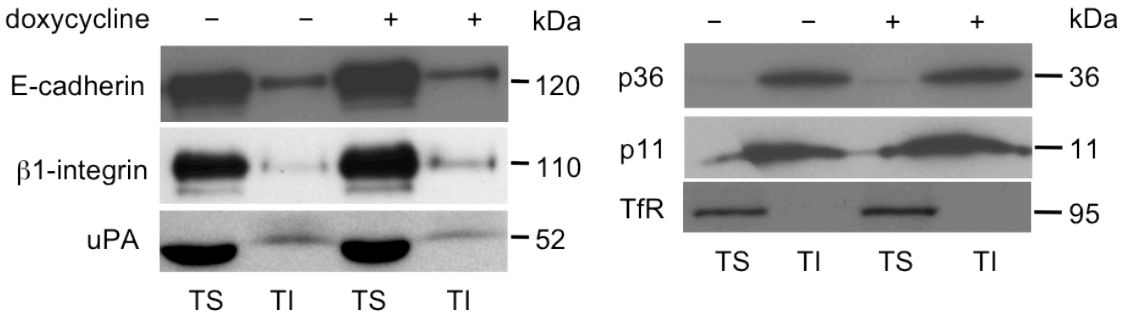

Figure 3.22. E-cadherin, β1-integrin, uPA, p36 and p11 are present in caveolae-enriched fractions of caveolin-1 knockdown SUM149 cells in 3D culture. Caveolae enriched fractions were isolated from clone F2 ± doxycycline by a detergent based method that separates Triton X-100-soluble (TS) from –insoluble (TI) membrane components. TS indicates non-caveolae fractions and TI indicates caveolae-enriched fractions. Equal volumes of each fraction were analyzed by SDS-PAGE and immunoblotted with anti-E-cadherin, anti-β1-integrin, anti-uPA, anti-p36, anti-p11 and anti-transferrin receptor (TfR) antibodies. TfR is a negative control as it is not associated with lipid rafts.

1 knockdown cells. We observed decreased EGFR in both TS and TI fractions of clone F2 cells when treated with 500 ng/ml doxycycline (Figure 3.23). These findings indicate that caveolin-1 may play a role in the expression of EGFR and mediate its cell surface localization in IBC cells.

Analysis of caveolin-1 expression and cathepsin B localization in a new IBC cell line. The human cell line MDA-IBC-3 (a kind gift of Dr. Wendy Woodward developed at The University of Texas MD Anderson Cancer Center, Texas) was obtained from a patient with IBC and generated from primary breast cancer cells isolated from pleural effusion fluid (Klopp et al., 2010). The SUM149 and SUM190 are the only commercially available IBC cell lines for *in vitro* investigation. Therefore, we thought it important to test our hypothesis with this additional IBC cell line. To initiate analysis of the new IBC cell line, we compared the protein expression of cathepsin B and caveolin-1 in three IBC cell lines (SUM149, SUM190 and MDA-IBC-3) when grown in monolayer cultures on plastic. MDA-IBC-3 cells express more cathepsin B protein as assessed by SDS-PAGE and immunoblotting (Figure 3.24A). We previously found that SUM190 does not have detectable caveolin-1 protein and surprisingly neither does the MDA-IBC-3 cell line (Figure 3.24A).

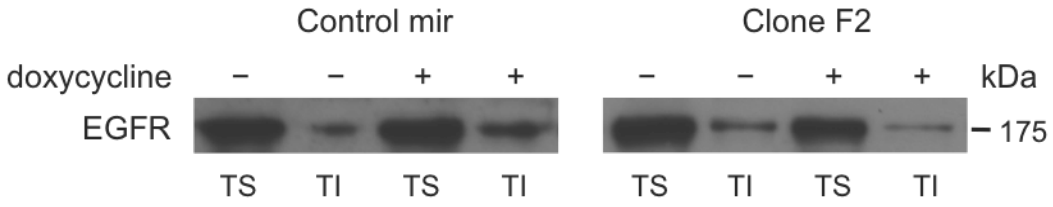

Figure 3.23. Knockdown of caveolin-1 decreases the expression and cell surface localization of EGFR in IBC cells. Control mir and clone F2 3D cultures were subjected to detergent-based cellular fractionation method, as described in Materials and Methods, that separate Triton X-100-soluble (TS; non-caveolae) from Triton X-100–insoluble (TI; caveolae-enriched) cellular fractions. (A) Equal volume aliquots of each fraction were analyzed by SDS-PAGE and immunoblotted with antibodies against EGFR.

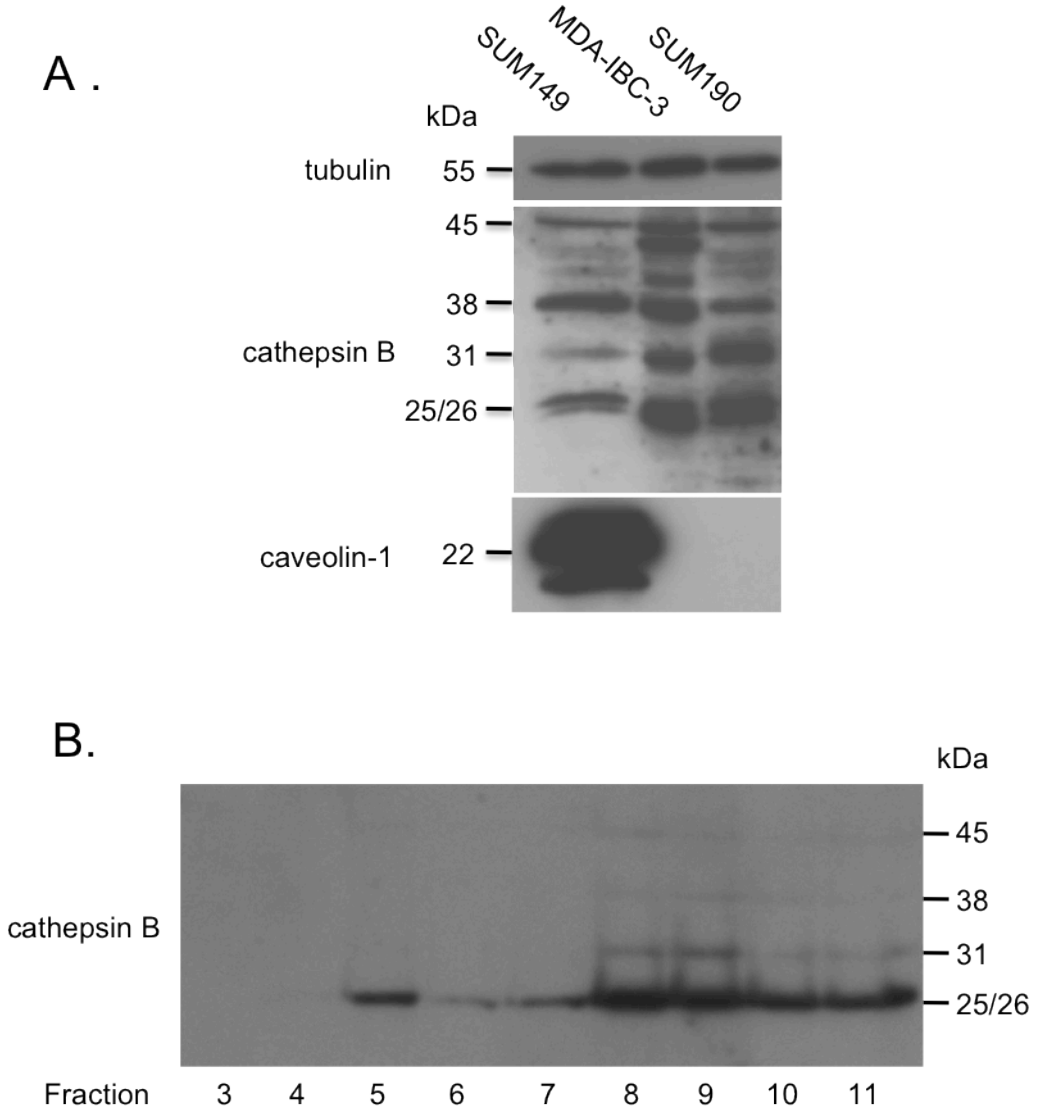

Figure 3.24. Cathepsin B expression and localization in a new IBC cell line MDA-IBC-3. (A) IBC cells (SUM149, MDA-IBC-3 and SUM190) grown on plastic were harvested in lysis buffer (10 mM Tris, pH 7.5, 50 mM NaCl, 1% Triton X-100, 60 mM octylglucoside) and equally loaded samples separated by 12% SDS-PAGE under reducing conditions. Proteins were transferred to nitrocellulose membrane and immunoblotted with anti-CTSB and anti-caveolin-1 polyclonal antibodies. The immunoblot for caveolin-1 was overexposed to ensure no observable caveolin-1 signal was detectable in MDA-IBC-3 and SUM190 lysate. (B) MDA-IBC-3 cells grown as a monolayer were subjected to subcellular fractionation on a sucrose gradient. Equal volumes of each fraction were analyzed by SDS-PAGE and immunoblotted for cathepsin B.

Cathepsin B localizes to plasma membrane domains other than caveolae. Caveolin-1 protein expression is essential to caveolae formation (Drab et al., 2001; Razani et al., 2001). Since caveolin-1 protein was not detected in both MDA-IBC-3 and SUM190 lysates, we hypothesized that these cells might not have caveolae. Subcellular fractionation of SUM190 cells showed that cathepsin B localized to low-density lipid fractions despite the absence of caveolin-1 (Cavallo-Medved, unpublished data). We also investigated the subcellular localization of cathepsin B in MDA-IBC-3 cells. We subjected MDA-IBC-3 cells grown in monolayer to the non-detergent based sucrose density fractionation gradient method. As expected cathepsin B localized to fractions 8-11, i.e., fractions containing endolysosomes (Figure 3.24B). Cathepsin B also distributed to a low-density lipid fraction, i.e., fraction 5, containing lipid microdomains. These data suggest that cathepsin B may localize to non-caveolar lipid microdomains in the plasma membrane of MDA-IBC-3 cells.

Treatment of IBC cells with lovastatin: a pharmacological approach to disrupt lipid microdomains. Statins are a class of drug primarily used in prevention, monitoring and treatment of cardiovascular disease. Statins prevent the catalysis of mevalonate by inhibiting the enzymatic activity of HMG-CoA reductase, an important rate-limiting step in the cholesterol biosynthesis pathway. Therefore, statins have lipid-lowering activity. Asymmetric distribution of cholesterol and other lipids in the plasma membrane results in lipid-enriched

domains or lipid rafts including caveolae (Simons and Ikonen, 1997; Simons and Toomre, 2000). Caveolae are a specialized and distinct type of lipid raft, which are highly enriched in and dependent on cholesterol for biosynthesis (Rothberg et al., 1992). We hypothesize that cholesterol depletion by statin drugs will disrupt lipid microdomains, including caveolae. Here we used a statin, lovastatin, as an alternative approach for testing our hypothesis that cell surface association of the cysteine protease cathepsin B, the serine proteases of the plasminogen cascade in caveolae enhances cell surface proteolysis, and ultimately, the aggressiveness of IBC cells.

Proliferation of IBC cell lines differs in response to lovastatin treatment. Statins have been reported to reduce proliferation of breast cancer cells *in vitro* and *in vivo* (Campbell et al., 2006). In the study by Campbell *et al.*, treatment with multiple statins, including lovastatin, inhibited growth of MDA-231, SKBr3 and MCF-7 cells. To determine the effects of lovastatin on growth of IBC cells, we performed MTT assays. Proliferation of SUM149, SUM190 and MDA-IBC-3 cells was quantified at 0, 24, 48 and 72 hours in the presence of 3 μM lovastatin or DMSO (vehicle control) (Figure 3.25). We observed no change in the proliferation of SUM190 cells at any time point (Figure 3.25B). A small, but insignificant, decrease in proliferation of SUM149 cells was observed, but only after treatment for 72 hours (Figure 3.25A). MDA-IBC-3 cells were most sensitive to lovastatin in that proliferation was significantly decreased beginning

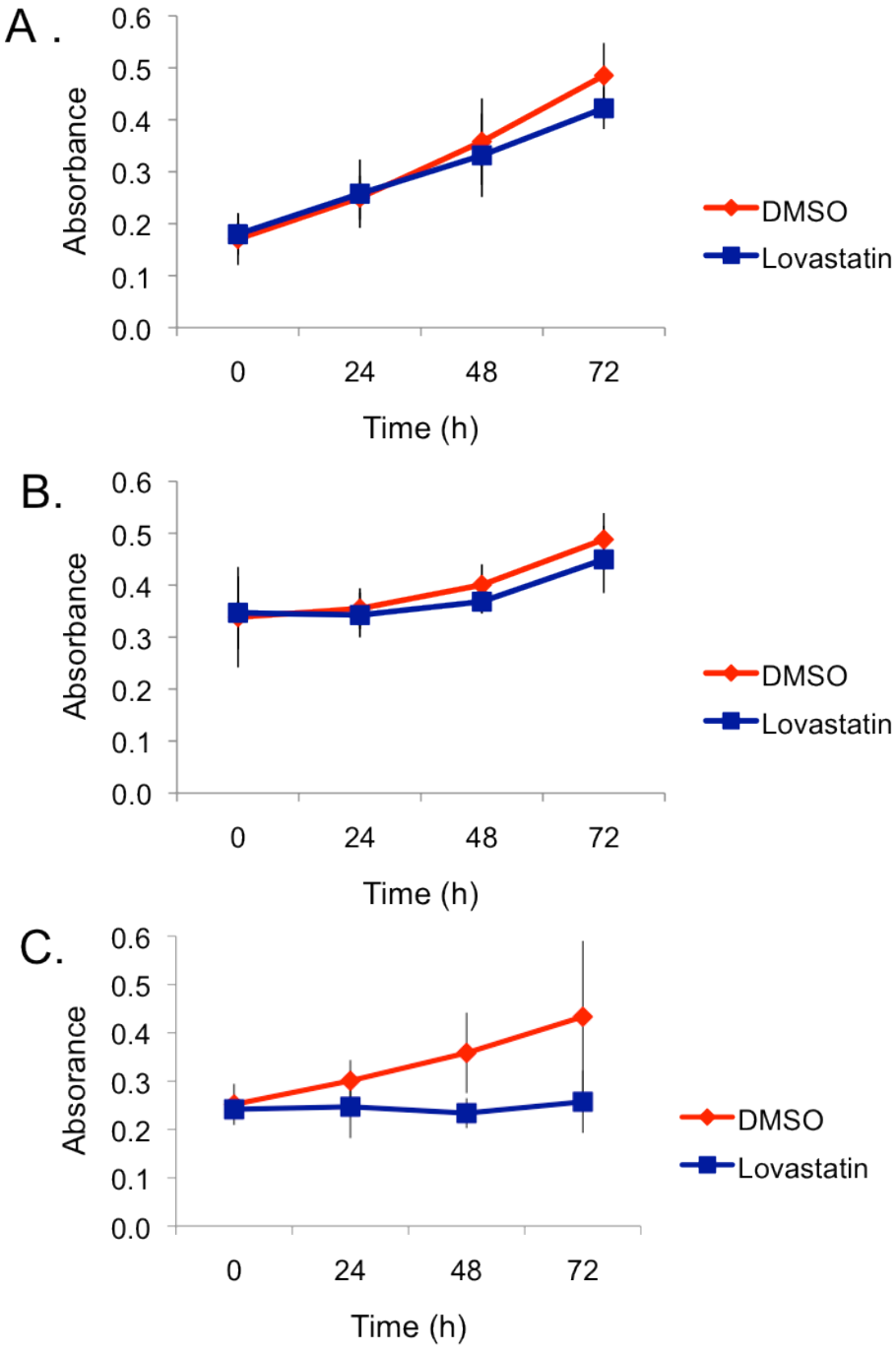
A .
Absorbance
0.6
0.5
0.4
0.3
0.2
0.1
0.0
0
24
48
72
Time (h)
DMSO
Lovastatin
B.
Absorbance
0.6
0.5
0.4
0.3
0.2
0.1
0.0
0
24
48
72
Time (h)
DMSO
Lovastatin
C.
Absorance
0.6
0.5
0.4
0.3
0.2
0.1
0.0
0
24
48
72
Time (h)
DMSO
Lovastatin

Figure 3.25. Lovastatin decreases proliferation of MDA-IBC-3 cells. (A) SUM149, (B) SUM190, and (C) MDA-IBC-3 cells were seeded in 96-well plates (5,000 per well) with 3 μM lovastatin or DMSO (vehicle control). At 0, 24, 48 and 72 h time points, 50 μl of MTT stock solution was added to each well and incubated at 37°C for 3 hours. Media was removed and 150 μl of DMSO added to each well dissolving the formazan precipitate. Absorbance values were measured at a 485-nm wavelength with a SpectraFluor Plus plate reader (Tecan, Salzburg, Austria). Results from three independent experiments are presented as mean ± SD.

48 hours after drug treatment (Figure 3.25C). These results indicate that the three IBC cells do not exhibit the same pattern of lovastatin responsiveness.

Lovastatin treatment of IBC cells decreases cathepsin B expression and activity. In models of cardiac hypertrophy and atherosclerosis, statin treatment has been shown to inhibit the expression and activity of proteases, including cathepsin B (Kim et al., 2009; Qin et al., 2010). We investigated the expression of cathepsin B protein in IBC cells following treatment with lovastatin. At 48, 72 and 96 hours, lysate samples were collected and assayed by SDS-PAGE and immunoblotting. We observed no changes in expression of cathepsin B in the presence of 1 μM lovastatin at any time point (data not shown). Three μM lovastatin did decrease levels of cathepsin B protein (Figure 3.26A). This effect of lovastatin treatment was not time-dependent as further decreases did not occur at 72 and 96 h, as assessed by densitometric analysis of immunoblots (data not shown). The differences in cathepsin B were most striking at the 48 hour time point (Figure 3.26B). We also measured intracellular cathepsin B activity in the lysates of lovastatin treated SUM149 cells. In agreement with the decreases in the mature (31 and 25/26 kDa) cathepsin B forms observed by immunoblotting, cathepsin B activity was reduced by treatment with lovastatin (Figure 3.26C). These findings were not exclusive to SUM149 cells; exposure to 3 μM lovastatin for 48 h reduced cathepsin B activity and protein levels in MDA-IBC-3 and modestly in SUM190 (Figure 3.27A-C) cells. The effect of lovastatin

A.

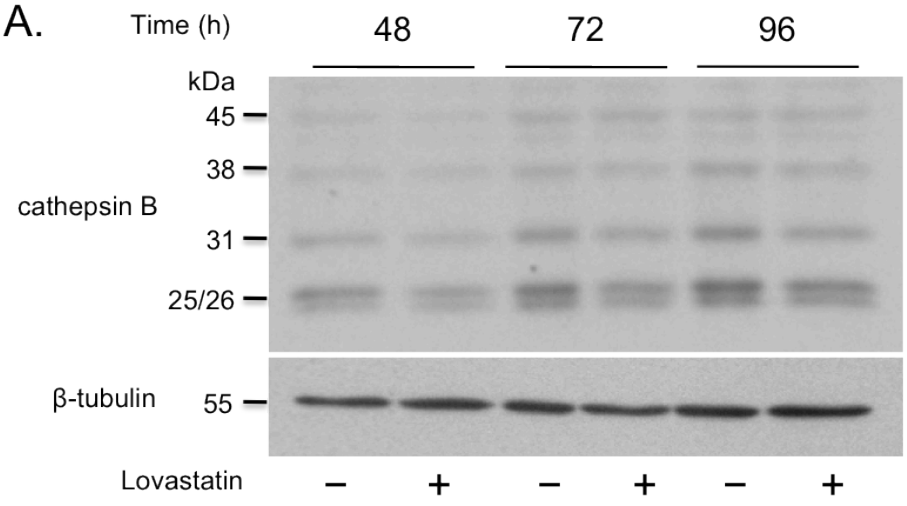
Time (h)
48
72
96
kDa
45
38
cathepsin B
31
25/26
β-tubulin
55
Lovastatin
–
+
–
+
–
+

B.

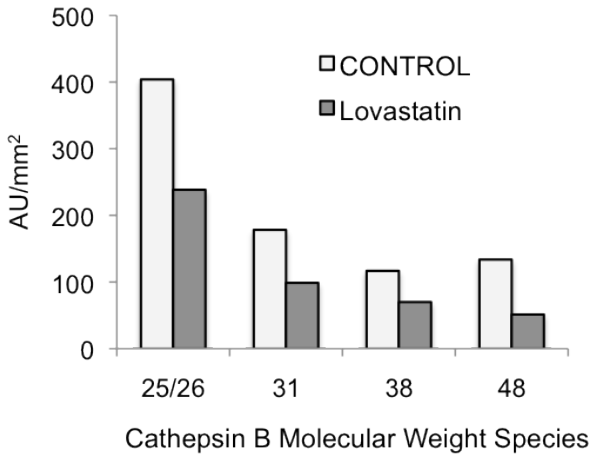
500
400
300
200
100
0
AU/mm²
CONTROL
Lovastatin
25/26
31
38
48
Cathepsin B Molecular Weight Species

C.

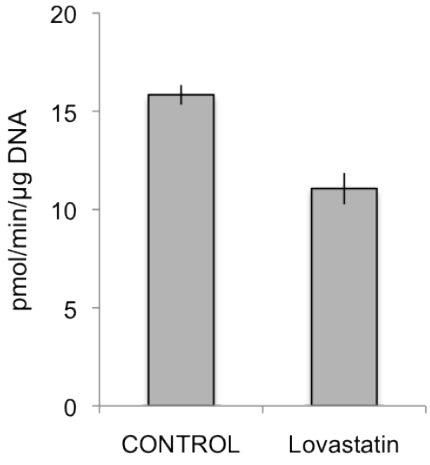
20
15
10
5
0
pmol/min/µg DNA
CONTROL
Lovastatin

Figure 3.26. Lovastatin treatment decreased cathepsin B expression and activity in SUM149 cells. 2D cultures of SUM149 were grown in the presence of 3 μM lovastatin for 48, 72 or 96 hours. (A) Lysates were equally loaded based on protein concentration and separated on 12% SDS-PAGE under reducing conditions. Proteins were transferred to nitrocellulose and immunoblotted with an anti-cathepsin B polyclonal antibody and anti-β-tubulin monoclonal antibody as a loading control. (B) Densitometric analysis (48 h exposure to lovastatin) of cathepsin B signal for the different molecular weight species of cathepsin B (expressed as AU/mm^2). Proform, 45 kDa; intermediate 38 kDa, single chain mature, 31 kDa; double chain mature, 25/26 kDa. (C) Enzymatic activity assay. Lovastatin treated and control SUM149 (48 hours) lysate samples were assayed for cathepsin B activity against the synthetic substrate Z-Arg-Arg-NHMec. Error bars represent standard deviation of three replicates in one experiment.

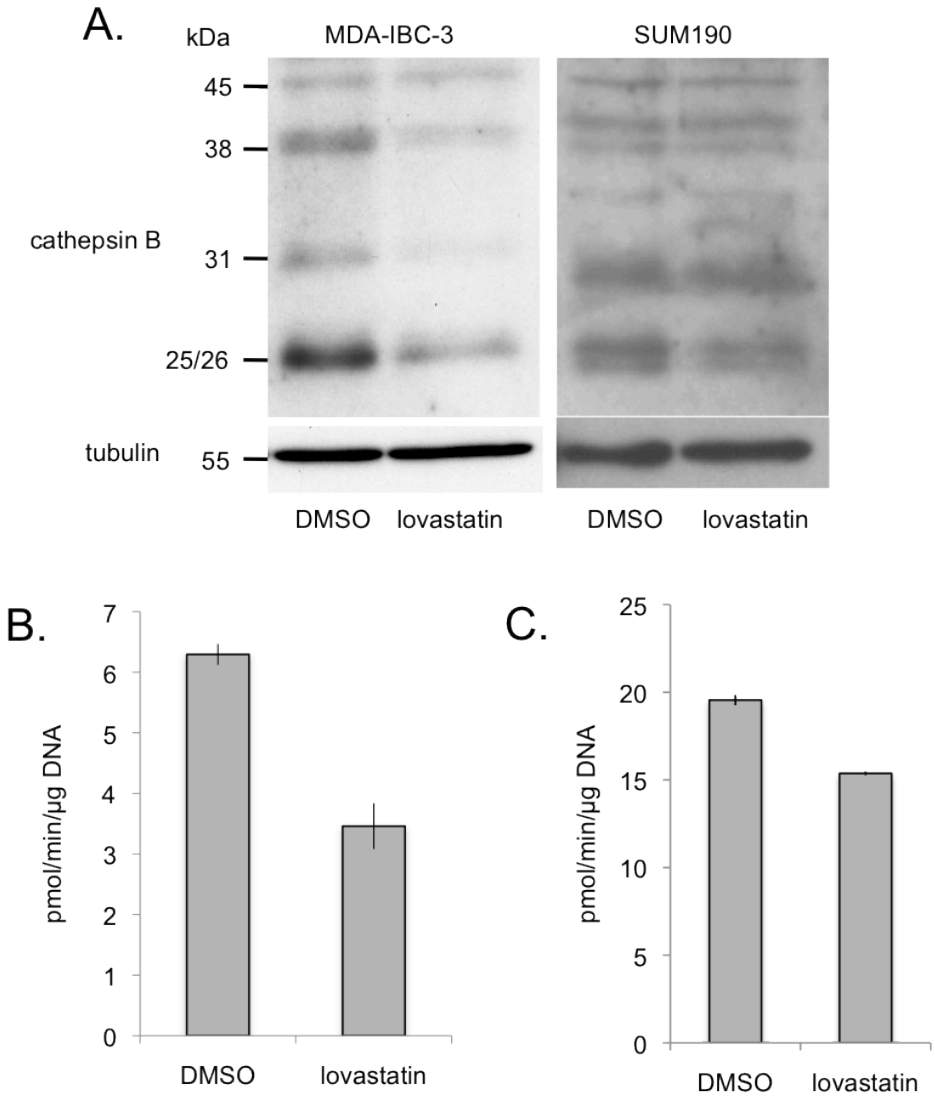

Figure 3.27. Lovastatin treatment decreased cathepsin B expression and activity in IBC cells. 2D cultures of MDA-IBC-3 and SUM149 cells were grown in the presence of 3 µM lovastatin for 48 hours. (A) Lysates were equally loaded based on protein concentration and samples were separated on 12% SDS-PAGE under reducing conditions. Proteins were transferred to nitrocellulose and immunoblotted with an anti-cathepsin B polyclonal antibody and anti-β-tubulin monoclonal antibody as a loading control. (B) MDA-IBC-3 and (C) SUM190 lysate samples were assayed for cathepsin B activity against the synthetic substrate Z-Arg-Arg-NHMec. Error bars represent standard deviation of three replicates in one experiment.

on cathepsin B protein and activity seems a general phenomenon since we observed similar results in three unrelated IBC cell lines.

Statins have shown promise in inhibiting fibrosis (Trebicka et al., 2010); proteases of the plasminogen cascade, including uPA, play a principal role in fibrinolysis. We also investigated if statin treatment can affect expression of uPA. Treatment with lovastatin reduced the amount of both secreted and intracellular uPA in SUM149 cells but no change was observed in its receptor uPAR (Figure 3.28).

Treatment with lovastatin decreases cholesterol in IBC cells. The fluorescent antifungal filipin has a high affinity for cholesterol or sterol molecules that contain a 3β-hydroxyl group and is commonly used to detect non-esterified cholesterol/sterols (Gimpl and Gehrig-Burger, 2007). Due to this property, filipin is widely used as a histochemical stain for cholesterol, e.g., filipin staining of cholesterol in cellular membranes is used as a diagnostic tool for Niemann-Pick disease (Ledvinova and Elleder, 1993). To further investigate the lipid lowering activity of lovastatin in IBC cells, SUM149 cells treated with 3 μM lovastatin or DMSO for 48 hours were fixed and stained with filipin III. In comparison to control cells, we observed decreased staining intensity for filipin III along the periphery of cells treated with lovastatin (Figure 3.29), indicative of decreases in total cellular cholesterol. These data provide an indirect indication that treatment

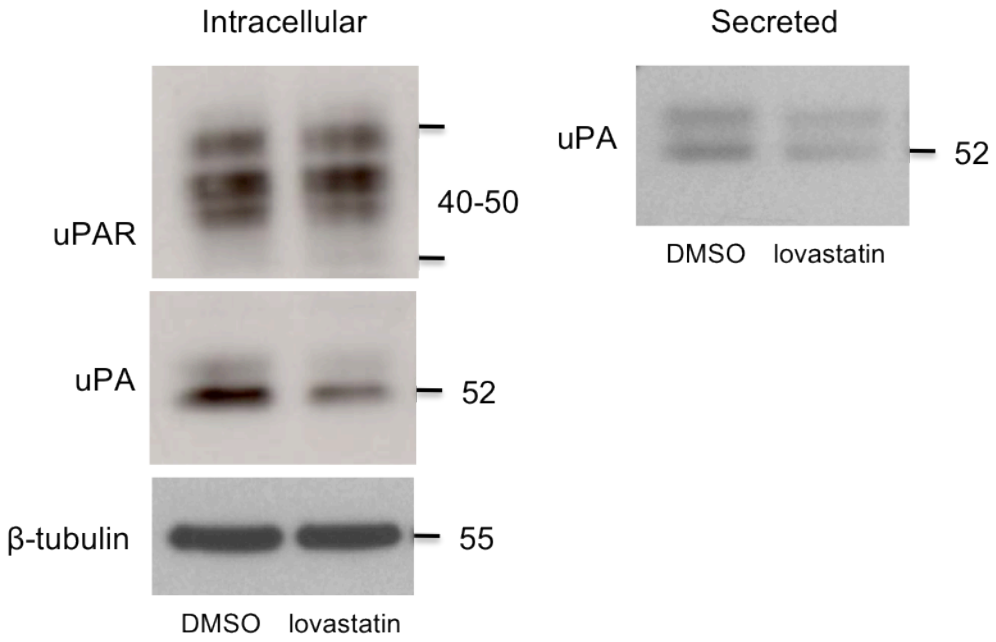

Figure 3.28. Lovastatin treatment decreases expression and secretion of uPA in SUM149 cells. Cell lysate (intracellular) and conditioned media (secreted) samples from 2D cultures of SUM149 treated with 3 μM lovastatin for 48 hours were separated on 12% SDS-PAGE under reducing conditions. Proteins were transferred to nitrocellulose and immunoblotted with an anti-uPA antibody, anti-uPAR and an anti-β-tubulin monoclonal antibody as a loading control.

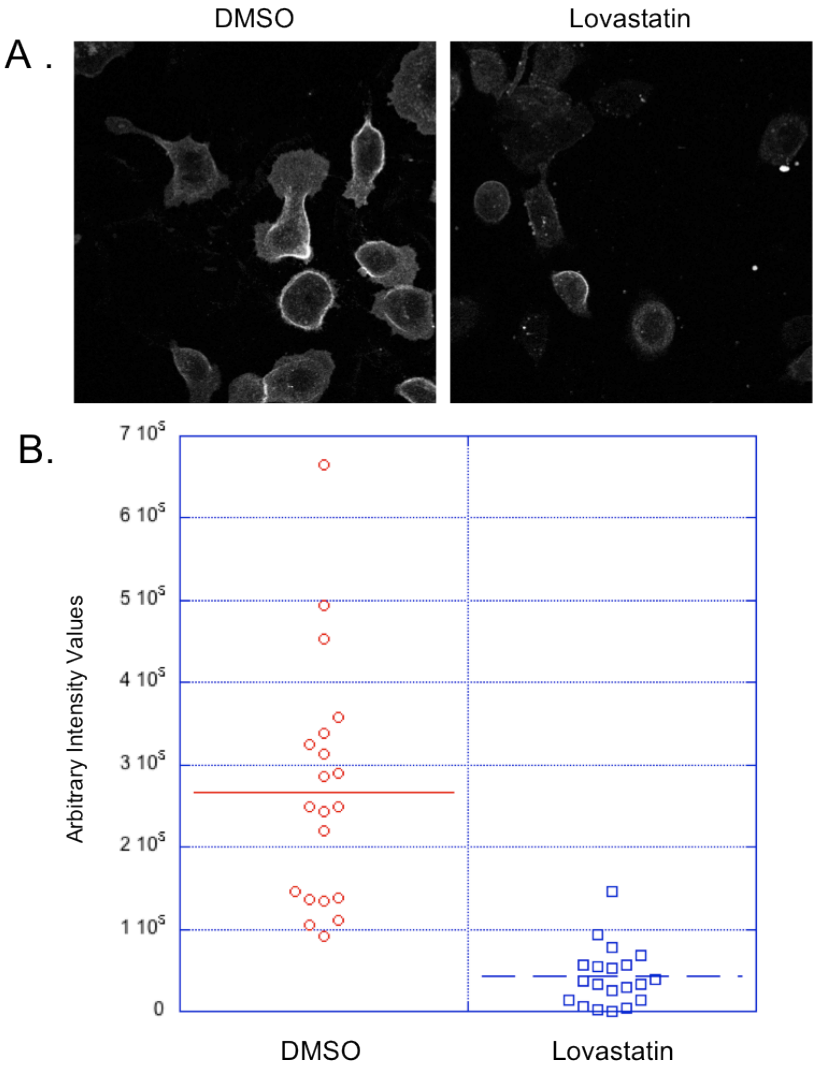

Figure 3.29. Lovastatin decreases cholesterol content in SUM149 cells. (A) Representative fluorescent images of SUM149 treated with 3 μM lovastatin or DMSO (vehicle control) for 48 hours and stained with filipin III. (B)Intensity of filipin III staining of SUM149 cells was analyzed with Metamorph software and represented as arbitrary intensity values (n=20).

with lovastatin decreased cholesterol in IBC cells and thereby affected lipid microdomains, including caveolae.

Lovastatin affects caveolin-1 levels in lipid-enriched fractions of SUM149 cells. Treatment with simvastatin, another member of the statin class of pharmaceuticals, decreases both cholesterol content and caveolin-1 expression in lipid fractions of human glioma cells (Wu et al., 2009). To determine if lovastatin elicits a similar effect on caveolin-1 in IBC cells, SUM149 cells were treated with lovastatin for 48 hours and subjected to subcellular fractionation on a sucrose gradient. Caveolin-1 primarily distributed to fractions 4-6 in control (DMSO) cells (Figure 3.30A) in agreement with previous data (Figure 3.3). We observed a decrease in the distribution of caveolin-1 to these lipid fractions when SUM149 cells were treated with lovastatin (Figure 3.30A). We also isolated caveolae-enriched fractions by a successive detergent based method: TS represents non-caveolae fractions and TI represents caveolae-enriched fractions. In the presence of lovastatin we observed decreased caveolin-1 in the TI fraction and a moderate increase in the TS fraction. This would be consistent with a change in localization of caveolin-1. In agreement with these data, we observed decreases in caveolin-1 localization when SUM149 were cells treated with lovastatin. The staining pattern for caveolin-1 in DMSO (diluent control) treated cells is along the plasma membrane. Following treatment with lovastatin,

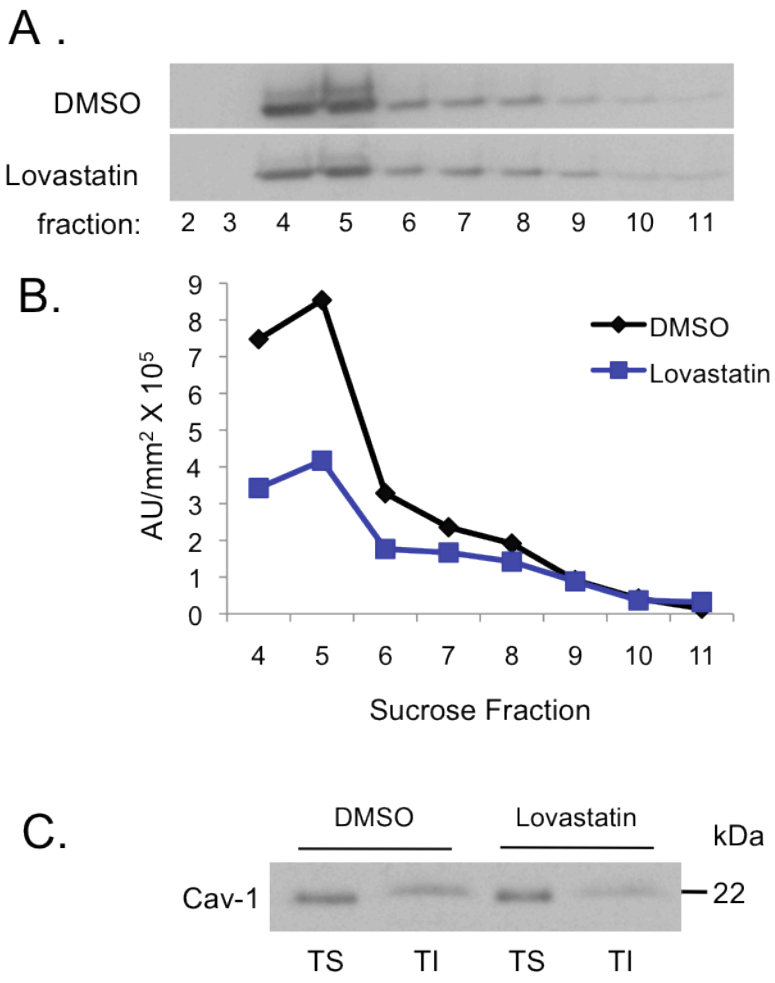

Figure 3.30. Lovastatin decreased caveolin-1 distribution to lipid fractions of IBC cells. SUM149 cells treated with 3 μM lovastatin or DMSO (vehicle control) for 48 hours were subjected to both non-detergent sucrose gradient (A) and detergent based (C) subcellular fractionations. Equal volumes of each fraction were analyzed by SDS-PAGE and immnoblotted for caveolin-1. (B) Protein bands were analyzed by densitometry. Graphical representation of caveolin-1 distribution in the sucrose gradient fractions.

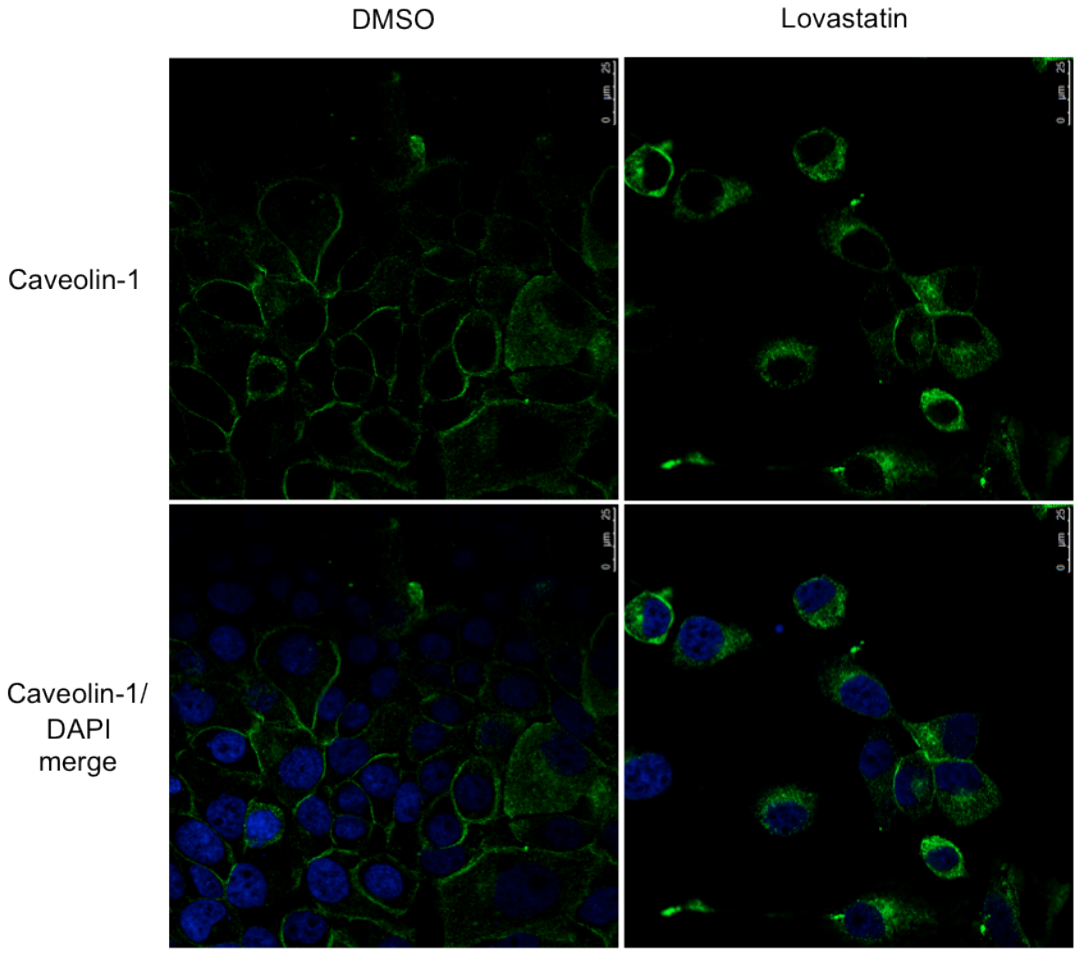

Figure 3.31. Immunostaining of lovastatin treated SUM149 reveals a decrease in caveolin-1 along the cell periphery. Immunostaining for caveolin-1 (green) was performed on permeabilized SUM149 monolayer cultures treated with 3 μM lovastatin or DMSO (vehicle control). Nuclei were stained with DAPI (blue). Confocal images were captured using a Leica TCS SP5 confocal microscope and 63X oil objective. Bar, 25 μm.

caveolin-1 staining exhibits a more cytoplasmic pattern with less staining at the plasma membrane (Figure 3.31).

Mevalonic Acid (MVA) rescues changes in cathepsin B subcellular distribution and decreases in cathepsin B activity in lovastatin treated IBC cells. Our knockdown studies revealed that cathepsin B membrane association is independent of caveolin-1 expression. However, lovastatin decreased cathepsin B protein levels, cholesterol content and caveolin-1 association with lipid fractions of IBC cells. To determine whether lovastatin affects the subcellular distribution of cathepsin B, 3D cultures of IBC cells were treated for 48 hours with 3 μM of drug and subjected to subcellular fractionation using the detergent based method. We also treated the cultures with MVA in the presence of lovastatin. HMG-CoA reductase, the direct target of statin drugs, catalyzes production of MVA in the cholesterol biosynthesis pathway. Therefore, we added exogenous MVA to test if this would rescue the lovastatin-induced phenotype. In agreement with the data in figure 3.4, cathepsin B was present in both the TS and TI fractions of SUM149 control (DMSO) cultures (Figure 3.32A). Treatment with lovastatin decreased the amount of cathepsin B in both the TS and TI fractions. MVA partially rescued the observed decreases (Figure 3.32A). We also performed this experiment of MDA-IBC-3 and SUM190 IBC cells. Similar to our findings in the SUM149 cultures, cathepsin B protein levels were decreased in both TS and TI fractions of MDA-IBC-3 cells when treated with lovastatin and

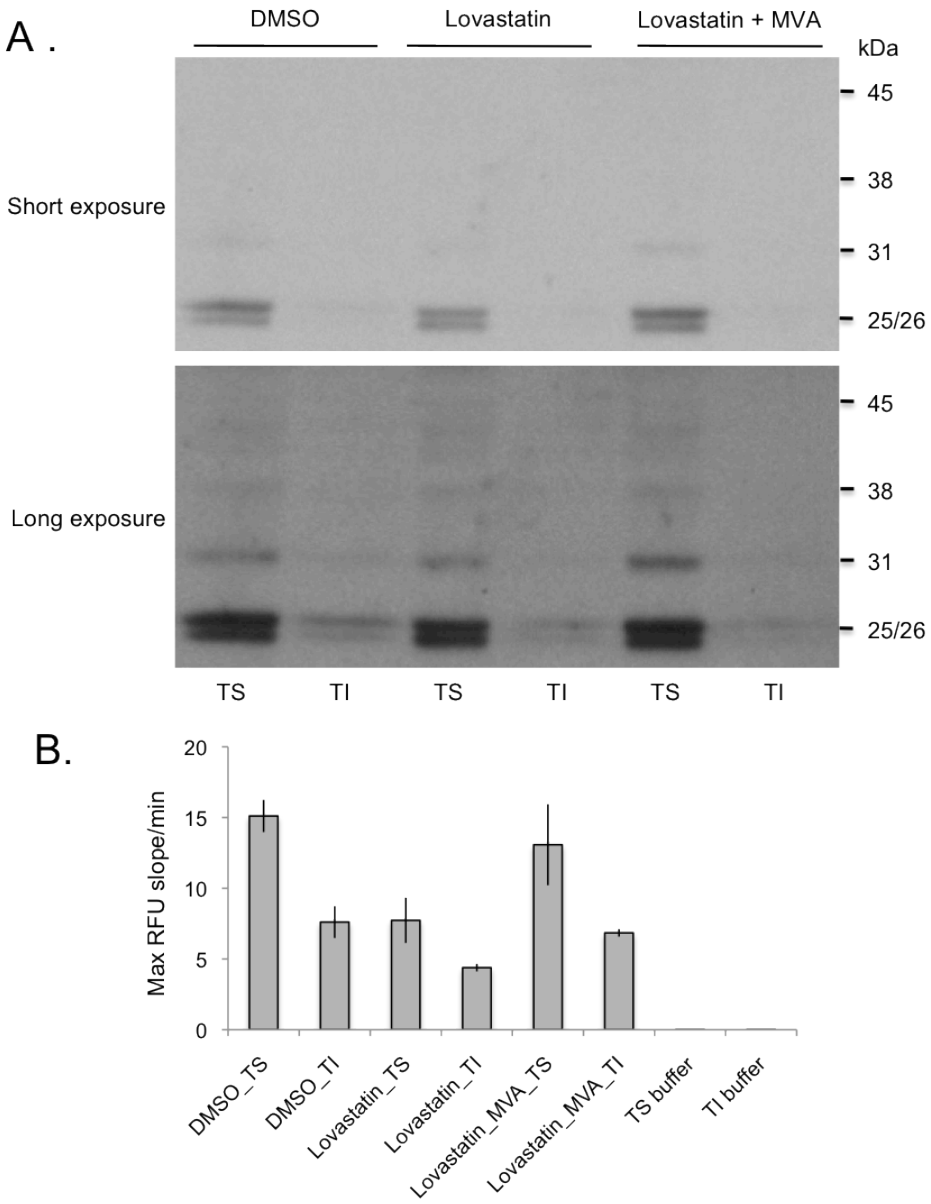

Figure 3.32. Mevalonic acid (MVA) partially rescues lovastatin-induced reduction of cathepsin B protein and activity in subcellular fractions of SUM149 3D cultures. SUM149 3D cultures were isolated by a detergent-based method, as described in Materials and Methods, that separate Triton X-100-soluble (TS) from Triton X-100–insoluble (TI) cellular fractions. (A) Equal volume aliquots of each fraction were analyzed by SDS-PAGE and immunoblotted with an antibody against cathepsin B. (B) TS and TI fractions were assayed for enzymatic activity against the synthetic cathepsin B substrate Z-Arg-Arg-NHMec. Cathepsin B activity in both TS and TI fractions was inhibited by 3 μM Lovastatin. MVA rescued this phenotype.

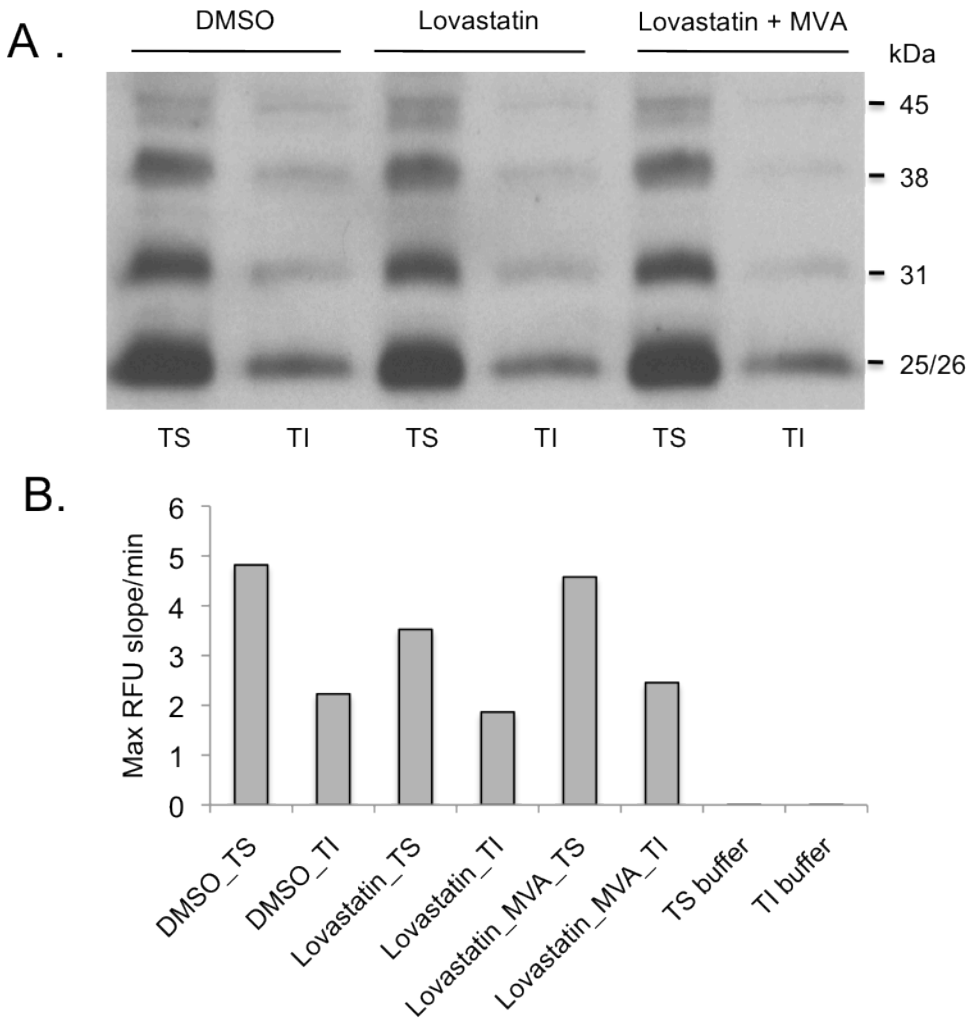

Figure 3.33. Mevalonate (MVA) partially rescues lovastatin-induced reduction of cathepsin B protein and activity in subcellular fractions of MDA-IBC-3 3D cultures. MDA-IBC-3 3D cultures were isolated by a detergent-based method, as described in Materials and Methods, that separate Triton X-100-soluble (TS) from Triton X-100–insoluble (TI) cellular fractions. (A) Equal volume aliquots of each fraction were analyzed by SDS-PAGE and immunoblotted with an antibody against cathepsin B. (B) TS and TI fractions were assayed for enzymatic activity against the synthetic cathepsin B substrate Z-Arg-Arg-NHMec. Cathepsin B activity in both TS and TI fractions was inhibited by 3 μM Lovastatin. MVA partially rescued this phenotype.

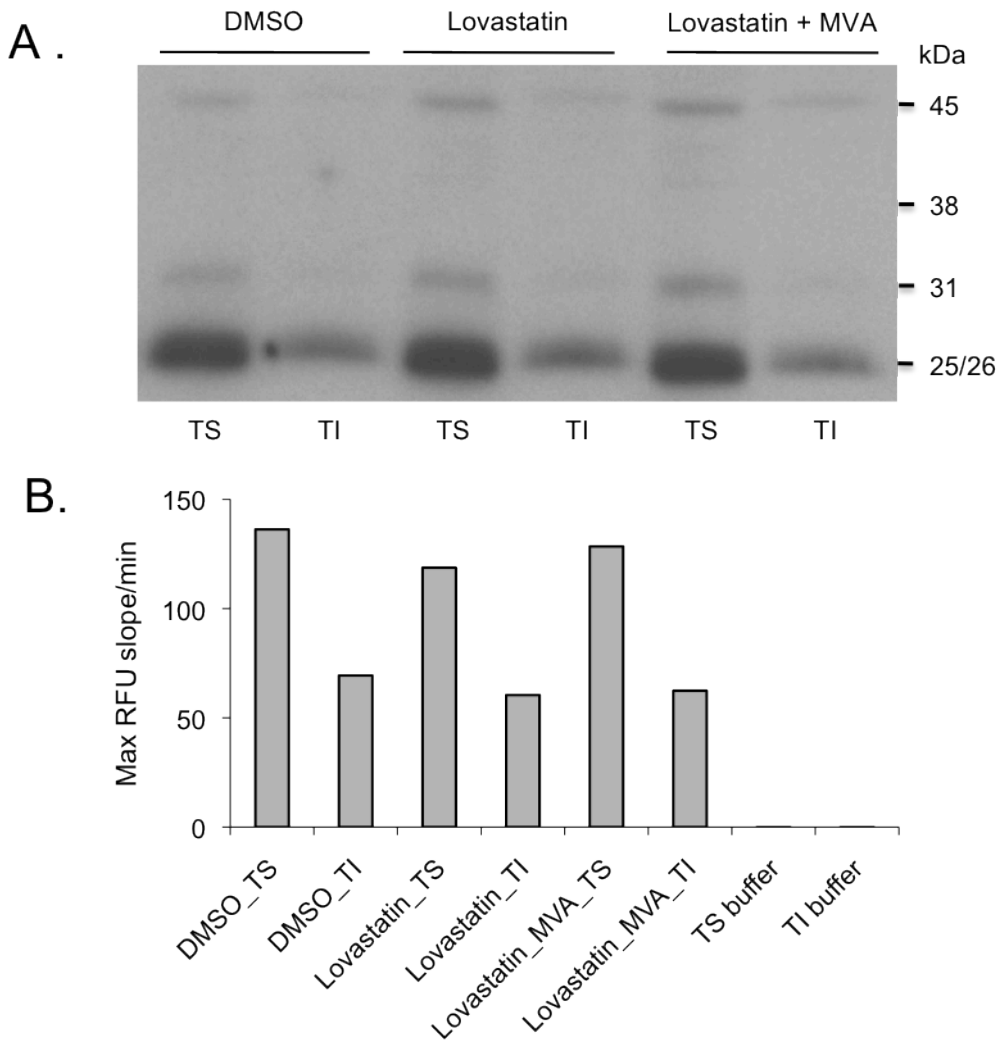

Figure 3.34. Lovastatin does not affect cathepsin B protein and activity in subcellular fractions of SUM190 3D cultures. SUM90 3D cultures were isolated by a detergent-based method, as described in Materials and Methods, that separate Triton X-100-soluble (TS) from Triton X-100–insoluble (TI) cellular fractions. (A) Equal volume aliquots of each fraction were analyzed by SDS-PAGE and immunoblotted with an antibody against cathepsin B. (B) TS and TI fractions were assayed for enzymatic activity against the synthetic cathepsin B substrate Z-Arg-Arg-NHMec. Cathepsin B activity in both TS and TI fractions was inhibited by 3 μM Lovastatin.

were modestly rescued by adding back exogenous MVA (Figure 3.33A). The SUM190 cells exhibited decreased sensitivity to lovastatin treatment in comparison to SUM149 and MDA-IBC-3 cells. Lovastatin treatment of SUM190 did not elicit the same decreases in cathepsin B protein levels or changes in subcellular distribution (Figure 3.34A).

Alterations in distribution of cathepsin B were further investigated by comparing the activity of cathepsin B in both TS and TI fractions of control, lovastatin treated cells and by adding MVA. We detected cathepsin B activity in both the TS and TI control fractions of all three IBC cell lines that were comparable to the levels of mature cathepsin B detected by immunoblotting (Figures 3.33B, 3.34B and 3.35B). Treatment with lovastatin reduced the activity of cathepsin B in both fractions of SUM149 and MDA-IBC-3 cultures but not in the SUM190 cells (Figure 3.34B). Addition of exogenous MVA in the presence of lovastatin partially restored the activity of cathepsin B in both the TS and TI fractions of SUM149 and MDA-IBC-3 cultures (Figures 3.32B and 33.3B).

Lovastatin treatment reduces type IV collagen degradation and invasion by IBC cells. Our subcellular fractionation and enzymatic assays indicated that active cathepsin B is associated with TI fractions of IBC cells. Lovastatin treatment diminished the levels of cathepsin B protein and activity in TI fractions. In addition, inhibiting cathepsin B activity significantly diminished degradation of DQ-collagen IV (Figure 3.6) and invasion (Figure 3.7), suggesting

that cathepsin B contributes to pericellular degradation and invasion by IBC cells. Therefore, we examined whether treatment with lovastatin would reduce degradation of DQ-collagen IV and invasion of IBC cells. For these studies, we used our live cell proteolysis assay to image the degradation of DQ-collagen IV by SUM149, MDA-IBC-3 and SUM190 cells grown for 48 hours and treated with 3 μM lovastatin or DMSO (vehicle control). Lovastatin significantly decreased the intensity of pericellular degradation products of DQ-collagen IV surrounding SUM149 3D structures (Figure 3.35A and B).

When grown in 3D rBM overlay cultures, MDA-IBC-3 cells form spheroid-like multicellular structures similar to those observed for SUM149 cells, yet exhibited a different pattern of proteolysis resembling that observed for SUM190 cells (Figure 3.2). The DQ-collagen IV cleavage products associated with MDA-IBC-3 structures appeared punctate or intracellular rather than pericellular (Figure 3.36). In addition, we observed the intensity of degradation products in MDA-IBC-3 cultures to be less than in SUM149 cultures, indicating that these cells degraded less collagen IV. Similar to the SUM149 cells, lovastatin treatment of MDA-IBC-3 cells changed cathepsin B subcellular distribution and decreased cathepsin B activity. When the MDA-IBC-3 cells were treated with lovastatin, degradation of DQ-collagen IV was not affected (Figure 3.36A and B). Degradation of DQ-collagen IV by SUM190 cells also was not affected by treatment with lovastatin (Figure 3.37A and B).

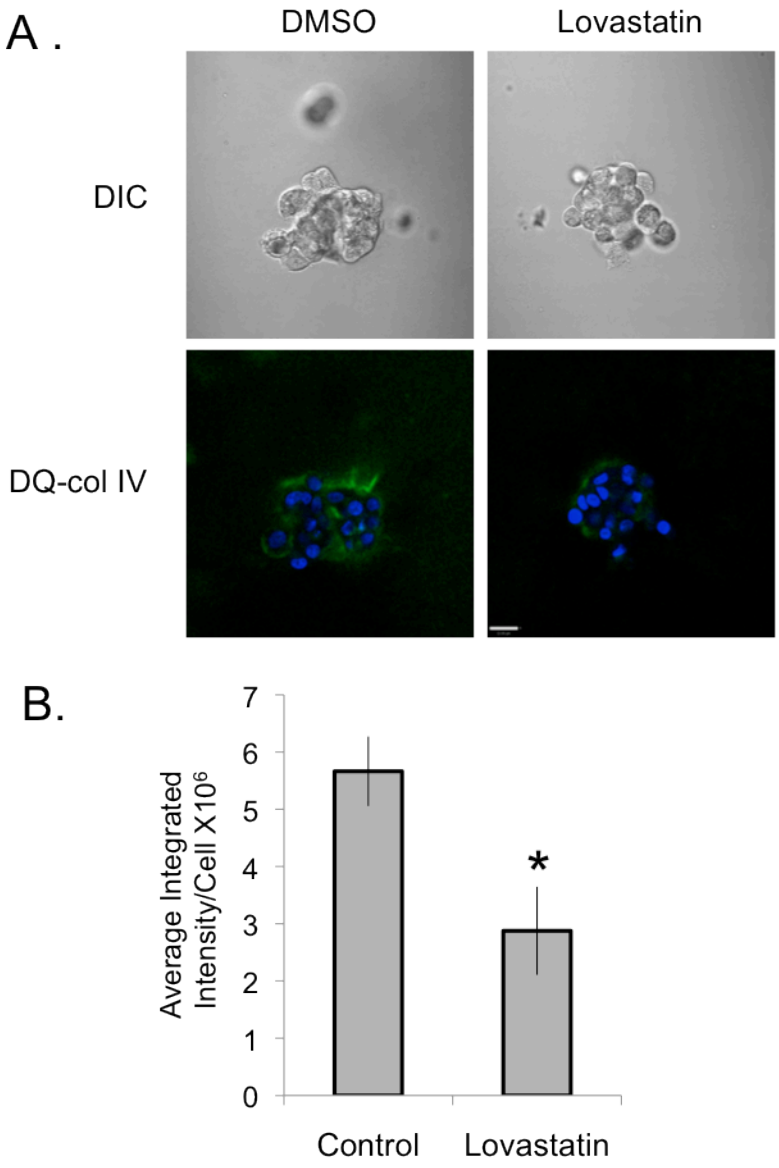

Figure 3.35. Lovastatin reduced degradation of DQ-collagen IV by SUM149 3D cultures. SUM149 cells grown in 3D rBM cultures containing DQ-collagen IV were treated with Lovastatin (3 μM) or DMSO (vehicle control) for 48 hours. (A) Representative confocal micrographs of the equatorial plane of the DQ-collagen IV degradation channel (green) and corresponding DIC channel are shown. Nuclei were stained with Hoechst (blue). Bar, 22 μm. (B) Data are represented as integrated fluorescence intensity due to proteolysis in the entire volume of 3D structures and was normalized to the number of cells. Results from three independent experiments are presented as mean ± SD; *, $P<0.008$ (Student's *t* test).

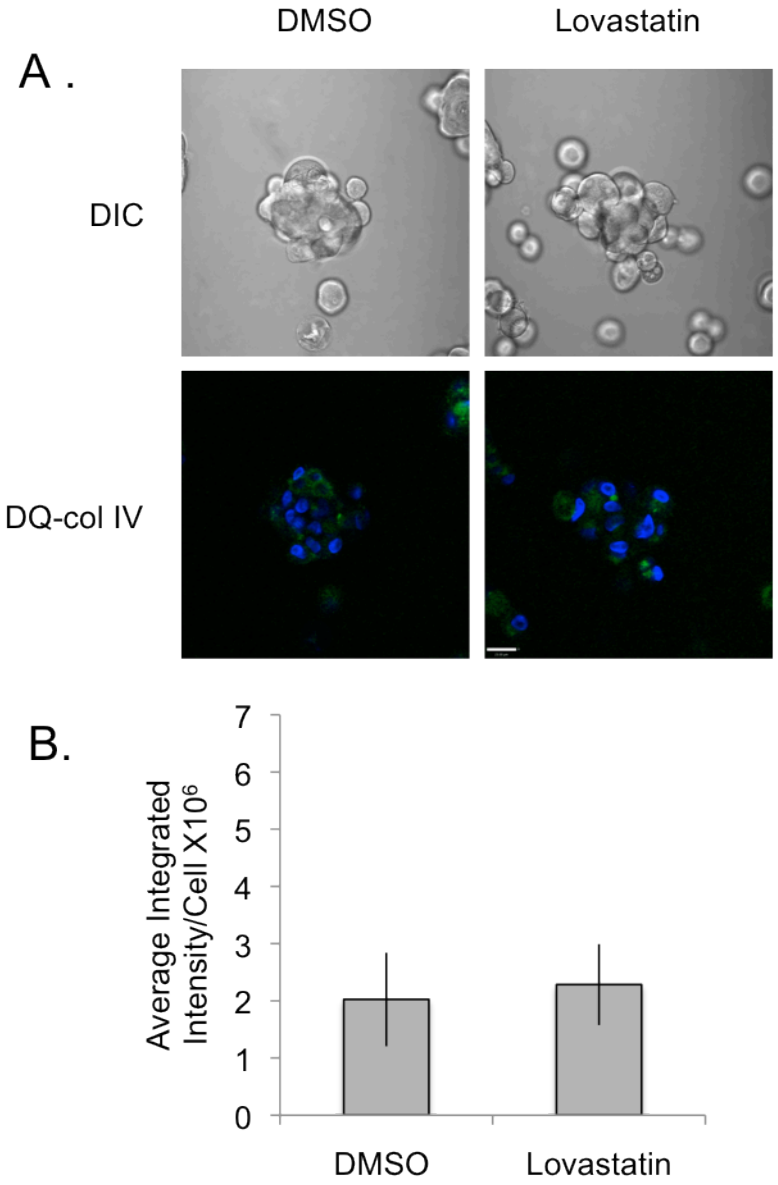

Figure 3.36. Lovastatin did not affect degradation of DQ-collagen IV by MDA-IBC-3 3D cultures. MDA-IBC-3 cells grown in 3D rBM cultures containing DQ-collagen IV were treated with Lovastatin (3 μM) or DMSO (vehicle control) for 48 hours. (A) Representative confocal micrographs of the equatorial plane of the DQ-collagen IV degradation channel (green) and corresponding DIC channel are shown. Nuclei were stained with Hoechst (blue). Bar, 23 μm. (B) Data are represented as integrated fluorescence intensity due to proteolysis in the entire volume of 3D structures and was normalized to the number of cells. Mean ± SD (n=8).

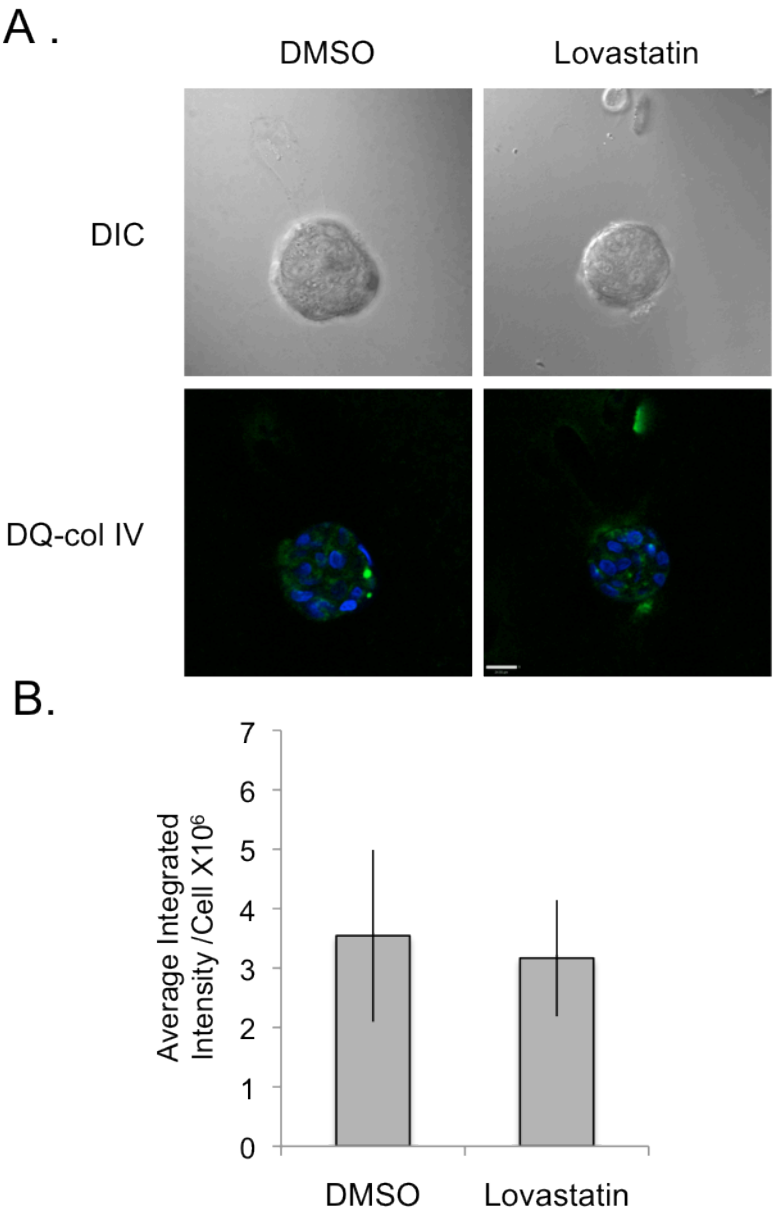

Figure 3.37. Lovastatin did not affect degradation of DQ-collagen IV by SUM190 3D cultures. SUM190 cells grown in 3D rBM cultures containing DQ-collagen IV were treated with Lovastatin (3 μM) or DMSO (Control) for 48 hours. (A) Representative confocal micrographs of the equatorial plane of the DQ-collagen IV degradation channel (green) and corresponding DIC channel are shown. Nuclei were stained with Hoechst (blue). Bar, 24 μm. (B) Data are represented as integrated fluorescence intensity due to proteolysis in the entire volume of 3D structures and was normalized to the number of cells. Results from three independent experiments are presented as mean ± SD.

Since lovastatin treatment significantly decreased the degradation of collagen IV by SUM149 cells, we also measured the effect the drug may have on invasiveness. For these studies, we performed invasion assays as previously described for the caveolin-1 knockdown studies [see page 76]. Briefly, equal numbers of SUM149 cells were suspended in serum free media and seeded on transwell filters coated with rBM. Medium containing serum, to stimulate invasion, was added to the chamber below the filter. Cells were incubated with lovastatin, lovastatin plus exogenous MVA, or DMSO (vehicle control) for 24 hours and the number of invaded cells was counted. Invasion of SUM149 cells was significantly reduced by lovastatin (Figure 3.38A and B). When MVA was added in the presence of lovastatin, IBC cells invaded comparably to the vehicle controls. Invasion assays were also performed with the other IBC cell lines; however, neither the MDA-IBC-3 or the SUM190 cells invaded under control conditions, even up to 5 days following their initial seeding.

Mevalonic Acid (MVA) rescues changes in EGFR subcellular distribution in lovastatin treated IBC cells. Knockdown of caveolin-1 in SUM149 cells decreased the localization of EGFR to caveolae-enriched subcelluar fractions (Figure 3.23). Lovastatin treatment also decreased caveolin-1 association with lipid microdomains of SUM149 cells. To investigate if lovastatin treatment also exerts this same affect on EGFR, we examined the subcellular distribution of EGFR in 3D cultures of SUM149 cells. When treated

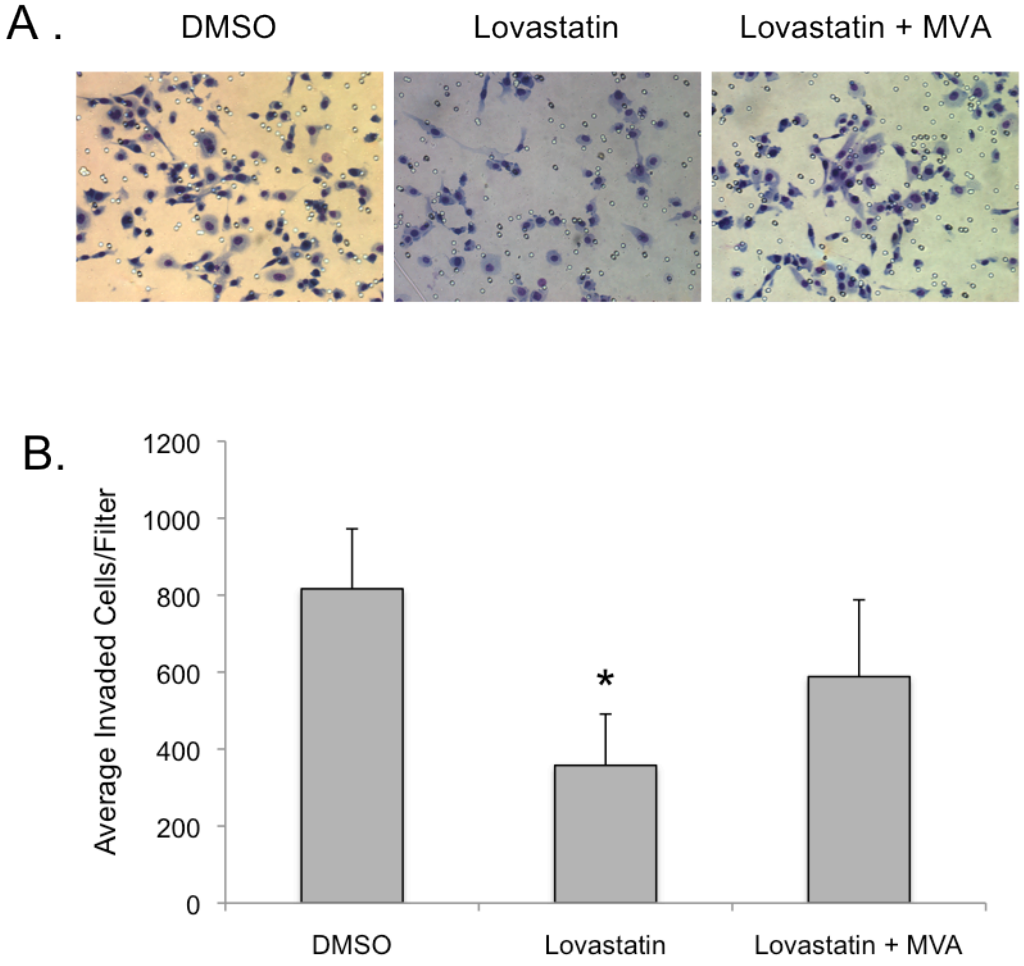

Figure 3.38. Lovastatin inhibits invasion of SUM149 cells. SUM149 cells were subjected to transwell invasion assays in the presence of DMSO (vehicle control), 3 μM Lovastatin or 3 μM Lovastatin + 1 mM MVA. (A) Images are SUM149 cells that have invaded through rBM-coated filters; bar, 150 μm. (B) Quantification of invaded cells was performed by counting the average number of invaded cells per filter (using Image J software). Results from three independent experiments are presented as mean ± SD; *, P< 0.001.

with lovastatin, less EGFR localized to the TI fraction in comparison to DMSO (vehicle control) controls (Figure 3.39). MVA rescued the observed decreases.

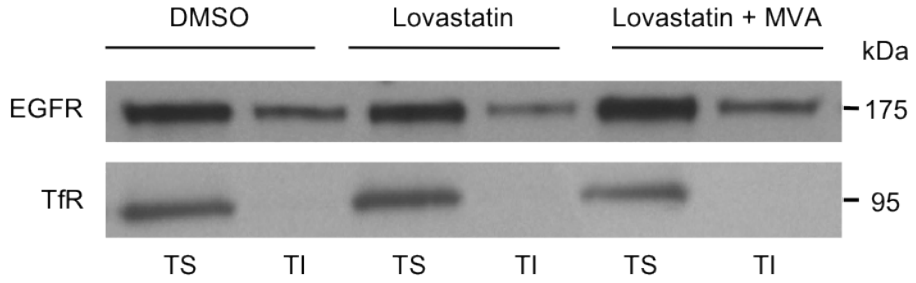

Figure 3.39. Mevalonic acid (MVA) rescues lovastatin-induced reduction of EGFR in subcellular fractions of SUM149 3D cultures. SUM149 3D cultures were isolated by a detergent-based method, as described in Materials and Methods, that separate Triton X-100-soluble (TS) from Triton X-100–insoluble (TI) cellular fractions. Equal volume aliquots of each fraction were analyzed by SDS-PAGE and immunoblotted with antibodies against EGFR and transferrin receptor (TfR). TfR is a negative control for lipid rafts. MVA rescued this phenotype.

CHAPTER 4

DISCUSSION

IBC is a rare but highly aggressive form of breast cancer with symptoms that develop rapidly (i.e., weeks or months) after initial diagnosis (Vermeulen et al., 2009). Current treatments for IBC are very limited so new therapeutics are needed, specifically therapies directed against pathways that mediate the aggressive IBC phenotype. Proteolytic activity is one important mediator of the invasion and metastatic spread that are hallmarks of aggressive cancer (Hanahan and Weinberg, 2011). Proteases of multiple catalytic classes are associated with caveolae, i.e. serine (Stahl and Mueller, 1995), cysteine proteases (Cavallo-Medved et al., 2005; Cavallo-Medved et al., 2009) and MMPs (Annabi et al., 2001; Puyraimond et al., 2001). Caveolin-1 is a necessary structural and functional component of caveolae. Caveolin-1 is highly expressed in and a potential marker of IBC *in vivo* (Van den Eynden et al., 2006; Nouh et al., 2011). Our approach in this study was to investigate which proteases expressed by IBC cells are associated with caveolae, participate in ECM degradation and invasion by IBC cells and are present in IBC patient samples.

Our findings implicate cathepsin B and uPA as contributors to a proteolytic pathway that mediates the aggressive IBC phenotype. Cathepsin B had previously been shown to activate pro-uPA, a serine protease and member of the plasminogen cascade involved in ECM degradation, matrix metalloproteinase

activation and tumor cell invasion (Kobayashi et al., 1991). In SUM149 cells, uPA and its receptor uPAR colocalize with active cathepsin B in caveolae (Figures 3.4 and 3.5). The presence of active cathepsin B in caveolae of IBC cells suggests a potential role for this enzyme in pericellular proteolysis as was previously shown in colon carcinoma cells (Cavallo-Medved et al., 2005). Downregulation of caveolin-1 in the colon carcinoma cells decreases cathepsin B localization to caveolae in parallel with decreases in ECM degradation and cell invasion (Cavallo-Medved et al., 2005). In the SUM149 cells used in this study, which express both cathepsin B and caveolin-1, we determined that degradation of type IV collagen was predominantly pericellular and that a cell impermeant cathepsin B inhibitor reduced degradation of type IV collagen and invasion (Figures 3.6 and 3.7). Although significant, the lack of complete inhibition suggests that cathepsin B was only one of several proteases in the SUM149 cells that degrade type IV collagen and mediate invasion. Others have established that cathepsin B interacts with other proteases in mediating invasion. For example, Rao and colleagues have demonstrated that downregulation of both cathepsin B and uPAR more effectively reduces invasion of human glioma cells *in vitro* and *in vivo* in an intracranial xenograft model than does downregulation of either protease alone. Furthermore, downregulation of both cathepsin B and matrix metalloproteinase 9 (MMP9) reduces invasion of prostate tumor cells *in vitro* and tumor growth *in vivo* more effectively than downregulation of either one of the two proteases (Nalla et al., 2010). These studies confirm that

proteases function in concert, and not alone, to facilitate neoplastic progression.

Proteases can exhibit functional redundancy, including cysteine cathepsins (Nagler and Menard, 2003; Mohamed and Sloane, 2006). A striking example occurs between cathepsin B and cathepsin X. Active cathepsin X is redistributed to the surface of MMTV-PyMT mammary tumor cells deficient in cathepsin B. Moreover, cathepsin X neutralizing antibodies reduce invasion of the cathepsin B-deficient mammary tumor cells, consistent with cathepsin X compensating for the absence of cathepsin B (Vasiljeva et al., 2006).

The studies above illustrate that observations from *in vitro* assays such as invasion and ECM degradation assays can be meaningful surrogates for *in vivo* tumor endpoints. In a recent collaborative study (N Withana, BF Sloane and BS Parker, unpublished observations), we demonstrated that either knockdown or inhibition of cathepsin B in 4T1 mammary carcinoma cells reduced collagen degradation *in vitro*, as assessed by our live-cell proteolysis assay, and bone metastasis *in vivo*. Here in the three IBC cell lines, we observed differences in the degradation of type IV collagen in our live-cell proteolysis assay (Figures 3.2 and 3.36). These differences were further supported by variations in expression of caveolin-1, cathespin B and uPA, secretion of cathepsin B and uPA and expression of known caveolae associated proteins, i.e. uPAR and β1-integrin (Figures 3.1 and 3.24). We propose that these differences may be due, in part, to the differences in receptor status of the three IBC cell lines. Although all three lack estrogen and progesterone receptors, only SUM149 is HER2 negative and

thus a triple negative breast cancer cell line. Triple negative breast cancer is a subtype of breast cancer characterized as extremely aggressive and having a poor prognosis due to difficulties in treating and high risks of both recurrence and death (Dawson et al., 2009; Venkitaraman, 2010). A role for cathepsin B has previously been reported in several triple negative breast cancer cell lines that are not IBC (e.g., BT20, BT549, MCF-10AneoT, and MDA-MB-231) (Sameni et al., 2000; Kos et al., 2005; Gianotti et al., 2008; Gillet et al., 2009); inhibition of cathepsin B activity in these cells reduced their invasion *in vitro*. *In vivo* studies also provide evidence for an association between cathepsin B and breast cancers that are triple negative (Prud'homme et al., 2010) (N Withana, BF Sloane and BS Parker, unpublished observations). In addition, a transgenic mouse model of mammary cancer characterized by loss of hormone receptors with progression of disease (Maglione et al., 2001) exhibits both reduced primary tumor growth and lung metastases when deficient in cathepsin B (Vasiljeva et al., 2008), suggesting a link between cathepsin B and metastatic breast disease. This may be especially true in IBC as expression of cathepsin B was found to be positively correlated with lymph node metastasis in IBC tissues, a correlation not observed in non-IBC tissues (Nouh et al., 2011). As such, cathepsin B has been proposed to be a prognostic marker for IBC and potentially a component of a proposed molecular signature for IBC (Nouh et al., 2011), a signature that already includes caveolin-1 (Van den Eynden et al., 2006). Our current findings show that cathepsin B and caveolin-1 were co-expressed in tumor cells of IBC

patient samples and not in those of non-IBC patients (Table 3.1). Ongoing work will determine if this co-expression is elevated in non-IBC triple-negative breast cancers.

Another enzyme implicated in the aggressive IBC phenotype is RhoC GTPase, which is increased in expression and activity (Kleer et al., 2004; Wu et al., 2010). We speculate that there may be a network that links proteases, caveolin-1 and Rho signaling pathways in IBC. In colon, prostate and non-IBC tumors, phosphorylated caveolin-1 has been shown to promote migration and invasion via a Rho signaling pathway (Joshi et al., 2008); this has not yet been assessed in IBC. Rho signal transduction pathways have been shown to enrich localization of mRNAs to cellular protrusions, pseudopodia, thought to play a role in translation of signaling cascades involved in tumor cell migration and metastasis (Stuart et al., 2008). Both cathepsin B and RhoC localize and function in podosome or invadopodia mediated tumor cell migration and invasion (Tu et al., 2008; MacGrath and Koleske, 2011). A P132L mutation in caveolin-1 confers a dominant-negative effect on invasiveness of human scirrhous breast cancers (Hayashi et al., 2001) and upregulates genes involved in invasiveness and metastasis, including Rho-related signaling molecules and genes expressed by stem cells (Bonuccelli et al., 2009). Studies in MDA-MB-231 breast carcinoma cells connect Rho, caveolin-1 and cathepsin B (Bourguignon et al., 2004). Rho kinase signaling events, mediated upstream by CD44-NHE1 interactions localized to lipid microdomains containing caveolin-1, result in

acidification of the microenvironment surrounding breast cancer cells, activate secretion of cathepsin B and promote cellular invasiveness. We have previously shown that slight acidification of the microenvironment of a variety of tumors (melanoma, colon and breast) increases secretion and activity of cathepsin B and proteolysis of type IV collagen (Rozhin et al., 1994; Robey et al., 2009; Rothberg et al., 2011). Whether there is a universal link between Rho, caveolin-1, cathepsin B and acidification of the tumor microenvironment has not yet been evaluated.

One goal of this study was to determine whether cell surface associations of proteolytic networks in caveolae enhance the aggressiveness of IBC. Our experimental approach was to downregulate expression of caveolin-1, a necessary structural and functional component of caveolae, in IBC cells. Two of the six shRNAmir clones tested, clones C8 and F2, diminished caveolin-1 protein levels approximately 40 and 95%, respectively (Figure 3.11B). Distribution of caveolin-1 to lipid enriched fractions was also decreased in knockdown SUM149 cells (Figure 3.14). We hypothesize that loss of caveolin-1 expression correlates with reduced caveolae biogenesis and thus a loss of caveolae present at the cell surface of SUM149 cells. This conclusion is consistent with previous reports in which downregulation of caveolin-1 significantly reduced the number of cell surface caveolae (Griffoni et al., 2000; Cho et al., 2003). We found that knockdown of caveolin-1 did not affect the subcellular distribution of cathepsin B. These results indicate that cathepsin B localization to lipid microdomains at the

cell surface of SUM149 cells is independent of caveolin-1 expression. This is consistent with our findings in the SUM190 and MDA-IBC-3 cell lines, which do not express caveolin-1. Cathepsin B is associated with non-caveolar lipid microdomains of both SUM190 cells (Cavallo-Medved, unpublished data) and MDA-IBC-3 cells (Figure 3.24). In contrast, knockdown of caveolin-1 did decrease the association of both uPA and EGFR with caveolar lipid microdomains. This suggests that the cell surface associated uPA and EGFR is mediated by the expression of caveolin-1 in SUM149 cells and that both proteins compartmentalize in caveolae. The available evidence support that some EGFR does localize to caveolae (Smart et al., 1995; Mineo et al., 1996). That said, there is conflict in the literature regarding the quantity of EGFR present in caveolae and conditions under which EGFR is found in caveolae [for review, see (Balbis and Posner, 2010)]. Caveolin-1 has been shown to function in uPAR-dependent activation of integrins α5 and β1, Src and EGFR (Monaghan-Benson et al., 2008). Monaghan-Benson and colleagues also report that phosphorylated caveolin-1 directs the trafficking of EFGR to focal adhesions.

Our findings demonstrated that knockdown of caveolin-1 decreased degradation of DQ-collagen IV and reduced invasion by SUM149 cells (Figures 3.18 and 3.19). This was true for clone F2, in which there was a greater reduction of caveolin-1 (cf. Figure 3.11 and Figure 3.14). In other studies, threshold levels of caveolin-1 protein expression have been shown to be required for the formation of caveolae at the plasma membrane (Fra et al., 1995; Breuza

et al., 2002). Perhaps caveolae biogenesis persists in the clone C8 knockdown cells; verification by means of electron microscopy would be necessary to validate this hypothesis.

Caveolin-1 oligomers can form functional plasma membranes domains other than caveolae (Head and Insel, 2007). Caveolin-1 is targeted, in a cell specific manner, to other intracellular compartments such as secretory vesicles, mitochondria and the cytoplasm (Li et al., 2001). Caveolin-1 is also a component of a cytosolic heat-shock protein chaperone complex functioning in transport of cholesterol from the ER to caveolae (Uittenbogaard et al., 1998). Caveolin-1 complexes with lipoproteins, is localized to the secretory pathway and secreted by pancreatic and exocrine cells (Liu et al., 1999). In addition, via a scaffolding domain of 20 amino acids located in the cytosolic N-terminus region, caveolin-1 interacts with several signaling molecules including Src tyrosine kinases, G alpha subunits, H-Ras, nitric oxide synthase and G-protein-coupled receptors (Li et al., 1995; Li et al., 1996; Garcia-Cardena et al., 1997). Indeed, multiple functions have been attributed to caveolin-1 that may be independent of caveolae [for review, see (Liu et al., 2002a)]. The many other functions of caveolin-1 cannot be ruled out as possibly contributing to the aggressiveness of IBC and warrant further investigation.

Our data indicate that the cysteine protease cathepsin B participates in degradation of type IV collagen and invasion by IBC cells, likely through its association with proteolytic networks in lipid microdomains at the cell surface.

Knockdown of caveolin-1 also resulted in decreases in degradation of type IV collagen and invasion by IBC cells. Our original hypothesis was not valid in that cathepsin B does not localize specifically to caveolae since downregulating caveolin-1 did not affect its association with caveolae. Therefore we conclude that cathepsin B and caveolin-1 both contribute to the aggressiveness of IBC, but do so by different mechanisms.

Statins directly target the activity of HMG-CoA reductase, the rate-limiting enzyme in the metabolic pathway that leads to production of cholesterol and other isoprenoids. High blood cholesterol is a risk factor for cardiovascular disease, the number one cause of mortality world wide, and statins are important in the treatment of this disease (Taylor et al., 2011). Interestingly, statins are associated with pleiotropic beneficial effects including improvement of endothelial dysfunction, increased nitric oxide bioavailability, antioxidant and anti-inflammatory effects (Davignon, 2004). The multifaceted effects of statins have led to investigating their potential use in the prevention and treatment of cancer. Long term statin use for five or more years does not reduce the incidence of most cancers, including breast cancers (Jacobs et al., 2011). Nonetheless, *in vitro* and *in vivo* studies indicate statins may be a useful therapeutic for treatment of breast cancer [for review see, (Demierre et al., 2005). Here as an alternative approach to disrupt lipid microdomains, including caveolae, and thereby test our hypothesis, we treated IBC cells with a statin drug, lovastatin, to decrease cholesterol biosynthesis.

Statins have anti-proliferative affects on breast cancer cells *in vitro* and *in vivo* (Rao et al., 1999; Campbell et al., 2006). In the present study, lovastatin elicited different effects on IBC proliferation as assessed by MTT assays (Figure 3.25). The MDA-IBC-3 cells were most sensitive to the drug, whereas SUM149 and SUM190 proliferation was unaffected. Campbell *et al.* (Campbell et al., 2006) found that hormone receptor and ErbB2 status may be indicators of responsiveness to statin treatment. In a recent clinical trial in which breast cancer patients were treated with fluvastatin, there was significantly reduced proliferation and increased apoptosis in tumors that were high grade as compared to low grade tumors (Garwood et al., 2010).

Cysteine cathepsins, including cathepsin B, play a potentially significant role in development and progression of many cardiovascular diseases [for review, see (Lutgens et al., 2007)]. In a murine model of atherosclerosis increased cathepsin B message and protein levels are associated with highly inflammatory lesions (Chen et al., 2002) and treatment with statins reduces cathepsin B expression and activity in these lesions (Kim et al., 2009). These same effects of statins are not specific to cysteine cathepsins but also extend to other classes of proteases, including both serine proteases (Denoyelle et al., 2001) and MMPs (Thunyakitpisal and Chaisuparat, 2004; Abisi et al., 2008). In our cultures of IBC cells, lovastatin decreased cathepsin B expression and activity (Figures 3.26 and 3.27). In addition, lovastatin treatment diminished both the protein level and activity of cathepsin B in both TS and TI fractions of 3D

cultures of IBC cells (Figures 3.32 and 3.33). These data indicate that lovastatin is capable of reducing the association of cathepsin B with membrane lipid microdomains. These findings are particularly interesting because we confirmed a functional role for cell surface cathepsin B. CA074, a cell impermeable and highly selective cathepsin B inhibitor, significantly reduced pericellular proteolysis and invasion by SUM149 cells (Figures 3.6 and 3.7). In agreement with these findings, lovastatin treatment, which diminished pericellular cathepsin B, also significantly reduced type IV collagen degradation and invasion by IBC cells (Figures 3.35 and 3.38). Others have also shown that lovastatin decreases migration and invasion of breast cancer cells (Silva et al., 2003; Kang et al., 2009), in part due to reduced expression of both MMP-2 and -9 (Kang et al., 2009). Another statin drug, cerivastatin, inhibits proliferation and invasion of highly aggressive MDA-MB-231 breast cancer cells, concomitantly with reduced expression of uPA, MMP-9, uPAR and PAI-1 (Denoyelle et al., 2001; Denoyelle et al., 2003). In our studies, treatment of SUM149 cells with lovastatin resulted in decreased uPA expression and secretion (Figure 3.28). The observed reduction of type IV collagen degradation and invasion by SUM149 cells are a result of lovastatin-induced decreases in expression of proteases, including cathepsin B and uPA.

EGFR expression is associated with more aggressive subtypes of breast cancer and increased expression is also higher in IBC than non-IBC patient tissues (Guerin et al., 1989). Therapies targeting EGFR (including the use of

small molecules against its tyrosine kinase domain, e.g. gefitinib and erlotinib, or cetuximab, a chimeric monoclonal antibody) resulted in little benefit (Rimawi et al., 2010). This has led to combination strategies to maximize the potential of drugs and improve patient outcome [for reviews, see (Fischgrabe and Wulfing, 2008; Sanchez-Munoz et al., 2009)]. In comparison to normal cells, cancer cells are highly dependent on products of the mevalonic pathway and generally have increased HMG-CoA reductase activity; therefore statins have been proposed for use as cancer therapeutics (Wong et al., 2002; Chan et al., 2003). In addition, mevalonate metabolites are also important for EGFR signaling and effects of statins on EGFR have been investigated. Lovastatin treatment inhibits autophosphorylation of EGFR and downstream signaling events (Mantha et al., 2005; Dimitroulakos et al., 2006); inhibits dimerization of EGFR, decreases both AKT phosphorylation and inactivation of RhoA (Zhao et al., 2010); and has also been shown to sensitize resistant cells to drug treatment (Park et al., 2010). In the current study, we demonstrated that lovastatin treatment of IBC cells reduced the localization of EGFR to lipid microdomains, which could be rescued by MVA (Figure 3.39). Irwin *et al.* have demonstrated that EGFR in lipid microdomains mediates tyrosine kinase resistance and that treatment with lovastatin causes decreased Akt phosphorylation in SUM149 cells (Irwin et al., 2011). Whether inhibition of downstream signaling is due to disrupted EGFR localization to lipid microdomains by lovastatin warrants further investigation.

Stromal components of the IBC tumor microenvironment were not a focus of the current study. However, previous findings by our laboratory have suggested that secreted factors from the conditioned media of human monocytes increase both expression and activity of cathepsin B in SUM149 cells (Mohamed et al., 2008). Monocytes recruited from the circulation into the tumor microenvironment differentiate into tumor-associated macrophages. The tumor-associated macrophges secrete angiogenic factors and thereby promote tumor growth and invasion and are associated with poor prognosis in invasive breast cancer (Leek et al., 1996). In addition, both tumor cell and macrophage associated cathepsin B promotes progression and metastatic spread in a murine model of mammary carcinogenesis (Vasiljeva et al., 2006). Therefore, cathepsin B is expressed by tumor cells and many other tumor-associated cells, including macrophages, fibroblasts, endothelial cells, neutrophils and osteoclasts which contribute to neoplastic progression [for review, see (Mohamed and Sloane, 2006)]. Therefore, statins, by decreasing both expression and activity of cathepsin B, may prove efficacious in treatment of malignancies associated with its overexpression and increased activity, such as IBC. Combinational therapeutic approaches targeting both cathepsin B and uPAR have been shown by Rao and colleagues to inhibit tumor progression (Gopinath et al., 2010) and neovascularization in malignant glioma (Malla et al., 2011). Several protease targeted drugs are routinely used in the clinic, e.g., ACE inhibitors, and others

are in pre-clinical development, including neutralizing antibodies against both cathepsin B and uPA for cancer treatment (for review, see (Turk, 2006)).

This study was undertaken to investigate factors, in particular proteolytic networks, which mediate the aggressive IBC phenotype. My overall hypothesis was that cell surface association of the cysteine protease cathepsin B, serine proteases of the plasminogen cascade and their binding partners in caveolae enhance cell surface proteolysis, and ultimately, the aggressiveness of IBC cells. We have demonstrated that there is active cathepsin B at the surface of IBC cells. Targeting caveolae, a specialized lipid raft, by knockdown of caveolin-1 expression in IBC cells reduces their ability to degrade ECM proteins and their invasiveness. These studies confirm that caveolin-1 and caveolae play a critical role in the aggressive phenotype of IBC. In IBC cells that express caveolin-1, proteases and signaling proteins are associated with caveolae, including uPA and EGFR. Our studies therefore provide a mechanism for the role of caveolae, i.e., association of proteolytic pathways with caveolae in IBC cells and specifically the association of uPA and uPAR, components of the plasminogen activation system. We have also demonstrated that targeting lipid rafts by treating IBC cells with lovastatin alters their aggressive phenotype. In IBC cells that do not express caveolin-1, we showed that proteases are also associated with lipid rafts in the plasma membrane. Those proteases include uPA and cathepsin B, an upstream activator of pro-uPA. We also confirmed the presence of EGFR pathways in lipid rafts of IBC cells. Thus, our studies demonstrate a

critical role for lipid rafts, both caveolar and non-caveolar, in the aggressive phenotype of IBC.

REFERENCES

Abisi S, Burnand KG, Humphries J, Waltham M, Taylor P and Smith A (2008) Effect of statins on proteolytic activity in the wall of abdominal aortic aneurysms. *Br J Surg* **95**:333-337.

Almholt K, Lund LR, Rygaard J, Nielsen BS, Dano K, Romer J and Johnsen M (2005) Reduced metastasis of transgenic mammary cancer in urokinase-deficient mice. *Int J Cancer* **113**:525-532.

Anderson RG and Jacobson K (2002) A role for lipid shells in targeting proteins to caveolae, rafts, and other lipid domains. *Science* **296**:1821-1825.

Andrews NW (2000) Regulated secretion of conventional lysosomes. *Trends Cell Biol* **10**:316-321.

Annabi B, Lachambre M, Bousquet-Gagnon N, Page M, Gingras D and Beliveau R (2001) Localization of membrane-type 1 matrix metalloproteinase in caveolae membrane domains. *Biochem J* **353**:547-553.

Bafetti LM, Young TN, Itoh Y and Stack MS (1998) Intact vitronectin induces matrix metalloproteinase-2 and tissue inhibitor of metalloproteinases-2 expression and enhanced cellular invasion by melanoma cells. *J Biol Chem* **273**:143-149.

Baillo A, Giroux C and Ethier SP (2011) Knock-down of amphiregulin inhibits cellular invasion in inflammatory breast cancer. *J Cell Physiol* **226**:2691-2701.

Balbis A and Posner BI (2010) Compartmentalization of EGFR in cellular membranes: role of membrane rafts. *J Cell Biochem* **109**:1103-1108.

Berquin IM, Cao L, Fong D and Sloane BF (1995) Identification of two new exons and multiple transcription start points in the 5'-untranslated region of the human cathepsin-B-encoding gene. *Gene* **159**:143-149.

Berx G and Van Roy F (2001) The E-cadherin/catenin complex: an important gatekeeper in breast cancer tumorigenesis and malignant progression. *Breast Cancer Res* **3**:289-293.

Birchmeier W and Behrens J (1994) Cadherin expression in carcinomas: role in the formation of cell junctions and the prevention of invasiveness. *Biochim Biophys Acta* **1198**:11-26.

Bonnier P, Charpin C, Lejeune C, Romain S, Tubiana N, Beedassy B, Martin PM, Serment H and Piana L (1995) Inflammatory carcinomas of the breast: a clinical, pathological, or a clinical and pathological definition? *Int J Cancer* **62**:382-385.

Bonuccelli G, Casimiro MC, Sotgia F, Wang C, Liu M, Katiyar S, Zhou J, Dew E, Capozza F, Daumer KM, Minetti C, Milliman JN, Alpy F, Rio MC, Tomasetto C, Mercier I, Flomenberg N, Frank PG, Pestell RG and Lisanti MP (2009) Caveolin-1 (P132L), a common breast cancer mutation, confers mammary cell invasiveness and defines a novel stem cell/metastasis-associated gene signature. *Am J Pathol* **174**:1650-1662.

Bouras T, Lisanti MP and Pestell RG (2004) Caveolin-1 in breast cancer. *Cancer Biol Ther* **3**:931-941.

Bourguignon LY, Singleton PA, Diedrich F, Stern R and Gilad E (2004) CD44 interaction with Na+-H+ exchanger (NHE1) creates acidic microenvironments leading to hyaluronidase-2 and cathepsin B activation and breast tumor cell invasion. *J Biol Chem* **279**:26991-27007.

Boussen H, Bouzaiene H, Ben Hassouna J, Dhiab T, Khomsi F, Benna F, Gamoudi A, Mourali N, Hechiche M, Rahal K and Levine PH (2010) Inflammatory breast cancer in Tunisia: epidemiological and clinical trends. *Cancer* **116**:2730-2735.

Breuza L, Corby S, Arsanto JP, Delgrossi MH, Scheiffele P and Le Bivic A (2002) The scaffolding domain of caveolin 2 is responsible for its Golgi localization in Caco-2 cells. *J Cell Sci* **115**:4457-4467.

Brix K, Lemansky P and Herzog V (1996) Evidence for extracellularly acting cathepsins mediating thyroid hormone liberation in thyroid epithelial cells. *Endocrinology* **137**:1963-1974.

Brown D (1994) GPI-anchored proteins and detergent-resistant membrane domains. *Braz J Med Biol Res* **27**:309-315.

Bugge TH, Lund LR, Kombrinck KK, Nielsen BS, Holmback K, Drew AF, Flick MJ, Witte DP, Dano K and Degen JL (1998) Reduced metastasis of Polyoma virus middle T antigen-induced mammary cancer in plasminogen-deficient mice. *Oncogene* **16**:3097-3104.

Caglic D, Pungercar JR, Pejler G, Turk V and Turk B (2007) Glycosaminoglycans facilitate procathepsin B activation through disruption of propeptide-mature enzyme interactions. *J Biol Chem* **282**:33076-33085.

Campbell MJ, Esserman LJ, Zhou Y, Shoemaker M, Lobo M, Borman E, Baehner F, Kumar AS, Adduci K, Marx C, Petricoin EF, Liotta LA, Winters M, Benz S and Benz CC (2006) Breast cancer growth prevention by statins. *Cancer Res* **66**:8707-8714.

Campo E, Munoz J, Miquel R, Palacin A, Cardesa A, Sloane BF and Emmert-Buck MR (1994) Cathepsin B expression in colorectal carcinomas correlates with tumor progression and shortened patient survival. *Am J Pathol* **145**:301-309.

Cao L, Taggart RT, Berquin IM, Moin K, Fong D and Sloane BF (1994) Human gastric adenocarcinoma cathepsin B: isolation and sequencing of full-length cDNAs and polymorphisms of the gene. *Gene* **139**:163-169.

Carmeliet P, Moons L, Dewerchin M, Rosenberg S, Herbert JM, Lupu F and Collen D (1998) Receptor-independent role of urokinase-type plasminogen activator in pericellular plasmin and matrix metalloproteinase proteolysis during vascular wound healing in mice. *J Cell Biol* **140**:233-245.

Cavallo-Medved D, Dosescu J, Linebaugh BE, Sameni M, Rudy D and Sloane BF (2003) Mutant K-ras regulates cathepsin B localization on the surface of human colorectal carcinoma cells. *Neoplasia* **5**:507-519.

Cavallo-Medved D, Mai J, Dosescu J, Sameni M and Sloane BF (2005) Caveolin-1 mediates the expression and localization of cathepsin B, pro-urokinase plasminogen activator and their cell-surface receptors in human colorectal carcinoma cells. *J Cell Sci* **118**:1493-1503.

Cavallo-Medved D, Rudy D, Blum G, Bogyo M, Caglic D and Sloane BF (2009) Live-cell imaging demonstrates extracellular matrix degradation in association with active cathepsin B in caveolae of endothelial cells during tube formation. *Exp Cell Res* **315**:1234-1246.

Cavallo-Medved D and Sloane BF (2003) Cell-surface cathepsin B: understanding its functional significance. *Curr Top Dev Biol* **54**:313-341.

Chan KK, Oza AM and Siu LL (2003) The statins as anticancer agents. *Clin Cancer Res* **9**:10-19.

Chang S, Buzdar AU and Hursting SD (1998a) Inflammatory breast cancer and body mass index. *J Clin Oncol* **16**:3731-3735.

Chang S, Parker SL, Pham T, Buzdar AU and Hursting SD (1998b) Inflammatory breast carcinoma incidence and survival: the surveillance, epidemiology, and end results program of the National Cancer Institute, 1975-1992. *Cancer* **82**:2366-2372.

Chen J, Tung CH, Mahmood U, Ntziachristos V, Gyurko R, Fishman MC, Huang PL and Weissleder R (2002) In vivo imaging of proteolytic activity in atherosclerosis. *Circulation* **105**:2766-2771.

Cho KA, Ryu SJ, Park JS, Jang IS, Ahn JS, Kim KT and Park SC (2003) Senescent phenotype can be reversed by reduction of caveolin status. *J Biol Chem* **278**:27789-27795.

Choong PF and Nadesapillai AP (2003) Urokinase plasminogen activator system: a multifunctional role in tumor progression and metastasis. *Clin Orthop Relat Res*:S46-58.

Chung CY and Erickson HP (1994) Cell surface annexin II is a high affinity receptor for the alternatively spliced segment of tenascin-C. *J Cell Biol* **126**:539-548.

Couet J, Belanger MM, Roussel E and Drolet MC (2001) Cell biology of caveolae and caveolin. *Adv Drug Deliv Rev* **49**:223-235.

Cubellis MV, Nolli ML, Cassani G and Blasi F (1986) Binding of single-chain prourokinase to the urokinase receptor of human U937 cells. *J Biol Chem* **261**:15819-15822.

Dalet-Fumeron V, Boudjennah L and Pagano M (1996) Competition between plasminogen and procathepsin B as a probe to demonstrate the in vitro activation of procathepsin B by the tissue plasminogen activator. *Arch Biochem Biophys* **335**:351-357.

Dalet-Fumeron V, Guinec N and Pagano M (1993) In vitro activation of pro-cathepsin B by three serine proteinases: leucocyte elastase, cathepsin G, and the urokinase-type plasminogen activator. *FEBS Lett* **332**:251-254.

Davignon J (2004) Beneficial cardiovascular pleiotropic effects of statins. *Circulation* **109**:III39-43.

Dawood S, Merajver SD, Viens P, Vermeulen PB, Swain SM, Buchholz TA, Dirix LY, Levine PH, Lucci A, Krishnamurthy S, Robertson FM, Woodward WA, Yang WT, Ueno NT and Cristofanilli M (2010) International expert panel on inflammatory breast cancer: consensus statement for standardized diagnosis and treatment. *Ann Oncol*.

Dawood S, Merajver SD, Viens P, Vermeulen PB, Swain SM, Buchholz TA, Dirix LY, Levine PH, Lucci A, Krishnamurthy S, Robertson FM, Woodward WA, Yang WT, Ueno NT and Cristofanilli M (2011) International expert panel on inflammatory breast cancer: consensus statement for standardized diagnosis and treatment. *Ann Oncol* **22**:515-523.

Dawson SJ, Provenzano E and Caldas C (2009) Triple negative breast cancers: clinical and prognostic implications. *Eur J Cancer* **45 Suppl 1**:27-40.

Debnath J and Brugge JS (2005) Modelling glandular epithelial cancers in three-dimensional cultures. *Nat Rev Cancer* **5**:675-688.

Delannoy-Courdent A, Mattot V, Fafeur V, Fauquette W, Pollet I, Calmels T, Vercamer C, Boilly B, Vandenbunder B and Desbiens X (1998) The expression of an Ets1 transcription factor lacking its activation domain decreases uPA proteolytic activity and cell motility, and impairs normal tubulogenesis and cancerous scattering in mammary epithelial cells. *J Cell Sci* **111 (Pt 11)**:1521-1534.

Demierre MF, Higgins PD, Gruber SB, Hawk E and Lippman SM (2005) Statins and cancer prevention. *Nat Rev Cancer* **5**:930-942.

Denoyelle C, Albanese P, Uzan G, Hong L, Vannier JP, Soria J and Soria C (2003) Molecular mechanism of the anti-cancer activity of cerivastatin, an inhibitor of HMG-CoA reductase, on aggressive human breast cancer cells. *Cell Signal* **15**:327-338.

Denoyelle C, Vasse M, Korner M, Mishal Z, Ganne F, Vannier JP, Soria J and Soria C (2001) Cerivastatin, an inhibitor of HMG-CoA reductase, inhibits the signaling pathways involved in the invasiveness and metastatic properties of highly invasive breast cancer cell lines: an in vitro study. *Carcinogenesis* **22**:1139-1148.

Di Vizio D, Solomon KR and Freeman MR (2008) Cholesterol and cholesterol-rich membranes in prostate cancer: an update. *Tumori* **94**:633-639.

Dimitroulakos J, Lorimer IA and Goss G (2006) Strategies to enhance epidermal growth factor inhibition: targeting the mevalonate pathway. *Clin Cancer Res* **12**:4426s-4431s.

Drab M, Verkade P, Elger M, Kasper M, Lohn M, Lauterbach B, Menne J, Lindschau C, Mende F, Luft FC, Schedl A, Haller H and Kurzchalia TV (2001) Loss of caveolae, vascular dysfunction, and pulmonary defects in caveolin-1 gene-disrupted mice. *Science* **293**:2449-2452.

Duffy MJ (2004) The urokinase plasminogen activator system: role in malignancy. *Curr Pharm Des* **10**:39-49.

Duffy MJ, O'Grady P, Devaney D, O'Siorain L, Fennelly JJ and Lijnen HJ (1988) Urokinase-plasminogen activator, a marker for aggressive breast carcinomas. Preliminary report. *Cancer* **62**:531-533.

Edge SB, American Joint Committee on Cancer. and American Cancer Society. (2010) AJCC cancer staging handbook from the AJCC cancer staging manual, in pp 1 online resource (xix, 718 p.), Springer, New York.

Elsheikh SE, Green AR, Rakha EA, Samaka RM, Ammar AA, Powe D, Reis-Filho JS and Ellis IO (2008) Caveolin 1 and Caveolin 2 are associated with breast cancer basal-like and triple-negative immunophenotype. *Br J Cancer* **99**:327-334.

Emmert-Buck MR, Roth MJ, Zhuang Z, Campo E, Rozhin J, Sloane BF, Liotta LA and Stetler-Stevenson WG (1994) Increased gelatinase A (MMP-2) and cathepsin B activity in invasive tumor regions of human colon cancer samples. *Am J Pathol* **145**:1285-1290.

Fernandez I, Ying Y, Albanesi J and Anderson RG (2002) Mechanism of caveolin filament assembly. *Proc Natl Acad Sci U S A* **99**:11193-11198.

Fischgrabe J and Wulfing P (2008) Targeted therapies in breast cancer: established drugs and recent developments. *Curr Clin Pharmacol* **3**:85-98.

Foekens JA, Peters HA, Look MP, Portengen H, Schmitt M, Kramer MD, Brunner N, Janicke F, Meijer-van Gelder ME, Henzen-Logmans SC, van Putten WL and Klijn JG (2000) The urokinase system of plasminogen activation and prognosis in 2780 breast cancer patients. *Cancer Res* **60**:636-643.

Foley J, Nickerson NK, Nam S, Allen KT, Gilmore JL, Nephew KP and Riese DJ, 2nd (2010) EGFR signaling in breast cancer: bad to the bone. *Semin Cell Dev Biol* **21**:951-960.

Fong D, Calhoun DH, Hsieh WT, Lee B and Wells RD (1986) Isolation of a cDNA clone for the human lysosomal proteinase cathepsin B. *Proc Natl Acad Sci U S A* **83**:2909-2913.

Fong D, Chan MM, Hsieh WT, Menninger JC and Ward DC (1992) Confirmation of the human cathepsin B gene (CTSB) assignment to chromosome 8. *Hum Genet* **89**:10-12.

Fra AM, Williamson E, Simons K and Parton RG (1995) De novo formation of caveolae in lymphocytes by expression of VIP21-caveolin. *Proc Natl Acad Sci U S A* **92**:8655-8659.

Galbiati F, Volonte D, Liu J, Capozza F, Frank PG, Zhu L, Pestell RG and Lisanti MP (2001) Caveolin-1 expression negatively regulates cell cycle progression by inducing G(0)/G(1) arrest via a p53/p21(WAF1/Cip1)-dependent mechanism. *Mol Biol Cell* **12**:2229-2244.

Garcia-Cardena G, Martasek P, Masters BS, Skidd PM, Couet J, Li S, Lisanti MP and Sessa WC (1997) Dissecting the interaction between nitric oxide synthase (NOS) and caveolin. Functional significance of the nos caveolin binding domain in vivo. *J Biol Chem* **272**:25437-25440.

Garwood ER, Kumar AS, Baehner FL, Moore DH, Au A, Hylton N, Flowers CI, Garber J, Lesnikoski BA, Hwang ES, Olopade O, Port ER, Campbell M

and Esserman LJ (2010) Fluvastatin reduces proliferation and increases apoptosis in women with high grade breast cancer. *Breast Cancer Res Treat* **119**:137-144.

Gerke V and Moss SE (2002) Annexins: from structure to function. *Physiol Rev* **82**:331-371.

Gianotti A, Sommer CA, Carmona AK and Henrique-Silva F (2008) Inhibitory effect of the sugarcane cystatin CaneCPI-4 on cathepsins B and L and human breast cancer cell invasion. *Biol Chem* **389**:447-453.

Gillet L, Roger S, Besson P, Lecaille F, Gore J, Bougnoux P, Lalmanach G and Le Guennec JY (2009) Voltage-gated Sodium Channel Activity Promotes Cysteine Cathepsin-dependent Invasiveness and Colony Growth of Human Cancer Cells. *J Biol Chem* **284**:8680-8691.

Gillies RJ, Raghunand N, Karczmar GS and Bhujwalla ZM (2002) MRI of the tumor microenvironment. *J Magn Reson Imaging* **16**:430-450.

Gimpl G and Gehrig-Burger K (2007) Cholesterol reporter molecules. *Biosci Rep* **27**:335-358.

Glenney JR, Jr. (1989) Tyrosine phosphorylation of a 22-kDa protein is correlated with transformation by Rous sarcoma virus. *J Biol Chem* **264**:20163-20166.

Glenney JR, Jr. and Soppet D (1992) Sequence and expression of caveolin, a protein component of caveolae plasma membrane domains

phosphorylated on tyrosine in Rous sarcoma virus-transformed fibroblasts. *Proc Natl Acad Sci U S A* **89**:10517-10521.

Gocheva V, Zeng W, Ke D, Klimstra D, Reinheckel T, Peters C, Hanahan D and Joyce JA (2006) Distinct roles for cysteine cathepsin genes in multistage tumorigenesis. *Genes Dev* **20**:543-556.

Goetz JG, Lajoie P, Wiseman SM and Nabi IR (2008) Caveolin-1 in tumor progression: the good, the bad and the ugly. *Cancer Metastasis Rev* **27**:715-735.

Gonzalez-Angulo AM, Sneige N, Buzdar AU, Valero V, Kau SW, Broglio K, Yamamura Y, Hortobagyi GN and Cristofanilli M (2004) p53 expression as a prognostic marker in inflammatory breast cancer. *Clin Cancer Res* **10**:6215-6221.

Gopinath S, Malla RR, Gondi CS, Alapati K, Fassett D, Klopfenstein JD, Dinh DH, Gujrati M and Rao JS (2010) Co-depletion of cathepsin B and uPAR induces G0/G1 arrest in glioma via FOXO3a mediated p27 upregulation. *PLoS One* **5**:e11668.

Griffoni C, Spisni E, Santi S, Riccio M, Guarnieri T and Tomasi V (2000) Knockdown of caveolin-1 by antisense oligonucleotides impairs angiogenesis in vitro and in vivo. *Biochem Biophys Res Commun* **276**:756-761.

Grondahl-Hansen J, Hilsenbeck SG, Christensen IJ, Clark GM, Osborne CK and Brunner N (1997) Prognostic significance of PAI-1 and uPA in cytosolic

extracts obtained from node-positive breast cancer patients. *Breast Cancer Res Treat* **43**:153-163.

Grondahl-Hansen J, Peters HA, van Putten WL, Look MP, Pappot H, Ronne E, Dano K, Klijn JG, Brunner N and Foekens JA (1995) Prognostic significance of the receptor for urokinase plasminogen activator in breast cancer. *Clin Cancer Res* **1**:1079-1087.

Guerin M, Gabillot M, Mathieu MC, Travagli JP, Spielmann M, Andrieu N and Riou G (1989) Structure and expression of c-erbB-2 and EGF receptor genes in inflammatory and non-inflammatory breast cancer: prognostic significance. *Int J Cancer* **43**:201-208.

Guicciardi ME, Deussing J, Miyoshi H, Bronk SF, Svingen PA, Peters C, Kaufmann SH and Gores GJ (2000) Cathepsin B contributes to TNF-alpha-mediated hepatocyte apoptosis by promoting mitochondrial release of cytochrome c. *J Clin Invest* **106**:1127-1137.

Gunhan-Bilgen I, Ustun EE and Memis A (2002) Inflammatory breast carcinoma: mammographic, ultrasonographic, clinical, and pathologic findings in 142 cases. *Radiology* **223**:829-838.

Guo M, Mathieu PA, Linebaugh B, Sloane BF and Reiners JJ, Jr. (2002) Phorbol ester activation of a proteolytic cascade capable of activating latent transforming growth factor-betaL a process initiated by the exocytosis of cathepsin B. *J Biol Chem* **277**:14829-14837.

Gurewich V (2000) Fibrinolysis: an unfinished agenda. *Blood Coagul Fibrinolysis* **11**:401-408.

Halangk W, Lerch MM, Brandt-Nedelev B, Roth W, Ruthenbuerger M, Reinheckel T, Domschke W, Lippert H, Peters C and Deussing J (2000) Role of cathepsin B in intracellular trypsinogen activation and the onset of acute pancreatitis. *J Clin Invest* **106**:773-781.

Han B, Nakamura M, Mori I, Nakamura Y and Kakudo K (2005) Urokinase-type plasminogen activator system and breast cancer (Review). *Oncol Rep* **14**:105-112.

Hanahan D and Weinberg RA (2011) Hallmarks of cancer: the next generation. *Cell* **144**:646-674.

Hance KW, Anderson WF, Devesa SS, Young HA and Levine PH (2005) Trends in inflammatory breast carcinoma incidence and survival: the surveillance, epidemiology, and end results program at the National Cancer Institute. *J Natl Cancer Inst* **97**:966-975.

Hanewinkel H, Glossl J and Kresse H (1987) Biosynthesis of cathepsin B in cultured normal and I-cell fibroblasts. *J Biol Chem* **262**:12351-12355.

Hayashi K, Matsuda S, Machida K, Yamamoto T, Fukuda Y, Nimura Y, Hayakawa T and Hamaguchi M (2001) Invasion activating caveolin-1 mutation in human scirrhous breast cancers. *Cancer Res* **61**:2361-2364.

Head BP and Insel PA (2007) Do caveolins regulate cells by actions outside of caveolae? *Trends Cell Biol* **17**:51-57.

Heuser J (1989) Changes in lysosome shape and distribution correlated with changes in cytoplasmic pH. *J Cell Biol* **108**:855-864.

Hirohashi S (1998) Inactivation of the E-cadherin-mediated cell adhesion system in human cancers. *Am J Pathol* **153**:333-339.

Irwin ME, Mueller KL, Bohin N, Ge Y and Boerner JL (2011) Lipid raft localization of EGFR alters the response of cancer cells to the EGFR tyrosine kinase inhibitor gefitinib. *J Cell Physiol* **226**:2316-2328.

Jacobs EJ, Newton CC, Thun MJ and Gapstur SM (2011) Long-term use of cholesterol-lowering drugs and cancer incidence in a large United States cohort. *Cancer Res* **71**:1763-1771.

Jane DT, Morvay LC, Koblinski J, Yan S, Saad FA, Sloane BF and Dufresne MJ (2002) Evidence that E-box promoter elements and MyoD transcription factors play a role in the induction of cathepsin B gene expression during human myoblast differentiation. *Biol Chem* **383**:1833-1844.

Jedeszko C, Sameni M, Olive MB, Moin K and Sloane BF (2008) Visualizing protease activity in living cells: from two dimensions to four dimensions. *Curr Protoc Cell Biol* **Chapter 4**:Unit 4 20.

Joshi B, Strugnell SS, Goetz JG, Kojic LD, Cox ME, Griffith OL, Chan SK, Jones SJ, Leung SP, Masoudi H, Leung S, Wiseman SM and Nabi IR (2008) Phosphorylated caveolin-1 regulates Rho/ROCK-dependent focal adhesion dynamics and tumor cell migration and invasion. *Cancer Res* **68**:8210-8220.

Kang HM, Choi KS, Kassam G, Fitzpatrick SL, Kwon M and Waisman DM (1999) Role of annexin II tetramer in plasminogen activation. *Trends Cardiovasc Med* **9**:92-102.

Kang S, Kim ES and Moon A (2009) Simvastatin and lovastatin inhibit breast cell invasion induced by H-Ras. *Oncol Rep* **21**:1317-1322.

Keppler D and Sloane BF (1996) Cathepsin B: multiple enzyme forms from a single gene and their relation to cancer. *Enzyme Protein* **49**:94-105.

Khan KM and Falcone DJ (1997) Role of laminin in matrix induction of macrophage urokinase-type plasminogen activator and 92-kDa metalloproteinase expression. *J Biol Chem* **272**:8270-8275.

Kim DE, Kim JY, Schellingerhout D, Shon SM, Jeong SW, Kim EJ and Kim WK (2009) Molecular imaging of cathepsin B proteolytic enzyme activity reflects the inflammatory component of atherosclerotic pathology and can quantitatively demonstrate the antiatherosclerotic therapeutic effects of atorvastatin and glucosamine. *Mol Imaging* **8**:291-301.

Kleer CG, van Golen KL, Braun T and Merajver SD (2001) Persistent E-cadherin expression in inflammatory breast cancer. *Mod Pathol* **14**:458-464.

Kleer CG, Zhang Y, Pan Q, Gallagher G, Wu M, Wu ZF and Merajver SD (2004) WISP3 and RhoC guanosine triphosphatase cooperate in the development of inflammatory breast cancer. *Breast Cancer Res* **6**:R110-115.

Klopp AH, Lacerda L, Gupta A, Debeb BG, Solley T, Li L, Spaeth E, Xu W, Zhang X, Lewis MT, Reuben JM, Krishnamurthy S, Ferrari M, Gaspar R, Buchholz TA, Cristofanilli M, Marini F, Andreeff M and Woodward WA (2010) Mesenchymal stem cells promote mammosphere formation and decrease E-cadherin in normal and malignant breast cells. *PLoS One* **5**:e12180.

Klose A, Wilbrand-Hennes A, Zigrino P, Weber E, Krieg T, Mauch C and Hunzelmann N (2006) Contact of high-invasive, but not low-invasive, melanoma cells to native collagen I induces the release of mature cathepsin B. *Int J Cancer* **118**:2735-2743.

Kobayashi H, Moniwa N, Sugimura M, Shinohara H, Ohi H and Terao T (1993) Effects of membrane-associated cathepsin B on the activation of receptor-bound prourokinase and subsequent invasion of reconstituted basement membranes. *Biochim Biophys Acta* **1178**:55-62.

Kobayashi H, Ohi H, Sugimura M, Shinohara H, Fujii T and Terao T (1992) Inhibition of in vitro ovarian cancer cell invasion by modulation of urokinase-type plasminogen activator and cathepsin B. *Cancer Res* **52**:3610-3614.

Kobayashi H, Schmitt M, Goretzki L, Chucholowski N, Calvete J, Kramer M, Gunzler WA, Janicke F and Graeff H (1991) Cathepsin B efficiently activates the soluble and the tumor cell receptor-bound form of the

proenzyme urokinase-type plasminogen activator (Pro-uPA). *J Biol Chem* **266**:5147-5152.

Koblinski JE, Ahram M and Sloane BF (2000) Unraveling the role of proteases in cancer. *Clin Chim Acta* **291**:113-135.

Koblinski JE, Dosescu J, Sameni M, Moin K, Clark K and Sloane BF (2002) Interaction of human breast fibroblasts with collagen I increases secretion of procathepsin B. *J Biol Chem* **277**:32220-32227.

Koopman JL, Slomp J, de Bart AC, Quax PH and Verheijen JH (1998) Mitogenic effects of urokinase on melanoma cells are independent of high affinity binding to the urokinase receptor. *J Biol Chem* **273**:33267-33272.

Kos J, Sekirnik A, Premzl A, Zavasnik Bergant V, Langerholc T, Turk B, Werle B, Golouh R, Repnik U, Jeras M and Turk V (2005) Carboxypeptidases cathepsins X and B display distinct protein profile in human cells and tissues. *Exp Cell Res* **306**:103-113.

Kostoulas G, Lang A, Nagase H and Baici A (1999) Stimulation of angiogenesis through cathepsin B inactivation of the tissue inhibitors of matrix metalloproteinases. *FEBS Lett* **455**:286-290.

Koukoulis GK, Gould VE, Bhattacharyya A, Gould JE, Howeedy AA and Virtanen I (1991) Tenascin in normal, reactive, hyperplastic, and neoplastic tissues: biologic and pathologic implications. *Hum Pathol* **22**:636-643.

Krepela E, Vicar J and Cernoch M (1989) Cathepsin B in human breast tumor tissue and cancer cells. *Neoplasma* **36**:41-52.

Ledvinova J and Elleder M (1993) Filipin test for diagnosis of Niemann-Pick disease type C. *Sb Lek* **94**:137-143.

Lee SW, Reimer CL, Oh P, Campbell DB and Schnitzer JE (1998) Tumor cell growth inhibition by caveolin re-expression in human breast cancer cells. *Oncogene* **16**:1391-1397.

Leek RD, Lewis CE, Whitehouse R, Greenall M, Clarke J and Harris AL (1996) Association of macrophage infiltration with angiogenesis and prognosis in invasive breast carcinoma. *Cancer Res* **56**:4625-4629.

Levine PH and Veneroso C (2008) The epidemiology of inflammatory breast cancer. *Semin Oncol* **35**:11-16.

Li Q, Chow AB and Mattingly RR (2010) Three-dimensional overlay culture models of human breast cancer reveal a critical sensitivity to mitogen-activated protein kinase kinase inhibitors. *J Pharmacol Exp Ther* **332**:821-828.

Li S, Couet J and Lisanti MP (1996) Src tyrosine kinases, Galpha subunits, and H-Ras share a common membrane-anchored scaffolding protein, caveolin. Caveolin binding negatively regulates the auto-activation of Src tyrosine kinases. *J Biol Chem* **271**:29182-29190.

Li S, Okamoto T, Chun M, Sargiacomo M, Casanova JE, Hansen SH, Nishimoto I and Lisanti MP (1995) Evidence for a regulated interaction between heterotrimeric G proteins and caveolin. *J Biol Chem* **270**:15693-15701.

Li WP, Liu P, Pilcher BK and Anderson RG (2001) Cell-specific targeting of caveolin-1 to caveolae, secretory vesicles, cytoplasm or mitochondria. *J Cell Sci* **114**:1397-1408.

Linebaugh BE, Sameni M, Day NA, Sloane BF and Keppler D (1999) Exocytosis of active cathepsin B enzyme activity at pH 7.0, inhibition and molecular mass. *Eur J Biochem* **264**:100-109.

Lisanti MP, Scherer PE, Vidugiriene J, Tang Z, Hermanowski-Vosatka A, Tu YH, Cook RF and Sargiacomo M (1994) Characterization of caveolin-rich membrane domains isolated from an endothelial-rich source: implications for human disease. *J Cell Biol* **126**:111-126.

Liu J, Oh P, Horner T, Rogers RA and Schnitzer JE (1997) Organized endothelial cell surface signal transduction in caveolae distinct from glycosylphosphatidylinositol-anchored protein microdomains. *J Biol Chem* **272**:7211-7222.

Liu P, Li WP, Machleidt T and Anderson RG (1999) Identification of caveolin-1 in lipoprotein particles secreted by exocrine cells. *Nat Cell Biol* **1**:369-375.

Liu P, Rudick M and Anderson RG (2002a) Multiple functions of caveolin-1. *J Biol Chem* **277**:41295-41298.

Liu W, Wang G and Yakovlev AG (2002b) Identification and functional analysis of the rat caspase-3 gene promoter. *J Biol Chem* **277**:8273-8278.

Lloyd PG and Hardin CD (2011) Caveolae in cancer: two sides of the same coin? Focus on "Hydrogen peroxide inhibits non-small cell lung cancer cell

anoikis through the inhibition of caveolin-1 degradation". *Am J Physiol Cell Physiol* **300**:C232-234.

Ludwig T, Ovitt CE, Bauer U, Hollinshead M, Remmler J, Lobel P, Ruther U and Hoflack B (1993) Targeted disruption of the mouse cation-dependent mannose 6-phosphate receptor results in partial missorting of multiple lysosomal enzymes. *EMBO J* **12**:5225-5235.

Lutgens SP, Cleutjens KB, Daemen MJ and Heeneman S (2007) Cathepsin cysteine proteases in cardiovascular disease. *FASEB J* **21**:3029-3041.

MacGrath SM and Koleske AJ (2011) Invadopodia: RhoC runs rings around cofilin. *Curr Biol* **21**:R280-282.

Mach L, Stuwe K, Hagen A, Ballaun C and Glossl J (1992) Proteolytic processing and glycosylation of cathepsin B. The role of the primary structure of the latent precursor and of the carbohydrate moiety for cell-type-specific molecular forms of the enzyme. *Biochem J* **282 (Pt 2)**:577-582.

Maciewicz RA, Wardale RJ, Etherington DJ and Paraskeva C (1989) Immunodetection of cathepsins B and L present in and secreted from human pre-malignant and malignant colorectal tumour cell lines. *Int J Cancer* **43**:478-486.

Mackie EJ, Halfter W and Liverani D (1988) Induction of tenascin in healing wounds. *J Cell Biol* **107**:2757-2767.

MacLeod TJ, Kwon M, Filipenko NR and Waisman DM (2003) Phospholipid-associated annexin A2-S100A10 heterotetramer and its subunits:

characterization of the interaction with tissue plasminogen activator, plasminogen, and plasmin. *J Biol Chem* **278**:25577-25584.

Maglione JE, Moghanaki D, Young LJ, Manner CK, Ellies LG, Joseph SO, Nicholson B, Cardiff RD and MacLeod CL (2001) Transgenic Polyoma middle-T mice model premalignant mammary disease. *Cancer Res* **61**:8298-8305.

Mai J, Finley RL, Jr., Waisman DM and Sloane BF (2000) Human procathepsin B interacts with the annexin II tetramer on the surface of tumor cells. *J Biol Chem* **275**:12806-12812.

Malla RR, Gopinath S, Gondi CS, Alapati K, Dinh DH, Gujrati M and Rao JS (2011) Cathepsin B and uPAR knockdown inhibits tumor-induced angiogenesis by modulating VEGF expression in glioma. *Cancer Gene Ther* **18**:419-434.

Mantha AJ, Hanson JE, Goss G, Lagarde AE, Lorimer IA and Dimitroulakos J (2005) Targeting the mevalonate pathway inhibits the function of the epidermal growth factor receptor. *Clin Cancer Res* **11**:2398-2407.

Mason SD and Joyce JA (2011) Proteolytic networks in cancer. *Trends Cell Biol* **21**:228-237.

Matrai J, Chuah MK and VandenDriessche T (2010) Recent advances in lentiviral vector development and applications. *Mol Ther* **18**:477-490.

Mauch C, Adelmann-Grill B, Hatamochi A and Krieg T (1989) Collagenase gene expression in fibroblasts is regulated by a three-dimensional contact with collagen. *FEBS Lett* **250**:301-305.

McCormick D (1993) Secretion of cathepsin B by human gliomas in vitro. *Neuropathol Appl Neurobiol* **19**:146-151.

McKerrow JH, Bhargava V, Hansell E, Huling S, Kuwahara T, Matley M, Coussens L and Warren R (2000) A functional proteomics screen of proteases in colorectal carcinoma. *Mol Med* **6**:450-460.

Miao H, Nickel CH, Cantley LG, Bruggeman LA, Bennardo LN and Wang B (2003) EphA kinase activation regulates HGF-induced epithelial branching morphogenesis. *J Cell Biol* **162**:1281-1292.

Mineo C, James GL, Smart EJ and Anderson RG (1996) Localization of epidermal growth factor-stimulated Ras/Raf-1 interaction to caveolae membrane. *J Biol Chem* **271**:11930-11935.

Mohamed MM, Cavallo-Medved D and Sloane BF (2008) Human monocytes augment invasiveness and proteolytic activity of inflammatory breast cancer. *Biol Chem* **389**:1117-1121.

Mohamed MM and Sloane BF (2006) Cysteine cathepsins: multifunctional enzymes in cancer. *Nat Rev Cancer* **6**:764-775.

Moin K, Day NA, Sameni M, Hasnain S, Hirama T and Sloane BF (1992) Human tumour cathepsin B. Comparison with normal liver cathepsin B. *Biochem J* **285 (Pt 2)**:427-434.

Moll R, Mitze M, Frixen UH and Birchmeier W (1993) Differential loss of E-cadherin expression in infiltrating ductal and lobular breast carcinomas. *Am J Pathol* **143**:1731-1742.

Monaghan-Benson E, Mastick CC and McKeown-Longo PJ (2008) A dual role for caveolin-1 in the regulation of fibronectin matrix assembly by uPAR. *J Cell Sci* **121**:3693-3703.

Monier S, Parton RG, Vogel F, Behlke J, Henske A and Kurzchalia TV (1995) VIP21-caveolin, a membrane protein constituent of the caveolar coat, oligomerizes in vivo and in vitro. *Mol Biol Cell* **6**:911-927.

Montesano R, Roth J, Robert A and Orci L (1982) Non-coated membrane invaginations are involved in binding and internalization of cholera and tetanus toxins. *Nature* **296**:651-653.

Mort JS and Buttle DJ (1997) Cathepsin B. *Int J Biochem Cell Biol* **29**:715-720.

Murata M, Miyashita S, Yokoo C, Tamai M, Hanada K, Hatayama K, Towatari T, Nikawa T and Katunuma N (1991) Novel epoxysuccinyl peptides. Selective inhibitors of cathepsin B, in vitro. *FEBS Lett* **280**:307-310.

Murata M, Peranen J, Schreiner R, Wieland F, Kurzchalia TV and Simons K (1995) VIP21/caveolin is a cholesterol-binding protein. *Proc Natl Acad Sci U S A* **92**:10339-10343.

Murphy G, Ward R, Gavrilovic J and Atkinson S (1992) Physiological mechanisms for metalloproteinase activation. *Matrix Suppl* **1**:224-230.

Nagler DK and Menard R (2003) Family C1 cysteine proteases: biological diversity or redundancy? *Biol Chem* **384**:837-843.

Nalla AK, Gorantla B, Gondi CS, Lakka SS and Rao JS (2010) Targeting MMP-9, uPAR, and cathepsin B inhibits invasion, migration and activates apoptosis in prostate cancer cells. *Cancer Gene Ther* **17**:599-613.

Netzel-Arnett S, Hooper JD, Szabo R, Madison EL, Quigley JP, Bugge TH and Antalis TM (2003) Membrane anchored serine proteases: a rapidly expanding group of cell surface proteolytic enzymes with potential roles in cancer. *Cancer Metastasis Rev* **22**:237-258.

Neve RM, Chin K, Fridlyand J, Yeh J, Baehner FL, Fevr T, Clark L, Bayani N, Coppe JP, Tong F, Speed T, Spellman PT, DeVries S, Lapuk A, Wang NJ, Kuo WL, Stilwell JL, Pinkel D, Albertson DG, Waldman FM, McCormick F, Dickson RB, Johnson MD, Lippman M, Ethier S, Gazdar A and Gray JW (2006) A collection of breast cancer cell lines for the study of functionally distinct cancer subtypes. *Cancer Cell* **10**:515-527.

Nguyen DM, Sam K, Tsimelzon A, Li X, Wong H, Mohsin S, Clark GM, Hilsenbeck SG, Elledge RM, Allred DC, O'Connell P and Chang JC (2006) Molecular heterogeneity of inflammatory breast cancer: a hyperproliferative phenotype. *Clin Cancer Res* **12**:5047-5054.

Nielsen BS, Sehested M, Duun S, Rank F, Timshel S, Rygaard J, Johnsen M and Dano K (2001) Urokinase plasminogen activator is localized in stromal cells in ductal breast cancer. *Lab Invest* **81**:1485-1501.

Nielsen BS, Sehested M, Timshel S, Pyke C and Dano K (1996) Messenger RNA for urokinase plasminogen activator is expressed in myofibroblasts adjacent to cancer cells in human breast cancer. *Lab Invest* **74**:168-177.

Nishimura Y, Kawabata T and Kato K (1988) Identification of latent procathepsins B and L in microsomal lumen: characterization of enzymatic activation and proteolytic processing in vitro. *Arch Biochem Biophys* **261**:64-71.

Nouh MA, Mohamed MM, El-Shinawi M, Shaalan MA, Cavallo-Medved D, Khaled HM and Sloane BF (2011) Cathepsin B: a potential prognostic marker for inflammatory breast cancer. *J Transl Med* **9**:1.

Oda T, Kanai Y, Oyama T, Yoshiura K, Shimoyama Y, Birchmeier W, Sugimura T and Hirohashi S (1994) E-cadherin gene mutations in human gastric carcinoma cell lines. *Proc Natl Acad Sci U S A* **91**:1858-1862.

Oh HY, Lee EJ, Yoon S, Chung BH, Cho KS and Hong SJ (2007) Cholesterol level of lipid raft microdomains regulates apoptotic cell death in prostate cancer cells through EGFR-mediated Akt and ERK signal transduction. *Prostate* **67**:1061-1069.

Oh P and Schnitzer JE (2001) Segregation of heterotrimeric G proteins in cell surface microdomains. G(q) binds caveolin to concentrate in caveolae, whereas G(i) and G(s) target lipid rafts by default. *Mol Biol Cell* **12**:685-698.

Oyama T, Kanai Y, Ochiai A, Akimoto S, Oda T, Yanagihara K, Nagafuchi A, Tsukita S, Shibamoto S, Ito F and et al. (1994) A truncated beta-catenin

disrupts the interaction between E-cadherin and alpha-catenin: a cause of loss of intercellular adhesiveness in human cancer cell lines. *Cancer Res* **54**:6282-6287.

Park IH, Kim JY, Jung JI and Han JY (2010) Lovastatin overcomes gefitinib resistance in human non-small cell lung cancer cells with K-Ras mutations. *Invest New Drugs* **28**:791-799.

Parton M, Dowsett M, Ashley S, Hills M, Lowe F and Smith IE (2004) High incidence of HER-2 positivity in inflammatory breast cancer. *Breast* **13**:97-103.

Parton RG, Joggerst B and Simons K (1994) Regulated internalization of caveolae. *J Cell Biol* **127**:1199-1215.

Pepper MS (2001) Role of the matrix metalloproteinase and plasminogen activator-plasmin systems in angiogenesis. *Arterioscler Thromb Vasc Biol* **21**:1104-1117.

Perou CM, Sorlie T, Eisen MB, van de Rijn M, Jeffrey SS, Rees CA, Pollack JR, Ross DT, Johnsen H, Akslen LA, Fluge O, Pergamenschikov A, Williams C, Zhu SX, Lonning PE, Borresen-Dale AL, Brown PO and Botstein D (2000) Molecular portraits of human breast tumours. *Nature* **406**:747-752.

Pinilla SM, Honrado E, Hardisson D, Benitez J and Palacios J (2006) Caveolin-1 expression is associated with a basal-like phenotype in sporadic and hereditary breast cancer. *Breast Cancer Res Treat* **99**:85-90.

Poole AR, Tiltman KJ, Recklies AD and Stoker TA (1978) Differences in secretion of the proteinase cathepsin B at the edges of human breast carcinomas and fibroadenomas. *Nature* **273**:545-547.

Prud'homme GJ, Glinka Y, Toulina A, Ace O, Subramaniam V and Jothy S (2010) Breast cancer stem-like cells are inhibited by a non-toxic aryl hydrocarbon receptor agonist. *PLoS One* **5**:e13831.

Puyraimond A, Fridman R, Lemesle M, Arbeille B and Menashi S (2001) MMP-2 colocalizes with caveolae on the surface of endothelial cells. *Exp Cell Res* **262**:28-36.

Pyke C, Graem N, Ralfkiaer E, Ronne E, Hoyer-Hansen G, Brunner N and Dano K (1993) Receptor for urokinase is present in tumor-associated macrophages in ductal breast carcinoma. *Cancer Res* **53**:1911-1915.

Qian F, Bajkowski AS, Steiner DF, Chan SJ and Frankfater A (1989) Expression of five cathepsins in murine melanomas of varying metastatic potential and normal tissues. *Cancer Res* **49**:4870-4875.

Qin YW, Ye P, He JQ, Sheng L, Wang LY and Du J (2010) Simvastatin inhibited cardiac hypertrophy and fibrosis in apolipoprotein E-deficient mice fed a "Western-style diet" by increasing PPAR alpha and gamma expression and reducing TC, MMP-9, and Cat S levels. *Acta Pharmacol Sin* **31**:1350-1358.

Rabbani SA and Mazar AP (2001) The role of the plasminogen activation system in angiogenesis and metastasis. *Surg Oncol Clin N Am* **10**:393-415, x.

Rao S, Porter DC, Chen X, Herliczek T, Lowe M and Keyomarsi K (1999) Lovastatin-mediated G1 arrest is through inhibition of the proteasome, independent of hydroxymethyl glutaryl-CoA reductase. *Proc Natl Acad Sci U S A* **96**:7797-7802.

Rastelli F, Biancanelli S, Falzetta A, Martignetti A, Casi C, Bascioni R, Giustini L and Crispino S (2010) Triple-negative breast cancer: current state of the art. *Tumori* **96**:875-888.

Razani B, Engelman JA, Wang XB, Schubert W, Zhang XL, Marks CB, Macaluso F, Russell RG, Li M, Pestell RG, Di Vizio D, Hou H, Jr., Kneitz B, Lagaud G, Christ GJ, Edelmann W and Lisanti MP (2001) Caveolin-1 null mice are viable but show evidence of hyperproliferative and vascular abnormalities. *J Biol Chem* **276**:38121-38138.

Reinheckel T, Deussing J, Roth W and Peters C (2001) Towards specific functions of lysosomal cysteine peptidases: phenotypes of mice deficient for cathepsin B or cathepsin L. *Biol Chem* **382**:735-741.

Reiser J, Adair B and Reinheckel T (2010) Specialized roles for cysteine cathepsins in health and disease. *J Clin Invest* **120**:3421-3431.

Rempel SA, Rosenblum ML, Mikkelsen T, Yan PS, Ellis KD, Golembieski WA, Sameni M, Rozhin J, Ziegler G and Sloane BF (1994) Cathepsin B expression and localization in glioma progression and invasion. *Cancer Res* **54**:6027-6031.

Rety S, Sopkova J, Renouard M, Osterloh D, Gerke V, Tabaries S, Russo-Marie F and Lewit-Bentley A (1999) The crystal structure of a complex of p11 with the annexin II N-terminal peptide. *Nat Struct Biol* **6**:89-95.

Rickli EE (1975) The activation mechanism of human plasminogen. *Thromb Diath Haemorrh* **34**:386-395.

Rimawi MF, Shetty PB, Weiss HL, Schiff R, Osborne CK, Chamness GC and Elledge RM (2010) Epidermal growth factor receptor expression in breast cancer association with biologic phenotype and clinical outcomes. *Cancer* **116**:1234-1242.

Riou G, Le MG, Travagli JP, Levine AJ and Moll UM (1993) Poor prognosis of p53 gene mutation and nuclear overexpression of p53 protein in inflammatory breast carcinoma. *J Natl Cancer Inst* **85**:1765-1767.

Rizzo V, Sung A, Oh P and Schnitzer JE (1998) Rapid mechanotransduction in situ at the luminal cell surface of vascular endothelium and its caveolae. *J Biol Chem* **273**:26323-26329.

Robertson FM, Bondy M, Yang W, Yamauchi H, Wiggins S, Kamrudin S, Krishnamurthy S, Le-Petross H, Bidaut L, Player AN, Barsky SH, Woodward WA, Buchholz T, Lucci A, Ueno NT and Cristofanilli M (2010) Inflammatory breast cancer: the disease, the biology, the treatment. *CA Cancer J Clin* **60**:351-375.

Robey IF, Baggett BK, Kirkpatrick ND, Roe DJ, Dosescu J, Sloane BF, Hashim AI, Morse DL, Raghunand N, Gatenby RA and Gillies RJ (2009)

Bicarbonate increases tumor pH and inhibits spontaneous metastases. *Cancer Res* **69**:2260-2268.

Robison AK and Collen D (1987) Activation of the fibrinolytic system. *Cardiol Clin* **5**:13-19.

Rodriguez A, Webster P, Ortego J and Andrews NW (1997) Lysosomes behave as Ca2+-regulated exocytic vesicles in fibroblasts and epithelial cells. *J Cell Biol* **137**:93-104.

Rohlich P and Allison AC (1976) Oriented pattern of membrane-associated vesicles in fibroblasts. *J Ultrastruct Res* **57**:94-103.

Roshy S, Sloane BF and Moin K (2003) Pericellular cathepsin B and malignant progression. *Cancer Metastasis Rev* **22**:271-286.

Rothberg JM, Sameni M, Moin K and Sloane BF (2011) Live-cell imaging of tumor proteolysis: Impact of cellular and non-cellular microenvironment. *Biochim Biophys Acta*.

Rothberg KG, Heuser JE, Donzell WC, Ying YS, Glenney JR and Anderson RG (1992) Caveolin, a protein component of caveolae membrane coats. *Cell* **68**:673-682.

Rowan AD, Mason P, Mach L and Mort JS (1992) Rat procathepsin B. Proteolytic processing to the mature form in vitro. *J Biol Chem* **267**:15993-15999.

Rozhin J, Sameni M, Ziegler G and Sloane BF (1994) Pericellular pH affects distribution and secretion of cathepsin B in malignant cells. *Cancer Res* **54**:6517-6525.

Sameni M, Cavallo-Medved D, Dosescu J, Jedeszko C, Moin K, Mullins SR, Olive MB, Rudy D and Sloane BF (2009) Imaging and quantifying the dynamics of tumor-associated proteolysis. *Clin Exp Metastasis* **26**:299-309.

Sameni M, Moin K and Sloane BF (2000) Imaging proteolysis by living human breast cancer cells. *Neoplasia* **2**:496-504.

San Segundo B, Chan SJ and Steiner DF (1986) Differences in cathepsin B mRNA levels in rat tissues suggest specialized functions. *FEBS Lett* **201**:251-256.

Sanchez-Munoz A, Perez-Ruiz E, Jimenez B, Ribelles N, Marquez A, Garcia-Rios I and Alba Conejo E (2009) Targeted therapy of metastatic breast cancer. *Clin Transl Oncol* **11**:643-650.

Santoro SA, Zutter MM, Wu JE, Staatz WD, Saelman EU and Keely PJ (1994) Analysis of collagen receptors. *Methods Enzymol* **245**:147-183.

Sargiacomo M, Sudol M, Tang Z and Lisanti MP (1993) Signal transducing molecules and glycosyl-phosphatidylinositol-linked proteins form a caveolin-rich insoluble complex in MDCK cells. *J Cell Biol* **122**:789-807.

Schmalhofer O, Brabletz S and Brabletz T (2009) E-cadherin, beta-catenin, and ZEB1 in malignant progression of cancer. *Cancer Metastasis Rev* **28**:151-166.

Schnitzer JE (2001) Caveolae: from basic trafficking mechanisms to targeting transcytosis for tissue-specific drug and gene delivery in vivo. *Adv Drug Deliv Rev* **49**:265-280.

Schnitzer JE, Allard J and Oh P (1995a) NEM inhibits transcytosis, endocytosis, and capillary permeability: implication of caveolae fusion in endothelia. *Am J Physiol* **268**:H48-55.

Schnitzer JE, McIntosh DP, Dvorak AM, Liu J and Oh P (1995b) Separation of caveolae from associated microdomains of GPI-anchored proteins. *Science* **269**:1435-1439.

Schnitzer JE, Oh P, Pinney E and Allard J (1994) Filipin-sensitive caveolae-mediated transport in endothelium: reduced transcytosis, scavenger endocytosis, and capillary permeability of select macromolecules. *J Cell Biol* **127**:1217-1232.

Schwab W, Gavlik JM, Beichler T, Funk RH, Albrecht S, Magdolen V, Luther T, Kasper M and Shakibaei M (2001) Expression of the urokinase-type plasminogen activator receptor in human articular chondrocytes: association with caveolin and beta 1-integrin. *Histochem Cell Biol* **115**:317-323.

Shuja S, Sheahan K and Murnane MJ (1991) Cysteine endopeptidase activity levels in normal human tissues, colorectal adenomas and carcinomas. *Int J Cancer* **49**:341-346.

Silva J, Beckedorf A and Bieberich E (2003) Osteoblast-derived oxysterol is a migration-inducing factor for human breast cancer cells. *J Biol Chem* **278**:25376-25385.

Simons K and Ikonen E (1997) Functional rafts in cell membranes. *Nature* **387**:569-572.

Simons K and Toomre D (2000) Lipid rafts and signal transduction. *Nat Rev Mol Cell Biol* **1**:31-39.

Simons K and van Meer G (1988) Lipid sorting in epithelial cells. *Biochemistry* **27**:6197-6202.

Sinha AA, Gleason DF, Deleon OF, Wilson MJ and Sloane BF (1993) Localization of a biotinylated cathepsin B oligonucleotide probe in human prostate including invasive cells and invasive edges by in situ hybridization. *Anat Rec* **235**:233-240.

Sinha AA, Wilson MJ, Gleason DF, Reddy PK, Sameni M and Sloane BF (1995) Immunohistochemical localization of cathepsin B in neoplastic human prostate. *Prostate* **26**:171-178.

Sloane BF, Dunn JR and Honn KV (1981) Lysosomal cathepsin B: correlation with metastatic potential. *Science* **212**:1151-1153.

Sloane BF, Yan S, Podgorski I, Linebaugh BE, Cher ML, Mai J, Cavallo-Medved D, Sameni M, Dosescu J and Moin K (2005) Cathepsin B and tumor proteolysis: contribution of the tumor microenvironment. *Semin Cancer Biol* **15**:149-157.

Smart EJ, Ying YS, Mineo C and Anderson RG (1995) A detergent-free method for purifying caveolae membrane from tissue culture cells. *Proc Natl Acad Sci U S A* **92**:10104-10108.

Solomon KR, Mallory MA and Finberg RW (1998) Determination of the non-ionic detergent insolubility and phosphoprotein associations of glycosylphosphatidylinositol-anchored proteins expressed on T cells. *Biochem J* **334 (Pt 2)**:325-333.

Song KS, Li S, Okamoto T, Quilliam LA, Sargiacomo M and Lisanti MP (1996) Co-purification and direct interaction of Ras with caveolin, an integral membrane protein of caveolae microdomains. Detergent-free purification of caveolae microdomains. *J Biol Chem* **271**:9690-9697.

Soric J and Gordon JA (1986) Calcium-dependent isolation of the 36-kilodalton substrate of pp60src-kinase. Fractionation of the phosphorylated and unphosphorylated species. *J Biol Chem* **261**:14490-14495.

Stahl A and Mueller BM (1995) The urokinase-type plasminogen activator receptor, a GPI-linked protein, is localized in caveolae. *J Cell Biol* **129**:335-344.

Staubach S and Hanisch FG (2011) Lipid rafts: signaling and sorting platforms of cells and their roles in cancer. *Expert Rev Proteomics* **8**:263-277.

Stegmeier F, Hu G, Rickles RJ, Hannon GJ and Elledge SJ (2005) A lentiviral microRNA-based system for single-copy polymerase II-regulated RNA

interference in mammalian cells. *Proc Natl Acad Sci U S A* **102**:13212-13217.

Stillfried GE, Saunders DN and Ranson M (2007) Plasminogen binding and activation at the breast cancer cell surface: the integral role of urokinase activity. *Breast Cancer Res* **9**:R14.

Stuart HC, Jia Z, Messenberg A, Joshi B, Underhill TM, Moukhles H and Nabi IR (2008) Localized Rho GTPase activation regulates RNA dynamics and compartmentalization in tumor cell protrusions. *J Biol Chem* **283**:34785-34795.

Sukoh N, Abe S, Nakajima I, Ogura S, Isobe H, Inoue K and Kawakami Y (1994) Immunohistochemical distributions of cathepsin B and basement membrane antigens in human lung adenocarcinoma: association with invasion and metastasis. *Virchows Arch* **424**:33-38.

Taggart CC, Lowe GJ, Greene CM, Mulgrew AT, O'Neill SJ, Levine RL and McElvaney NG (2001) Cathepsin B, L, and S cleave and inactivate secretory leucoprotease inhibitor. *J Biol Chem* **276**:33345-33352.

Taipale J and Keski-Oja J (1997) Growth factors in the extracellular matrix. *Faseb J* **11**:51-59.

Tarui T, Andronicos N, Czekay RP, Mazar AP, Bdeir K, Parry GC, Kuo A, Loskutoff DJ, Cines DB and Takada Y (2003) Critical role of integrin alpha 5 beta 1 in urokinase (uPA)/urokinase receptor (uPAR, CD87) signaling. *J Biol Chem* **278**:29863-29872.

Taylor F, Ward K, Moore TH, Burke M, Davey Smith G, Casas JP and Ebrahim S (2011) Statins for the primary prevention of cardiovascular disease. *Cochrane Database Syst Rev*:CD004816.

Thunyakitpisal PD and Chaisuparat R (2004) Simvastatin, an HMG-CoA reductase inhibitor, reduced the expression of matrix metalloproteinase-9 (Gelatinase B) in osteoblastic cells and HT1080 fibrosarcoma cells. *J Pharmacol Sci* **94**:403-409.

Trebicka J, Hennenberg M, Odenthal M, Shir K, Klein S, Granzow M, Vogt A, Dienes HP, Lammert F, Reichen J, Heller J and Sauerbruch T (2010) Atorvastatin attenuates hepatic fibrosis in rats after bile duct ligation via decreased turnover of hepatic stellate cells. *J Hepatol* **53**:702-712.

Tu C, Ortega-Cava CF, Chen G, Fernandes ND, Cavallo-Medved D, Sloane BF, Band V and Band H (2008) Lysosomal cathepsin B participates in the podosome-mediated extracellular matrix degradation and invasion via secreted lysosomes in v-Src fibroblasts. *Cancer Res* **68**:9147-9156.

Turk B (2006) Targeting proteases: successes, failures and future prospects. *Nat Rev Drug Discov* **5**:785-799.

Uittenbogaard A, Ying Y and Smart EJ (1998) Characterization of a cytosolic heat-shock protein-caveolin chaperone complex. Involvement in cholesterol trafficking. *J Biol Chem* **273**:6525-6532.

Ulisse S, Baldini E, Sorrenti S and D'Armiento M (2009) The urokinase plasminogen activator system: a target for anti-cancer therapy. *Curr Cancer Drug Targets* **9**:32-71.

Van den Eynden GG, Van Laere SJ, Van der Auwera I, Merajver SD, Van Marck EA, van Dam P, Vermeulen PB, Dirix LY and van Golen KL (2006) Overexpression of caveolin-1 and -2 in cell lines and in human samples of inflammatory breast cancer. *Breast Cancer Res Treat* **95**:219-228.

Van der Auwera I, Van Laere SJ, Van den Eynden GG, Benoy I, van Dam P, Colpaert CG, Fox SB, Turley H, Harris AL, Van Marck EA, Vermeulen PB and Dirix LY (2004) Increased angiogenesis and lymphangiogenesis in inflammatory versus noninflammatory breast cancer by real-time reverse transcriptase-PCR gene expression quantification. *Clin Cancer Res* **10**:7965-7971.

van der Stappen JW, Williams AC, Maciewicz RA and Paraskeva C (1996) Activation of cathepsin B, secreted by a colorectal cancer cell line requires low pH and is mediated by cathepsin D. *Int J Cancer* **67**:547-554.

van Kempen LC, Rhee JS, Dehne K, Lee J, Edwards DR and Coussens LM (2002) Epithelial carcinogenesis: dynamic interplay between neoplastic cells and their microenvironment. *Differentiation* **70**:610-623.

Van Laere S, Van der Auwera I, Van den Eynden GG, Fox SB, Bianchi F, Harris AL, van Dam P, Van Marck EA, Vermeulen PB and Dirix LY (2005)

Distinct molecular signature of inflammatory breast cancer by cDNA microarray analysis. *Breast Cancer Res Treat* **93**:237-246.

Vasiljeva O, Korovin M, Gajda M, Brodoefel H, Bojic L, Kruger A, Schurigt U, Sevenich L, Turk B, Peters C and Reinheckel T (2008) Reduced tumour cell proliferation and delayed development of high-grade mammary carcinomas in cathepsin B-deficient mice. *Oncogene* **27**:4191-4199.

Vasiljeva O, Papazoglou A, Kruger A, Brodoefel H, Korovin M, Deussing J, Augustin N, Nielsen BS, Almholt K, Bogyo M, Peters C and Reinheckel T (2006) Tumor cell-derived and macrophage-derived cathepsin B promotes progression and lung metastasis of mammary cancer. *Cancer Res* **66**:5242-5250.

Vasiljeva O, Reinheckel T, Peters C, Turk D, Turk V and Turk B (2007) Emerging roles of cysteine cathepsins in disease and their potential as drug targets. *Curr Pharm Des* **13**:387-403.

Vassalli JD, Baccino D and Belin D (1985) A cellular binding site for the Mr 55,000 form of the human plasminogen activator, urokinase. *J Cell Biol* **100**:86-92.

Venkitaraman R (2010) Triple-negative/basal-like breast cancer: clinical, pathologic and molecular features. *Expert Rev Anticancer Ther* **10**:199-207.

Vermeulen PB, Van Laere SJ and Dirix LY (2009) Inflammatory breast carcinoma as a model of accelerated self-metastatic expansion by intravascular growth. *Br J Cancer* **101**:1028-1029; author reply 1030.

Vincent-Salomon A and Thiery JP (2003) Host microenvironment in breast cancer development: epithelial-mesenchymal transition in breast cancer development. *Breast Cancer Res* **5**:101-106.

Visscher DW, Sloane BF, Sameni M, Babiarz JW, Jacobson J and Crissman JD (1994) Clinicopathologic significance of cathepsin B immunostaining in transitional neoplasia. *Mod Pathol* **7**:76-81.

Walshe JM and Swain SM (2005) Clinical aspects of inflammatory breast cancer. *Breast Dis* **22**:35-44.

Watanabe M, Higashi T, Watanabe A, Osawa T, Sato Y, Kimura Y, Tominaga S, Hashimoto N, Yoshida Y, Morimoto S and et al. (1989) Cathepsin B and L activities in gastric cancer tissue: correlation with histological findings. *Biochem Med Metab Biol* **42**:21-29.

Wei Y, Yang X, Liu Q, Wilkins JA and Chapman HA (1999) A role for caveolin and the urokinase receptor in integrin-mediated adhesion and signaling. *J Cell Biol* **144**:1285-1294.

Weigelt B and Bissell MJ (2008) Unraveling the microenvironmental influences on the normal mammary gland and breast cancer. *Semin Cancer Biol* **18**:311-321.

Wike-Hooley JL, Haveman J and Reinhold HS (1984) The relevance of tumour pH to the treatment of malignant disease. *Radiother Oncol* **2**:343-366.

Williams TM and Lisanti MP (2005) Caveolin-1 in oncogenic transformation, cancer, and metastasis. *American journal of physiology* **288**:C494-506.

Wong WW, Dimitroulakos J, Minden MD and Penn LZ (2002) HMG-CoA reductase inhibitors and the malignant cell: the statin family of drugs as triggers of tumor-specific apoptosis. *Leukemia* **16**:508-519.

Wu H, Jiang H, Lu D, Xiong Y, Qu C, Zhou D, Mahmood A and Chopp M (2009) Effect of simvastatin on glioma cell proliferation, migration, and apoptosis. *Neurosurgery* **65**:1087-1096; discussion 1096-1087.

Wu M, Wu ZF, Rosenthal DT, Rhee EM and Merajver SD (2010) Characterization of the roles of RHOC and RHOA GTPases in invasion, motility, and matrix adhesion in inflammatory and aggressive breast cancers. *Cancer* **116**:2768-2782.

Yan S, Berquin IM, Troen BR and Sloane BF (2000) Transcription of human cathepsin B is mediated by Sp1 and Ets family factors in glioma. *DNA Cell Biol* **19**:79-91.

Yan S, Sameni M and Sloane BF (1998) Cathepsin B and human tumor progression. *Biol Chem* **379**:113-123.

Yan S and Sloane BF (2003) Molecular regulation of human cathepsin B: implication in pathologies. *Biol Chem* **384**:845-854.

Zhao TT, Le Francois BG, Goss G, Ding K, Bradbury PA and Dimitroulakos J (2010) Lovastatin inhibits EGFR dimerization and AKT activation in squamous cell carcinoma cells: potential regulation by targeting rho proteins. *Oncogene* **29**:4682-4692.

Zhuang L, Kim J, Adam RM, Solomon KR and Freeman MR (2005) Cholesterol targeting alters lipid raft composition and cell survival in prostate cancer cells and xenografts. *J Clin Invest* **115**:959-968.

Zhuang L, Lin J, Lu ML, Solomon KR and Freeman MR (2002) Cholesterol-rich lipid rafts mediate akt-regulated survival in prostate cancer cells. *Cancer Res* **62**:2227-2231.

ABSTRACT

FUNCTIONAL IN VITRO ANALYSES OF LIPID RAFT-ASSOCIATED CATHEPSIN B: IMPLICATION FOR THE INVASIVE PHENOTYPE OF INFLAMMATORY BREAST CANCER

by

BERNADETTE C. VICTOR

December 2011

Advisor: Dr. Bonnie F. Sloane

Major: Cancer Biology

Degree: Doctor of Philosophy

Inflammatory breast cancer (IBC) is an aggressive, metastatic and highly angiogenic form of locally advanced breast cancer. Breast cancer invasion has been linked to proteolytic activity at the tumor cell surface. We observed that uPA, uPAR and enzymatically active cathepsin B were all present in caveolae fractions isolated from SUM149 cells. Using a live-cell proteolysis assay, we demonstrated that both IBC cell lines degrade type IV collagen. The SUM149 cells exhibit predominantly pericellular proteolysis, consistent with localization of constituents of a proteolytic pathway to membrane microdomains. A functional role for cathepsin B was confirmed by the ability of CA074, a cell impermeable and highly selective cathepsin B inhibitor, to significantly reduce pericellular proteolysis and invasion by SUM149 cells. A statistically significant co-expression of cathepsin B and caveolin-1 was found in IBC patient biopsies, thus validating our *in vitro* data. To determine whether the uPA and cathepsin B

present at the cell surface is localized specifically to caveolae and investigate if caveolae are a functional component of the IBC phenotype, we knocked down the expression of caveolin-1 in SUM149 cells. The subcellular distribution of cathepsin B was unchanged in caveolin-1 knockdown SUM149 cells. In contrast, knockdown decreased the association of both uPA and EGFR with caveolae. Knockdown of caveolin-1 also decreased degradation of type IV collagen and invasion by IBC cells. We also determined that targeted disruption of lipid microdomains by use of lovastatin diminished the aggressiveness of IBC cells. Cathepsin B activity and association with lipid microdomains was reduced in lovastatin treated IBC cells. Lovastatin treatment also reduced type IV collagen degradation and invasion by IBC cells. In conclusion, we have shown that cathepsin B and caveolin-1 both contribute to the aggressiveness of IBC, albeit by different mechanisms.

AUTOBIOGRAPHICAL STATEMENT

BERNADETTE C. VICTOR

EDUCATION:
Bachelor of Science Biology, Wayne State University 2002

PROFESSIONAL APPOINTMENTS:
Research Assistant, Barabara Ann Karmanos Cancer Institute/Wayne State University, 2003-4

HONORS/AWARDS:
Wayne State University Presidential Scholarship, 1997-2001
Wayne State University School of Medicine Honor for "Exceptional Academic and Research Accomplishments in Cancer Biology for the 2008–2009 Academic Year", 2009

GRANT SUPPORT (active):
Cathepsin B and Its Binding Partners in the Aggressiveness of Inflammatory Breast Cancer. DoD Breast Predoctoral Fellowship, B.C. Victor. B.F. Sloane, Mentor. 1/15/09-2/14/12; $92,000.

PUBLICATIONS:

Victor B.C, Sloane B.F.: Cysteine cathepsin non-inhibitory binding partners: modulating intracellular trafficking and function. *Biol Chem* 2007, 388:1131-1140.

Jedeszko, C.*, Victor, B.C.*, Podgorski, I. and Sloane, B.F.: Fibroblast hepatocyte growth factor promotes invasion of human mammary ductal carcinoma in situ. *Cancer Res* 2009, 69:9148-9155.*Joint first authors

Victor, B.C., Anbalagan, A., Mohamed, M.M., Sloane, B.F. and Cavallo-Medved, D.: Inhibition of cathepsin B activity attenuates extracellular matrix degradation and inflammatory breast cancer invasion. *Breast Cancer Research* 2011, *Accepted pending minor revisions*

Moin, K., Sameni, M., Victor, B.C., Rothberg J.M., Mattingly, R.R. and Sloane, B.F.: 3D/4D functional imaging of tumor-associated proteolysis: impact of microenvironment. *Methods in Enzymology*, *In press.*

Wojtkowiak, J.W., Victor, B.C., Jedeszko, C., Sloane, B.F., Reiners, J.J. and Mattingly, R.R.: Farnesyl transferase inhibitor and lovastatin co-treatment disrupts trafficking and processing of procathepsins. *In preparation.*